Nazlı TEKİN ENERGY HARVESTING WIRELESS MULTIMEDIA SENSOR NETWORKS IN INDUSTRIAL ENVIRONMENTS AGU 2020

ENERGY HARVESTING WIRELESS MULTIMEDIA SENSOR NETWORKS IN INDUSTRIAL ENVIRONMENTS

A Ph.D. Thesis

By

Nazlı TEKİN

July 2020

ENERGY HARVESTING WIRELESS MULTIMEDIA SENSOR NETWORKS IN INDUSTRIAL ENVIRONMENTS

A THESIS
SUBMITTED TO THE DEPARTMENT OF ELECTRICAL AND COMPUTER ENGINEERING
AND THE GRADUATE SCHOOL OF ENGINEERING AND SCIENCE OF ABDULLAH GUL UNIVERSITY
IN PARTIAL FULFILLMENT OF THE REQUIREMENTS
FOR THE DEGREE OF
DOCTOR OF ELECTRICAL AND COMPUTER ENGINEERING

By
Nazlı TEKİN
July 2020

SCIENTIFIC ETHICS COMPLIANCE

I hereby declare that all information in this document has been obtained in accordance with academic rules and ethical conduct. I also declare that, as required by these rules and conduct, I have fully cited and referenced all materials and results that are not original to this work.

Nazlı TEKİN

REGULATORY COMPLIANCE

Ph.D. thesis titled "Energy Harvesting Wireless Multimedia Sensor Networks in Industrial Environments" has been prepared in accordance with the Thesis Writing Guidelines of the Abdullah Gül University, Graduate School of Engineering & Science.

Prepared By	Advisor
Nazlı TEKIN	Prof. Dr. V. Çağrı GÜNGÖR

Head of the Electrical and Computer Engineering Program
Prof. Dr. V. Çağrı GÜNGÖR

ACCEPTANCE AND APPROVAL

Ph.D. thesis titled "Energy Harvesting Wireless Multimedia Sensor Networks in Industrial Environments" and prepared by Nazlı TEKİN has been accepted by the jury in the Electrical and Computer Engineering Graduate Program at Abdullah Gül University, Graduate School of Engineering & Science.

22 / 07 / 2020

JURY:

Advisor : Prof. Dr. V. Çağrı GÜNGÖR

Member : Asst. Prof. Gülay YALÇIN ALKAN

Member : Asst. Prof. Muhammed SÜTÇÜ

Member : Assoc. Prof. Özlem DURMAZ İNCEL

Member : Assoc. Prof. Berk CANBERK

APPROVAL:

The acceptance of this Ph.D. thesis has been approved by the decision of the Abdullah Gül University, Graduate School of Engineering & Science, Executive Board dated ….. /….. / …….. and numbered ……..……. .

…….. /…….. / ……..

(Date)

Graduate School Dean

Prof. Dr. İrfan ALAN

ABSTRACT

ENERGY HARVESTING WIRELESS MULTIMEDIA SENSOR NETWORKS IN INDUSTRIAL ENVIRONMENTS

Nazlı TEKİN
Ph.D. in Electrical and Computer Engineering
Supervisor: Prof. Dr. V. Çağrı GÜNGÖR

July 2020

Providing energy efficient and reliable communication for Industrial Wireless Sensor Networks (IWSNs) is of great significance when considering the harsh channel characteristics of industrial environment. However, prolonging a network lifetime while ensuring reliability becomes a major challenge.

The main goal of this thesis is to maximize the network lifetime of Industrial Wireless Sensor Networks (IWSNs). The Energy Harvesting (EH) methods based on indoor solar, thermal and vibration that are suitable for industrial environments are defined and their contributions on network lifetime are investigated. A novel Mixed Integer Programming (MIP) model is formulated to maximize network lifetime by jointly considering path loss, application reliability and EH methods.

Furthermore, communication in Wireless Multimedia Sensor Networks (WMSNs) causes the expense of extra energy consumption due to its huge data size. Therefore, reducing huge data size before transmission becomes important. To this end, the impact of the data size reduction methods such as compressive sensing and image compression while considering energy dissipation of both communication and computation on industrial network lifetime is evaluated. On the other hand, to solve the MIP model in a feasible time is hard especially when the large amount of sensor nodes deployed in the network. Heuristic based optimization methods are developed to overcome the time complexity of MIP problem.

Keywords: Energy harvesting, Network lifetime, Error control, Industrial wireless sensor networks

ÖZET

ENDÜSTRİYEL ORTAMLARDA ENERJİ HASATLAYAN ÇOĞUL ORTAM KABLOSUZ ALGILAYICI AĞLARI

Nazlı TEKİN
Elektrik ve Bilgisayar Mühendisliği Bölümü Doktora
Tez Yöneticisi: Prof. Dr. V. Çağrı GÜNGÖR
Temmuz-2020

Sert kanal koşullarına sahip olan Endüstriyel Kablosuz Algılayıcı Ağ'larda (EKAA), enerji verimli ve güvenilir kablosuz iletişim sağlamak büyük önem taşımaktadır. Ağ güvenirliğini sağlarken aynı zamanda ağın ömrünü uzatmak da zor bir problemdir. Bu çalışmanın amacı, EKAA'ların ömrünün eniyilenmesidir. Bunu yaparken, endüstriyel ortamlar için uygun olan iç mekan güneş, termal ve titreşime dayalı Enerji Hasatlama (EH) yöntemleri tanımlanmış ve bunların ağ ömrüne katkıları araştırılmıştır. Uygulama güvenilirliğini ve EH yöntemlerini birlikte değerlendirerek, ağ ömrünü eniyilemek için yeni bir Karma Tamsayılı Programlama (KTP) modeli formüle edilmiştir.

Ayrıca, Kablosuz Çoğul Ortam Algılayıcı Ağ'larında (KÇOAA) iletişim, büyük veri boyutu nedeniyle fazladan enerji tüketimine sebep olur. Bu nedenle, büyük veri boyutunu iletimden önce azaltmak önemli hale gelir.Bu amaçla, iletişim ve enerji dağıtım hesaplamalarını dikkate alırken, sıkıştırıcı algılama ve görüntü sıkıştırma gibi veri boyutu küçültme yöntemlerinin endüstriyel ağ ömrü üzerindeki etkisi değerlendirilir.

Öte yandan, özellikle çok sayıda algılayıcılar bulunduran ağlar için KTP modelini uygun bir zamanda çözmek bir hayli zordur. KTP'nin zaman karmaşıklığı sorununun üstesinden gelmek için sezgisel tabanlı yöntemler geliştirilmiştir.

Anahtar kelimeler: Enerji hasatlama, Ağ ömrü, Hata kontrol, Endüstriyel kablosuz algılayıcı ağları

Acknowledgements

At first, I would like to express my sincerest appreciation to my advisor, Prof. Dr. V. Çağrı Güngör for continuous support of my research, for his patience and motivation. I gained valuable experiences during this Ph. D. My research would not have been possible without his guidance and efforts.

I would like to thanks my thesis committee members, Assist. Prof. Gülay Yalçın and Assist. Prof. Muhammed Sütçü for their support and valuable suggestions.

I would like to thanks YÖK for providing 100/2000 YÖK Ph.D. scholarship.

I would like to great thanks to my parents who made me who I am today. Thanks to my father, Hüseyin for making me always go forward, my mother, Özay for unrequited love, my twin, Esra for getting me up when I lost my motivation, my little sister, Büşra and little brother, Mehmet for being my joy.

Table of Contents

List of Tables

List of Figures

To my family

Chapter 1

Introduction

1.1 Wireless Sensor Networks

Wireless Sensor Networks (WSNs) are composed of number of small sensor nodes that can sense data from environment, process them locally and communicate with each other or base station through wireless links. The sensing, processing and communication capabilities of sensor nodes give ability to monitor and react the events in environment. The sensors provide low cost and low power wireless communication in short range. Since the communication range is limited, multi-hop communication systems are often adopted in most of the networks. A typical WSNs is shown in Figure 1.1.1.

In recent years, WSNs have gain great interest due to their wide usage area. For instance, WSNs have been employed in military, health care, structural health monitoring, home and agriculture applications [30, 36] - [8, 21, 62, 108] - [33, 99]. Military applications include intrusion detection, border surveillance, and target monitoring. Intrusion can be detected by using sensors which are able to sense motion and sound. In border surveillance systems, the illegal activities can be noticed with the help of WSNs. Vehicles and missiles can be monitored and controlled in target monitoring systems. In health care systems, patient can be remotely controlled by utilizing WSNs. In addition, structural health monitoring systems prevents any possible damage on buildings and bridges by detecting any change. Precision agriculture systems increase efficiency and productivity by monitoring the development of crop production. Furthermore, real time monitoring systems help farmers to be aware of emergency issues and make a decision [104].

WSNs have gained much more importance to provide efficient automation systems for industrial applications. Since, Industrial WSNs (IWSNs) offers flexible, low cost and easy installation compared to conventional wired systems [103]. IWSNs can be

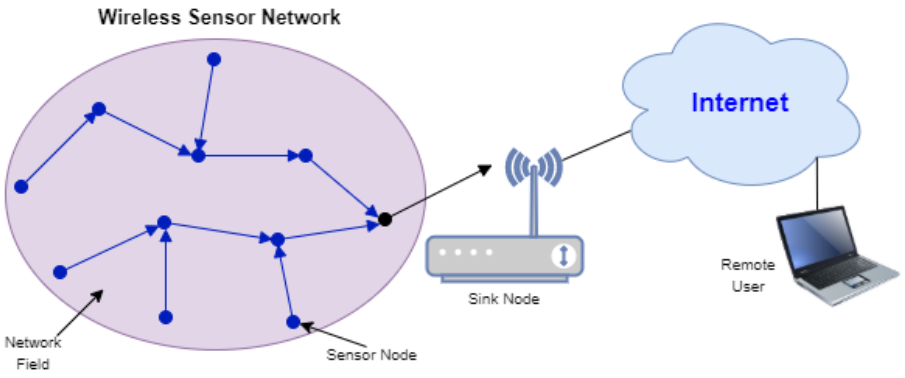

Figure 1.1.1. A typical wireless sensor networks

applied to variety of applications. These applications include some feedback systems, monitoring and controlling processes with covering a wide area of industrial aspects including automation systems. For instance, as to fulfill the operational requirements and making sure all the safety concerns are eradicated, industrial plants are provided with sensors making their performance potential at maximum level. Some conventional parameters such as conditions of equipment, outbreaks of fire, leakage of gas, humidity conditions, temperature parameters, pressure conditions and some others including flow are monitored. Sensors are operated in such a way that they present quick responses by making immediate decisions by analyzing plants performance and their circumstances. In addition, some applications have been developed to analyze historical sensor data and operational performance.

Figure 1.1.2 illustrates the wireless communication processes in IWSNs and its entities. The wireless communication system in IWSNs composes of three main parts namely, Inter-IWSNs, Beyond-IWSNs, displayers and servers [61]. In Inter-IWSNs, smart entities such as wireless sensors, mobile robots, machines etc. acquire and compute data from environment. In Beyond-IWSNs, access points and gateways are utilized as a bridge to other network such as Internet to relay the information. Finally, management systems get the information and use for controlling and making decision.

1.1.1 Industrial Wireless Sensor Network Applications

In this section, various key applications in which IWSNs are utilized such as industrial mobile robots, inventory management systems, equipment monitoring systems,

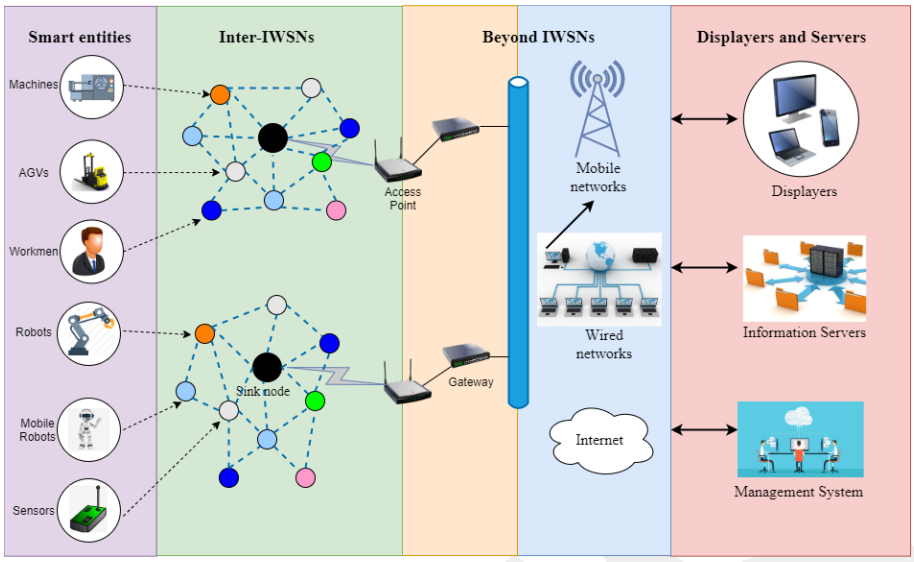

Figure 1.1.2. IWSNs schematic diagram

industrial process automation systems and environmental monitoring systems are presented.

1.1.1.1 Industrial Mobile Robots

With the help of industrial mobile robots, periodic data management is carried out in the industrial applications. Sensor nodes are used to notify faults occurring in operating systems due to error in processes regarding security and operating actions. The mobile robots visit sensor nodes in the plant area to gather data by avoiding obstacle and collision along the paths [102]. By periodically monitoring and controlling, the applications can minimize the cost of labors and cut down human error. Thus, the production downtime is minimized. Furthermore, re-calibration of sensor nodes is done by mobile robots which are attached with calibrated sensors.

1.1.1.2 Inventory Management System

The inventory management systems are used to avoid the scenarios such as out-of-stocks, manufacturing stoppages, increased in buffer inventory, and invoicing delays. By using WSN technology, it is possible to keep track of the inventory and asset all the time from the delivery of raw material to management decisions. For instance, General Motors is making use of the live inventory tracing tools [63]. This tool keeps track of the process which is starting from the supply of raw material to assembly of vehicles in the facility

and the purchase orders. By using the WSN with live inventory tracing, the supply chain efficiency can be greatly improved.

1.1.1.3 Equipment Monitoring and Process Automation

With the help of condition monitoring systems using WSNs, industries have ability to reduce the probability of malfunctions in equipment (*i.e.,* machine, motors etc.) [101]. The systems increase the efficiency and performance by detecting any undesirable change data (*i.e.,* pressure, temperature, vibration etc.) on machines. The advantages of WSNs condition monitoring systems over conventional wired systems are low cost and easy installations. Moreover, industrial automation systems provide to carry out the remote management used in the industrial tools and procedures by persistently analyzing time dependent manufacturing data including the range of temperature, pressure, level of humidity, vibration, and energy consumption [104].

1.1.1.4 Environment Monitoring

Environment monitoring systems involve leakage recognition, weather reports, radioactivity analysis, and external invasion messages identification. By using WSNs, the detection of anomalies including toxins, bio-toxins, radioactive agent or unwanted human intrusion could be detected anytime in the facility. Moreover, if there is any outflow of liquids and gases which could catch fire, the petrochemical facility may have to suffer many losses while putting people and personnel at risk and disrupting the climate. With the help of wireless sensors which are able to point out the leakage, the emergency response could be triggered as soon as possible to minimize the damage.

1.1.2 Industrial Standards

The IWSN applications require different standards compared to traditional WSN applications. Recently, several industrial alliances introduce the standards for IWSNs. In this section, a few standards, namely, Zigbee, WirelessHART and ISA100.11a suitable for IWSNs are briefly described.

1.1.2.1 Zigbee

This standard was initiated by ZigBee Alliance group who target building automation systems, industrial monitoring and controlling, and industrial automation systems. Zigbee is the wireless network protocol based on low data rate, low energy consumption, low cost [83]. Zigbee standards use the physical and MAC layer of IEEE 802.15. The higher layers are defined by Zigbee group. It also links UWB (802.15.3) to IEEE 802.4. It provides top communication data rate of 250 kbps with an range of 10–70 m. It also makes use of three band frequencies: 915 MHz (America), 868 MHz (Europe), and 2.4 GHz (Japan). Wireless Personal Area Network (WPAN) family are composed of ZigBee and Bluetooth. By comparing both, it has been found that there are differences in data rate, array and Quality of Service (QoS). It is established that ZigBee benefits from physical radio in comparison with standard IEEE 802.15.4. This allows to add up logic features and application tools. The recent ZigBee protocols are designed to support the beacon and non-beacon-enabled networks. An unslotted CSMA/CA technique is utilized in non-beacon-enabled networks. In this case, the ZigBee Routers keep the receivers in active mode which consume much power. This makes the heterogeneous networks to receive signal continuously while others transmit only the external stimulus is determined at the earliest. One useful example of a heterogeneous channel which is quite popular is wireless light switch. In this, the ZigBee node which is located at the lamp receives the signals persistently when it is joined to main supply.

1.1.2.2 WirelessHART

WirelessHART is linked with IEEE 802.15.4 physical layer. It comes with 2.4 GHz operation frequency while making use of 15 channels. The platform uses Time Synchronized Mesh Protocol (TSMP). TSMP utilizes the TDMA to carry out the process of channel access, channel hop and channel blacklist. All of these processes happen at the network layer. The channel hop is defined as the data transfer can be carried out at variable frequencies at variable time period. The WirelessHART standard makes use of 15 channels at variable times. Any channel which shows huge interference in the signal is backlisted. The interference and noise are alleviated by incorporating TDMA with channel hop and blacklists. WirelessHART provides redundant routing to increase reliability. Although

WirelessHART is robust, energy saving and reliable, many enhancements will be required to be done in it since it is in its early stages. WirelessHART was created, established, and standardized according to the industrial organizations in concern and supports the legacy systems made on the wired HART.

1.1.2.3 ISA100.11a

This standard was initiated by ISA100 working group to aid robust and reliable communication channels for process automation systems. With familiarity to wireless HART, it uses the physical layer of IEEE 802.15.4. They also use ISA100.11a which utilizes channel hop and blacklist to minimize the interference consequences. ISA100.11a has been incorporating various ways to carry out the channel hop like slow or rapid processing. Also at the level of data link layer, it links TDMA to CSMA to reap the benefits of outcomes. It has been known that the ISA100.11a's actual layer devices incorporates the IEEE 802.15.4-2006 hardware. It has been quite clear that the ISA100.11a incorporates 16 channels that work at a rate of 250 kbps. While operating, timing slots are divided into 10 to 12 ms. The compatibility with IPv6 provides users to link to the Internet at the network layer. The ISA standard supports communication with wiredHART and wirelessHART.

1.1.3 IWSN Challenges and Design Goals

The major design challenges of IWSNs are listed below. Table 1.1.1 presents the challenges and design goals for IWSNs.

1.1.3.1 Resource Constraints

The required resources to design and implement IWSNs such as energy, bandwidth, storage and processing are limited [38]. Due to battery-powered, sensor nodes face with limited energy problem. In the meantime, sensor nodes have limited computational capabilities because of their memory constraint. The limited bandwidth restricts the simultaneous data transmissions. Resource efficient design should be addressed, such as energy aware network and link layer be addressed.

1.1.3.2 Hazardous Environmental Conditions

The industrial environments have dynamic topology hence, the network connectivity may change because of sensor node and link failures. The topology may change dynamically because of mobility and sensor node failures. Motors and machines in industrial field may lead the harsh signal interference that result in signal loss. Moreover, vibrations and other environmental conditions such as high humidity and temperature, dirt and dust may affect the performance of sensor nodes in IWSNs. Adaptive network operation should be considered and adaptive communication protocols should be design for balancing the tradeoffs.

1.1.3.3 Quality of Services Requirements

The Quality of Services (QoS) vary for different type of IWSNs applications. QoS involves reliability, real time communication, longevity, privacy and security. To provide these requirements is very critical for IWSNs applications. For instance, in alarm notification systems, to sent information to controller on time is important. In addition, in monitoring system, collected data should be sent on time and reliably otherwise it is outdated and lead to wrong decisions. To meet all these requirements, a cross layer design which considers all layers, needs to be implemented [61]. In addition, application specific design should be considered.

1.1.3.4 Security

It is crucial to design and implement secure IWSNs by taking account of low cost hardware and energy efficiency. The possible attacks on the IWSNs are node controlling or tampering, denial of service, radio interference. The security attacks are categorized into two type, namely, passive attacks and active attacks, such that passive attackers monitor and listen to channel whereas active attackers both listen and change the data to be transmitted [56]. Low and high level security design should be addressed.

1.1.3.5 Packet Errors and Variable Link Capacity

Though IWSNs technology is advantageous by offering low cost, flexibility and easy deployment, posing some limitations and challenges because of harsh environment

Challenges	Design Goals
Resource Constraint Battery energy Limited memory Limited processing capabilities Bandwidth constraint	Resource efficient design Energy aware network (routing) layer Energy aware MAC layer Hardware optimizations (Sleep schedule algorithms)
Harsh channel conditions Varying topology and connectivity due to node failure	Adaptive network operation Adaptive signal processing algorithm and communication protocol design
QoS requirements Time sensitive Different IWSN application different QoS specification	Application specific design Adaptive and scalable time-synchronization protocol design Application specific design
Security External denial of attacks Intrusion	Secure design Trust control, secrecy, authentication, secure routing, intrusion detection, robust communication design
Variable link capacity Interference Noisy environment High error rate	Reliable design Error control and correction design
Limited lifetime Limited energy source	Energy efficient design Energy recovery and acquisition Energy harvesting methods

Table 1.1.1. Challenges versus design goals for IWSNs

conditions in industries. Interference due to high noise, multi-path distortion and radiations obstruction leads to high packet loss ratio. Besides, in the industrial environments radio propagation may suffer from machinery obstruction such as engine vibration and noise. Therefore, it is critical to achieve the maintenance of reliable data communications in IWSNs. The data transmission has to be safe and secure and must be transmitted on time as well. There might be issues in production and machinery if the data transfer is not carried out on time and in a safe manner. Error Control (EC) methos, namely, Forward Eror Correction (FEC), Automatic Repeat Request (ARQ) and Hybrid ARQ (HARQ) provide solutions to cope with unreliable data transmission.

1.1.3.6 Lifetime

Wireless communication provides a great advantage for industrial applications in terms of flexibility and low cost compared to wired systems. However, the energy given through battery to run the wireless sensors is a big challenge. It is required to ensure that power of a wireless sensor is consumed less and saved as well to enhance the battery lifetime. Since, battery replacement is a time consuming task and needs a lot of resources as well as cost to carry out the maintenance where many hundreds of wireless sensors are a

part of the facility. Therefore, it is critical to prolong the battery lifetime of wireless sensor nodes. A Energy Harvesting (EH) methods provide valuable solution to battery-powered sensor nodes. EH sensor nodes are capable of scavenging and storing the energy from the environment.

1.2 Contributions of This Thesis

The main contributions of this thesis can be grouped as follows:

i Survey of Energy Harvesting (EH) Methods for IWSNs and implementation of EH

- The EH methods that can be used for industrial environment are examined.
- The WSN applications with EH methods are comprehensively reviewed.
- The average power that can be scavenged from indoor solar, thermal and vibration is determined and properly applied to network lifetime analysis.

ii Reliability and Lifetime Analysis for IWSNs

- The lifetime of wireless multimedia sensor nodes which utilizes EH methods is analyzed. Moreover, the impact of EH methods such as indoor solar, thermal and vibration on sensor node lifetime is evaluated.
- To what extent compressing the image before transmitting affects the sensor node lifetime in industrial environment is investigated.
- The effect of different duty cycle requirements of applications using schedule-driven power management scheme on sensor node lifetime is examined.
- The impact of exploiting EC schemes, such as ARQ, FEC (*i.e.,* BCH(31,11,5), BCH(31,21,5), RS(15,11,5)) and HARQ (*i.e.,* HARQ-I, HARQ-II) on IWSNs lifetime is investigated while meeting desired application reliability. The performance evaluations have been conducted based on the power consumption characteristics of Mica2 and Telos motes.
- The contributions of EH methods on IWSN lifetime are evaluated.

- The realistic channel model which is log normal shadowing model is used to better performs the path loss characteristics and error rates on the industrial propagation environments. The different topographies for industrial environment are analyzed.
- The novel Mixed Integer Programming (MIP) with network-level EC scheme approach (*i.e.,* all sensor nodes adopt the same type of EC scheme) and node-level EC scheme approach (*i.e.,* each node adopts different type of EC scheme which is optimum one) are formulated with the objective of maximizing network lifetime by jointly considering realistic channel, energy dissipation models of the EC schemes and EH methods. The performances of MIP with network-level EC scheme approach and MIP with node-level EC scheme approach are quantitatively compared.
- The network lifetime with different data types, namely, scalar and image communication is analyzed. To this respect, MIP model is extended with energy dissipation of Compressive Sensing (CS) and image compression methods. The impacts of utilizing CS, image compression and EH methods on network lifetime is examined. For a realistic assessment, the performance evaluations have been conducted by considering acquisition, computation and communication energy dissipation of real-world WMSNs.

iii Meta-heuristic Methods Analysis

- Several meta-heuristic methods such as Golden Section Search (GSS), Extended GSS (EGSS), Simulated Annealing (SA), Extended SA (ESA) and Genetic Algorithm (GA) are applied to our MIP problem to get near-optimal solutions within a reasonable amount of time. Their solution performance and time complexity analysis are investigated.

1.3 Thesis Outline

This thesis is organized as follows. In Chapter 2, we provide comprehensive review of Energy Harvesting (EH) methods (*i.e.,* indoor solar, thermal and vibration) that are utilized for Industrial Wireless Sensor Network (IWSN) applications. In Chapter 3, we specify the system models that are used throughout the thesis. The channel model for industrial environment and Error Control (EC) schemes and the energy dissipation of them are explained. In Chapter 4, we examine the lifetime of EH multimedia sensor nodes in industrial environment. In Chapter 5, we analyze the effect of EC schemes on EH wireless sensor networks lifetime for industrial environment. We develop MIP model with network-level EC scheme approach to maximize the network lifetime. In Chapter 6, we investigate the effect of Compressive Sensing (CS) and image compression methods on EH wireless multimedia sensor networks. We develop MIP with node-level EC scheme approach for network lifetime maximization. In Chapter 7, we provide meta-heuristic methods (*i.e.,* Golden Section Search (GSS), Extended GSS (EGSS), Simulated Annealing (SA), Extended SA (ESA) and Genetic Algorithm (GA)) to jointly improve lifetime and reliability. Finally, in Chapter 8, we draw conclusion of the thesis.

Chapter 2

Energy Harvesting Methods for Industrial Wireless Sensor Networks

Industrial WSN applications include hundreds of battery-powered sensor nodes which spread over wide area. Due to battery-powered sensor nodes, the network lifetime for industrial applications is limited. To replace or recharge the exhausted battery is very challenging and costly especially when nodes are inaccessible. Recently, renewable energy harvesting technologies have gained great interest to power wireless sensor node with rechargeable batteries.

A typical EH sensor is shown in Figure 2.0.3. The harvesters generate electric energy from ambient sources. The generated energy has great potential to power sensor node. The common renewable energy sources for industrial environment are solar, thermal and vibration. The analysis of advantages and disadvantages of available energy sources for industrial environment are presented in Table 2.0.2.

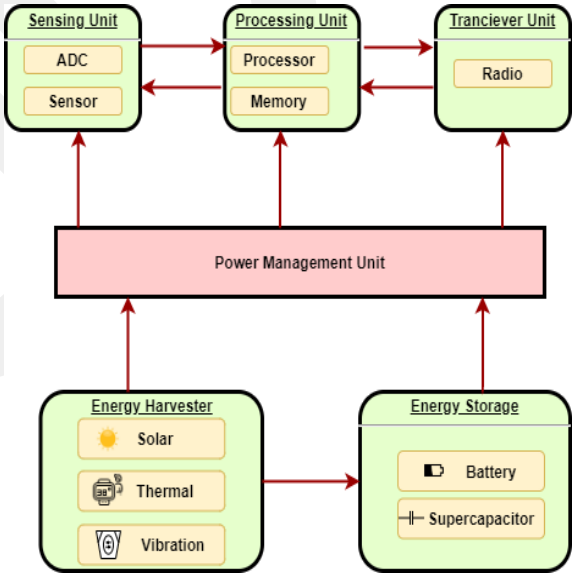

Figure 2.0.3. The units of energy harvesting sensor node

In the following sub section, we explain EH methods (*i.e., solar, thermal and*

Source	Type	Characteristics	Advantages	Disadvantages
Light	**Solar**	Uncontrollable, Predictable	High output voltage; Renewable, inexhaustible, green energy source; Highly efficient energy conversion.	Not always available, affected by weather, regions; Sensitive structure, deployment constraint; With high cost and pollution.
	Artificial	Partly controllable,Predictable	Abundant in indoor; Easy to implement.	Low power density; Sensitive structure.
Heat	**Thermal**	Uncontrollable, Unpredictable	Low maintenance, scalable; High durability, precision, small volume; Safety and reliability.	Not always available; Low power density; Low conversion efficiency.
Motion	**Vibration**	Controllable, Partly predictable	Higher power density, high output voltage; Compact and simple architectures; Scalable;	Weak device structure; Work at a low and narrow frequency band; Manufacturing complexity.

Table 2.0.2. Comparison of energy sources for IWSNs

vibration used in industrial environments. Table 2.4.5 provides the review of studies that use EH methods for WSNs.

2.1 Solar Energy Harvesting System

Sun is a renewable and efficient energy sources for industrial applications however it is time varying and unstable [101]. The solar energy harvesting is a method that converts harvested solar energy into electrical energy. Photovoltaic cells are used to gather the sunlight or artificial light energy and generate the electricity. The important characteristic of Photovoltaic (PV) cells is current-voltage curve where the current is obtained by [102]

$$I_{PV} = I_L - I_0 exp(\frac{V_{PV} + I_{PV} \times R_s}{n_s \times V_t}) - 1. \tag{2.1}$$

In (2.1), I_L is the current generated by light (A), I_0 is the reverse saturation current of the p-n diodes, , R_s refers the cell resistance (Ω) and V_t is cell voltage. The voltage is obtained by

$$V_t = \frac{kT_c}{q}, \tag{2.2}$$

where k denotes the Boltzmann's constant, T_c refers to the cell temperature (K), and q is the electron charge. The maximum harvested power is estimated as

$$P = V_{PV} I_L - V_{PV} I_0 [exp(\frac{V_{PV}}{n_s k T_c / q})]. \tag{2.3}$$

2.1.1 Applications

There are two types of light EH system namely, solar and artificial lights. Solar energy harvesting is great solution for sensor nodes with limited energy where used in outdoor industrial environments. There exist many studies [46, 58, 60] that use solar energy harvesting method to extend the lifetime of network. In [60], they introduced study that prolongs the industrial network lifetime by combining solar energy harvester and sleep schedule algorithm. For saving energy, some non-harvesting nodes turn into sleep state when harvester nodes scavenge more energy. In [58], they proposed the renewable energy system which utilizes the solar energy harvesting for the multimedia communication. They searched new approaches that optimize the EH wireless multimedia sensor networks. In [46], they developed solar energy harvesting mechanism for industrial wireless sensors. Mihajlovic et al. [68] proposed the solar EH system for water surface monitoring application. They designed solar EH system by using 6L7020-A20 solar cell and use super capacitor as an energy storage device. Their experimental results show that they can harvest power up to 0.3 W. Sharma et al. [93] utilize the solar EH system to maximize the network lifetime for agriculture monitoring applications. Using solar EH system increases network lifetime up to 115.75 days.

Additionally, ambient energy from artificial lights is used for indoor industrial environments [13, 19, 44, 74, 77, 82]. The artificial lights are controllable, however provide less energy compared to solar energy source. Carval et al. [19] discussed the availability of indoor solar EH. The amount of power harvested from light is presented. In a worst case scenario, they obtained 11.51 μW power from indoor light. Huang et. al [44] examined the feasibility of use of indoor solar harvesting system in WSN. They analyzed the amount of harvested power from different light irradiance. The results confirmed that the feasibility of harvesting light energy to power wireless sensor nodes. Nasiri et al. [74] argued that the use of PV cells to supply extra power for sensor nodes. They have tested the various light illumination levels. In addition, they have evaluated the energy storage options such as battery and capacitors. Pubill et al. [82] presented the harvested power from artificial light. Berger et al. [13] investigated whether the indoor light harvesting system can be practically applied or not in wireless sensor nodes. They have proved that it enables to power sensor nodes in real industrial environment with

$4W/m^2$ irradiance. Othman et al. [77] presented the design of indoor light harvesting system and their elements such as photovoltaic panel, circuit and energy storage items. Toh et. al [106] introduced Flexible EH (FEH) systems for monitoring human body health. To power wearable sensor nodes, super-capacitor stores the energy generated from indoor lights. According to experimental results that they conducted, 56 μW energy can be generated from 320 lux light intensity. Decker et. al [23] developed the indoor and outdoor energy harvesting system and examined the feasibility for autonomous field devices. Simulation results show that 2 W and 0.16 W power can be generated in indoor and outdoor EH systems, respectively. Eidaks et al. [26] presented hybrid energy harvester which integrates the indoor solar and Radio Frequency (RF) energy sources. Solar energy harvester provides 164 μW power whereas RF energy harvester provides 26 μW power on average. Aoki et al. [11] constructed and analyzed the Organic Photovoltaic (OPV) cell. They have compared OPV with traditional amorphous silicon solar cells (a-Si). The experimental results show that the harvested power is 43.4 $\mu W\ cm^{-2}$ and 28.5 $\mu W\ cm^{-2}$ for OPV and a-Si, respectively. Rasheduzzaman et. al [84] designed a energy harvesting autonomous wireless sensor node. They have compared the six different solar cell. They achieved 77.40 μW generated power by using Dye-sensitized solar cells (DSSC). For energy storage devices they utilized 3.0 V Magnesium Lithium rechargeable battery and 2000 uF capacitor.

2.2 Thermal Energy Harvesting System

Thermoelectric generator harvests energy from difference of temperature by utilizing Seebeck effects [107]. In other words, it produces the voltage from temperature difference between electrical conductors. The voltage of open-circuit (V_{oc}) is given by

$$V_{oc} = S * \Delta T = n * \alpha(T_H - T_C), \tag{2.4}$$

where S is the Seebeck's coefficient of TEG and α is the thermocouples. n is the number of thermocouples in TEG. T_H represents high temperature and T_C represents low temperature..

The current is obtained by

$$I_{TEG} = \frac{V_{oc} - V_{TEG}}{R_{s,TEG}}, \tag{2.5}$$

where $R_{s,TEG}$ denotes the TEG internal resistance. The average power harvested from TEG is calculated as:

$$P_{TEG} = V_{TEG} I_{TEG} = \frac{V_{TEG} n\alpha(T_H - T_C) - V_{TEG}^2}{R_{s,TEG}}. \tag{2.6}$$

2.2.1 Applications

Thermal energy harvesters can be used in industrial applications to extend lifetime. Hou et al. [42] designed thermal energy harvesting system to power industrial devices. They have evaluated the feasibility of thermal energy harvester. They have extended the previous work [43] to propose TEG system and investigate whether it can power sensor node which is used for monitoring the Industrial Internet of Things (IIoT). They utilized the two TGM287-1.0-1.3 module for energy conversion since one is not enough to supply energy for a sensor node. The results showed that the sensor node can be powered when the sleep time exceeds 16s. Allmen et al.[9] introduced the thermal energy harvesting system for aircraft strain monitoring. The thermal harvester utilizes the temperature difference of takeoff and landing to generate the power. Meng et al. [67] introduced the practical TEG system model utilizing automobile exhaust heat sources.

Guan et al. [37] introduced and investigated thermal EH system for wireless sensor nodes. BQ25504 converter is utilized. The experimental results show that the efficiency of thermal EH system is between 72.1 and 86.8 $\%$. 62–400 mV TEG voltage is achieved. Abdal et. al [3] presented thermal energy harvesting method to prolong the WSNs lifetime. The have used the Peltier devices for thermoelectric circuit which generates voltage up to 5V where there is at least 30 ° C gradient. They showed that the electrical power harvested form mechanical machinery heat difference can supply intermittent energy to wireless sensor nodes. In addition, they have surveyed the amount of power harvested from low level heat sources.

Additionally, thermal harvesters can be used in wireless body area sensor network applications. Thielen et al. [105] examined the feasibility and efficiency of utilizing

wearable thermal energy harvesting for human body. They conducted simulation and experimental study to investigate the usage of thermal energy harvester for human wrist. The experimental results showed that the harvested power reaches 280 μW on the average while 800 μW in outdoor activity scenario. Wahbah et al. [112] investigated the thermal and vibration based energy harvester for human body wearable devices. They have utilized off-the-shelf TEG and PE harvester. The experimental study showed that TEG generates up to 20 μW power whereas Piezoelectric (PE) harvester generates up to 3.7 μW . Kim et al. [54, 55] depicted and tested the TEG for human clothes and human body. The fabricated TEG harvests 224 nW power when it is worn it can generate 146.8 nW. They showed practicality of thermal energy harvester to power wireless sensor nodes. They have designed the flexible TEG (f-TEG) which is usable and scalable. Leonov et. al [59] studied on thermal energy harvesting system for wearable sensors. They did experiment in different ambient condition by placing sensors on garments or a person. 5 and 0.5 mW power are generated from 15 ° C and 27 ° C, respectively. Verma et al. [109] presented heat harvesting systems for environmental monitoring applications. They designed TEG by utilizing a Bi2Te3. They evaluated the measured data and show that 64 mW power can be harvested. Chottirapong et al. [22] utilized thermal and solar energy harvesting for organic fertilizer plant application. The source of heat is obtained by deodorizer tank for thermal energy harvester in that application. The experimental results show that the total harvested power from thermal and solar reaches up to 290mW.

2.3 Vibration Energy Harvesting System

Utilizing vibration energy harvester for powering sensors in industrial applications where the source of mechanical energy comes from machine vibrations is great interest. The electricity is harvested from mechanical energy by utilizing piezoelectricity [102]. The average harvested power is calculated as:

$$\mid P \mid = \frac{m\zeta_e A^2}{4\omega\zeta_T^2}, \tag{2.7}$$

where m is the proof mass, ω is the frequency and A is the acceleration amplitude. ζ_e is the electrical damping ratio and ζ_T is the combined electrical and mechanical damping ratio (*i.e.,* $\zeta_T = \zeta_e + \zeta_m$).

2.3.1 Applications

There are several studies that works on piezoelectric energy harvester for IWSNs [78, 86, 88]. Panthongsy et al. [78] proposed piezoelectric EH system to extend the WSNs lifetime. They have utilized the machine vibrations to generate electrical power. The resonant type piezoelectric is used foe energy harvester. They have showed that the proposed harvester supply power up to 82.29 μW which is usable for sensor nodes. Ren et al. [86] proposed electromagnetic vibration energy harvester for industrial application which includes planar spring, annular magnetic circuit and planar spring. The proposed vibration energy harvester can scavenge 10 mW power to sensor node. Sankman et al. [88] presented a solution for time varying (*i.e.,* unpredictable) vibration energy harvester. The harvester is designed considering vibration amplitude instead of frequencies. With the help of online adaptive impedance controller, the maximum power can be obtained regardless of changing vibrations. The authors proved that the adaptive impedance matching technique enhance the lifetime of WSNs. Akbar et al. [6] introduced piezoelectric energy harvester for aircraft design. They have designed and evaluated dynamic response of piezoelectric energy harvesters and obtained power of 25.24 kW. Petrini et al. [79] evaluated the vibration energy harvesters using to power sensor node for Heating Ventilation and Air Conditioning (HVAC) ducts. The vibration that is occured because of air flow in HVAC ducts is used as power sources. The maximum power harvested is between 200 and 400 μW for sensor nodes.

Vibration energy harvester can be used also in other WSN applications such as agriculture and intrusion detection applications. Dondi et al. [24] developed vibration energy harvester (VIBester) to provide energy for agriculture application. They introduced the application utilizes WSNs to monitor and control the trailer. Therefore, the application notifies the driver if there is any unacceptable changes in trailer conditions. The power harvested from VIBester is about 850 μW. Kassan et al. [53] introduced the vibration based energy harvesting model for WSNs applications. Switching mode is adjusted by

using controller unit.

Dong et al. [25] introduced vibration-threshold-triggered energy harvesters (VTT-EHs) to intrusion detection algorithm. They proved that the proposed harvesting system is sufficient for powering sensor odes. Wang et al. [113] designed and evaluated the piezoelectric devices for pavement applications. Modified polypropylene and aluminum plates are used in design of harvesting devices. They accomplished 50.41 mW power by using 15cm x 15cm device. Finally, Roshani et al. [87] examined the feasibility of piezoelectric device usage for EH in pavement.

2.4 Energy Storage

Since the applicability of powering sensor nodes directly from harvesters is difficult task, energy storage element are utilized. Rechargeable batteries are utilized as energy store devices for energy harvesting wireless sensors. For instance, Alkaline, Nickel-Metal hydride (Ni-MH), Lithium-ion (Li-Ion), or Lithium iron disulfide (Li-FeS2) batteries are used to power wireless sensor nodes. Li-FeS2 batteries has higher capacity and longer lifetime than alkaline batteries. The Li-Ion batteries which is rechargeable introduced in the early 2000s and enhanced the battery capacity and the network lifetime. However, the batteries still need to be changed after 1 or 2 years due to limited number of recharge cycles [97]. On the other hands, super-capacitors are utilized to store the energy for sensor nodes. Unlike rechargeable batteries, super-capacitors provide much more higher recharge cycle and efficiency. Therefore, they offer to longer lifetime than rechargeable batteries. However, the self discharge rate is high compared to batteries.

2.4.1 Super Capacitor

Super-capacitors accomplish higher capacitance by having larger surface area and thinner dielectrics than conventional capacitors. With this feature, it also achieve better power and energy densities. Super-capacitors charge and discharge quickly compared to regular capacitor. Practically super-capacitors have infinite life cycle [92]. The comparison

Capacitor	Capacitance (F)	Voltage (V)	Temperature (° C)	Diameter (mm)	Length (mm)
Panasonic	4.7	2.5	-25 to + 60	10	20
Nichicon	4.7	2.7	−25 to + 70	10	20
Elna	1	2.5	−25 to + 70	8	22
Maxwell	5	2.7	−40 to + 65	10	20

Table 2.4.3. Comparison of supercapacitors

of existing super-capacitors is given in Table 2.4.3 [5].

2.4.2 Rechargeable Batteries

Rechargeable batteries are utilized as an energy storage devices for wireless sensor nodes. Nickel-Metal Hydride (NiMH), Lithium Ion (Li-Ion), and Lithium Ion Polymer (LiPo) are the example of commonly used rechargeable batteries. The comparison of these rechargeable batteries is presented in Table 2.4.4 [5]. Lithium rechargeable batteries supply higher voltage and charging cycle. However, NiMH has higher capacity compared to the others. NiMH batteries can be charged directly from ambient energy sources whereas lithium batteries can be charged from primary buffer.

Battery Type	Voltage (V)	Capacity(mAh)	Energy (Wh)	Cycle
NiMH	1.25	2500	3.0	300-500
Li-Ion	3.6	730	2.7	500-1000
LiPo	3.6	930	3.4	300-500

Table 2.4.4. Comparison of rechargeable batteries

Table 2.4.5. Summary of energy harvesting applications

Source	Paper	Year	Power / Voltage	Testing Environment	Harvester Hardware	Node Hardware	Energy Storage	Application
Solar	[60]	2016	N/A	Simulation	N/A	N/A	N/A	Industrial WSNs
	[58]	2013	N/A	Simulation	N/A	N/A	N/A	Parking lot surveillance
	[23]	2013	0.16 W	Simulation	a-Si:H solar panel (4 x 4 cm^2)	N/A	LiSOCl2	Autonomous field devices
	[46]	2017	7.88 W	Simulation	N/A	N/A	Li-Po	WirelessHART sensor node
	[68]	2015	0.3 W	Experimental	6L7020-A20 solar cell	MSP430G2553	0.47F SuperCapacitor	Surface water monitoring
	[93]	2019	N/A	Simulation	N/A	MICAz	NiCd/NiMH	Smart agriculture monitoring
Indoor Solar	[23]	2013	2 W	Simulation	a-Si:H solar panel (20 x 20 cm^2)	N/A	LiSOCl2	Autonomous field devices
	[19]	2014	11.51 μW	Simulation	N/A	N/A	N/A	WSN
	[106]	2014	56 μW	Experimental	Sundance Solar MPT3.6−75 flexible PV panel	TI eZ430-RF2500T	Super capacitor	Health monitoring
	[74]	2009	380 μW	Simulation	N/A	N/A	NiMH	Low-Power Applications
	[84]	2016	77.40 $\mu W/cm^2$	Experimental	Dye-sensitized solar cells (DSSC)	Texas Instruments BQ25504	3.0 V Magnesium Lithium & capacitor	Indoor autonomous wireless sensor
	[82]	2018	N/A	Experimental	MP3-25 photovoltaic cell	Zolertia Z1	3V coin	Internet of Things (IoT) scenarios
	[13]	2015	112 μW	Simulation	SLMD 121 H06L solar cell	nRF51822	N/A	Indoor industrial applications
	[77]	2018	N/A	Experimental	Monocrystalline photovoltaic cell	N/A	Ni-MH	Internet Of Things application
	[26]	2018	164 μW	Experimental	EZ430-RF2500-SEH	MSP430F2274	capacitor	Indoor WSN
	[11]	2017	118.8 μW	Experimental	Organic photovoltaic (OPV)	EnOcean STM 431J	N/A	Indoor WSN
Thermal	[43]	2017	3.6 mW	Experimental	TGM287-1.0-1.3	Jennic JN5139	N/A	Industrial Internet of Things
	[55]	2018	272 mW	Experimental	f-TEG	LoRa Module	Li-Po	WSN
	[37]	2017	N/A	Experimental	F40550 / Xinghe Electronics	N/A	Li-Ion / LIR2032, OAHE Co.	WSN
	[105]	2017	280 μW	Simulation/Experimental	(Micropelt TPG-651/Quick-cool QC32-0.6-1.2	N/A	Li-Ion	Human body application
	[3]	2017	5 V	Experimental	Hanna (HI 93552R) KJT-Thermocopule	ATmega328P	7.4V lithium polymer	WSN
	[59]	2013	0.5-5 mW	Experimental	BiTe thermocouples	N/A	Alkaline battery	Wearable wireless sensors
	[112]	2014	20 μW	Experimental	(G230–0313) / Tellurex	N/A	N/A	Human body application
	[54]	2014	146.9	Experimental	Bi0.5Sb1.5Te3 (p-type),Bi2Se0.3Te2.7 (n-type)	N/A	N/A	Human body application
	[67]	2016	98.3 mW	Simulation	p-type /n-type	N/A	N/A	Automobile exhaust waste heat recovery
	[109]	2018	64 mW	Experimental	TEC1-12706 TE coolers	TPS61220	Li-ion	Environmental monitoring applications
	[22]	2015	290 mW	Experimental	TEC1–12706	MSP430G2231	super capacitor /Li-ion	Organic fertilizer plant
Vibration	[86]	2016	10 mW	Experimental	N/A	N/A	N/A	Industrial wireless sensor networks
	[78]	2015	82.29 μW	Experimental	PSI-5A4E piezoelectric cantilever	N/A	capacitor	Machine vibrations wsn
	[88]	2014	80 μW	Experimental	MIDE v25w piezoelectric cantilever	N/A	capacitor/NiMH or Li-Ion	Industrial applications
	[12]	2014	5.1 V	Experimental	N/A	MicaZ	AA batteries	Agriculture
	[24]	2012	845 μW	Experimental	N/A	MSP430	Li-ion	Safety of machinery with trailer
	[53]	2019	N/A	Simulation	N/A	Mica2	N/A	WSN
	[6]	2016	25.24 kW	Simulation	Bimorph piezoelectric / PZT-5A	N/A	N/A	Aircraft wingbox structure
	[79]	2017	200 - 400 μW	Experimental	PI Ceramic P-876K015 DuraAct Patch	N/A	N/A	Smart buildings/HVAC ducts
	[25]	2019	23.43 - 183.27 μW	Experimental	N/A	CC1110	capacitor	Identifying intrusion activities
	[113]	2018	50.41 mW	Experimental	N/A	N/A	N/A	Pavement applications
	[87]	2016	N/A	Experimental	N/A	N/A	capacitor	Pavement roadways
	[120]	2016	3.106 mW	Experimental	lead-zirconate-titanate (PZT)	N/A	N/A	Public roadway

Chapter 3

System model

3.1 Channel Model

By virtue of harsh industrial environment effects, signal may be diffracted, reflected and scattered along the propagation. Therefore, to determine path loss due to weakening signal, the log-normal shadowing model is adopted in this thesis [127].

According to the this model, the path loss, $PL_{ij}(d)$, over link-(i,j) (**i.e.,** between node i and node j) is given by

$$PL_{ij}(d) = PL(d_0) + 10n \log_{10}\left(\frac{d_{ij}}{d_0}\right) + X_\sigma, \tag{3.1}$$

where d_{ij} denotes the distance over link-(i,j). n denotes the path loss exponent. X_σ is a zero-mean random variable (in dB) with standard deviation, σ. $PL(d_0)$ is the path loss at reference distance, d_0 (in dB). The signal-to-noise ratio (SNR) over link-(i,j) is given by

$$\gamma_{ij} = P_t - PL_{ij}(d_{ij}) - P_n, \tag{3.2}$$

where P_t and P_n are the output power and the noise floor, respectively. Bit Error Rate (BER) is determined according to the modulation schemes of motes. Mica2 and Telos are implemented with FSK and O-QPSK, respectively [111]. For Mica2, the BER is given by

$$P_{b,ij}^{FSK} = \frac{1}{2} exp^{-\frac{E_b/N_0}{2}}, \tag{3.3}$$

where

$$E_b/N_0 = \gamma \frac{B_N}{R}, \tag{3.4}$$

where γ_{ij} is the received SNR, B_N is the noise bandwidth, and R is the data rate. The

probability of successfully transmitting a packet from node i to node j, p_{ij}^s, is given by [7]

$$p_{ij}^s(q) = (1 - \frac{1}{2} exp^{-\frac{\gamma_{ij}}{2}\frac{1}{0.64}})^{8q}, \tag{3.5}$$

where q refers to size of packet (in bits). For Telos, the BER is given by

$$P_{b,ij}^{O-QPSK} = Q(\sqrt{(E_b/N_0)_{DS}}), \tag{3.6}$$

where

$$(E_b/N_0)_{DS} = \frac{2NE_b/N_0}{N + 4E_b/N_0(K-1)/3}. \tag{3.7}$$

In Eq.(3.7), N is the number of chips per bit and K is the number of simultaneous users. The packet success rate over link-(ij), p_{ij}^s, is given by

$$p_{ij}^s(q) = (1 - Q(\sqrt{(E_b/N_0)_{DS}}))^{8q}. \tag{3.8}$$

For ARQ, the Packet Error Rate (PER) is given by

$$PER_{ij}^{ARQ}(q) = 1 - p_{ij}^s(q). \tag{3.9}$$

For FEC, the Block Error Rate (BLER) is shown by

$$BLER_{ij}(n,k,t) = \sum_{l=t+1}^{n} \binom{n}{l} P_{b,ij}^l (1 - P_{b,ij})^{n-l}, \tag{3.10}$$

where n refers to the block length, k refers to length of payload and t refers to the capability of error correction. Therefore, PER for FEC is given by

$$PER^{FEC}(q,n,k,t) = 1 - (1 - BLER(n,k,t))^{\lceil \frac{q}{k} \rceil}, \tag{3.11}$$

where $\lceil \frac{q}{k} \rceil$ is the number of blocks that is needed to transmit packet with q bits.

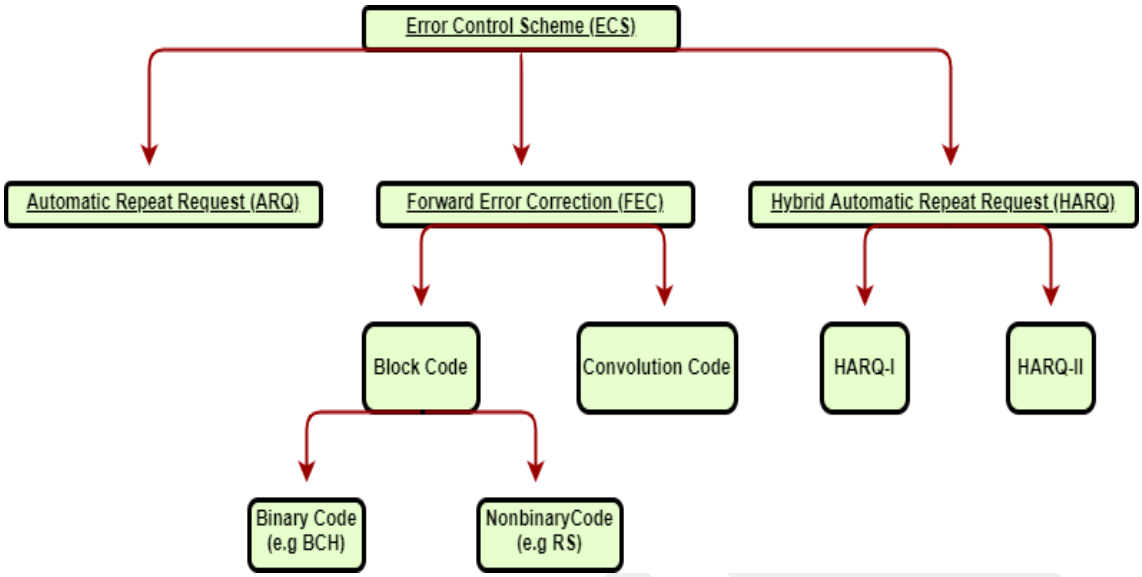

Figure 3.2.4. A classification of error control scheme

3.2 Error Control Schemes

In literature, different types of Error Control (EC) schemes, namely, Automatic Repeat Request (ARQ), Forward Error Correction (FEC) and Hybrid Automatic Repeat Request (HARQ) are introduced. Figure 3.2.4 presents the classification of EC schemes for WSNs.

3.2.1 Automatic Repeat Request (ARQ)

ARQ is one of the EC system that utilizes retransmission to achieve reliable data transmission. In ARQ, retransmission of data packets occurs if the receiver detects any error on the packets or the data packets are not received. The error can be detected by receiver by utilizing error detection algorithms. Parity checking and Cyclic Redundancy Check (CRC) are example of error detection algorithms that receiver uses. If error is detected, receiver sends Negative Acknowledgement (NACK) packet to transmitter. After received NACK packet, transmitter resends the packet. The retransmission also occurs if ACK packet does not received by transmitter within in predefined time [51]. The general representation of ARQ process is shown in Figure 3.2.5.

On the other hand, the disadvantage of ARQ schemes are energy costly and delay

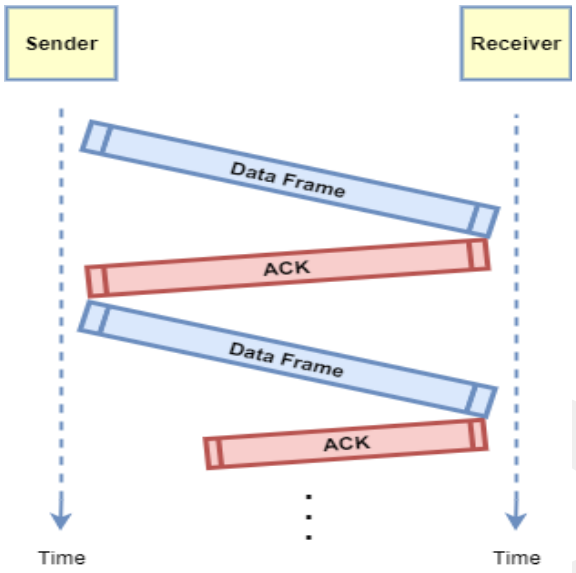

Figure 3.2.5. The representation of ARQ scheme

sensitive due to retransmission especially in harsh channel conditions and in long range communication. The communication energy cost includes energy consumed in transmission and reception phase.

For ARQ, the transmission energy cost over link-(i,j) is given by

$$E_{tx,ij}^{ARQ} = E_{enc} + n_{ret,ij}^{ARQ}\{(E_{tx}(L_P) + E_{rx}(L_A)) + E_{to}\}. \tag{3.12}$$

The reception energy cost over link-(i,j) is given by

$$E_{rx}^{ARQ} = n_{ret,ij}^{ARQ} \times (E_{rx}(L_P) + E_{tx}(L_A)), \tag{3.13}$$

L_P and L_A denote the length of data packets in bits, respectively. $E_{tx}(q)$ and $E_{rx}(q)$, are energy cost to transmit and receive q bits data and calculated as:

$$\begin{aligned} E_{tx}(q) &= E_{elec} \times q + P_{tx}(\frac{q}{R}) \\ E_{rx}(q) &= E_{elec} \times q + P_{rx}(\frac{q}{R}), \end{aligned} \tag{3.14}$$

where R and E_{elec} stand for the data rate and energy cost of transmitter electronics, respectively. E_{to} is the time until propagation of signal (T_{pd}) plus waiting for ACK packet (*i.e.,* guard time (T_{grd})).

$$E_{to} = P_{std} \times (T_{pd} + T_{grd}) \tag{3.15}$$

where P_{std} is the standby power. In order to say a successful communication data packet must be received by receiver and ACK packet must be received by transmitter. Therefore, the number of retransmission is given by

$$n_{ret,ij} = [p^s_{ij}(L_P) \times p^s_{ji}(L_A)]^{-1}. \tag{3.16}$$

The probability of successful packet transmission ($p^s_{ij}(q)$) is expressed in Section 3.1 Equation 3.5. The packet success rate over link-(i,j) (ϕ_{ij}) after the retransmission is expressed as [90]:

$$\phi_{ij} = 1 - [1 - [p^s_{ij}(L_P) \times p^s_{ji}(L_A)]]^{(n_{ret,ij}+1)}. \tag{3.17}$$

The time for transmitting L_P bits and waiting ACK packet is given by

$$T^{ARQ}_{tx,ij} = \frac{L_P}{R} + T_{pd} + T_{grd}. \tag{3.18}$$

The time for receiving L_P bits is given by

$$T^{ARQ}_{rx,ij} = \frac{L_P}{R}. \tag{3.19}$$

3.2.2 Forward Error Correction (FEC)

In FEC, transmitter adds redundancy bits to data packet so that receiver can detect and correct the errors on packet. Hence, no more retransmision is needed in that scheme. The retransmission cost eliminated however, encoding and decoding a packet cost and extra bits transmission cost emerge for FEC schemes. FEC scheme is advantageous in noisy channel environment because it avoid many retransmissions [32].

Block codes and convolution codes are the two types of FEC schemes defined in literature. In block code, data packets are divided into blocks with fixed length to be transmitted. Transmitter encode each block with codewords. Typically, block code is represented by three number (n,k,t) in which n is block length in bits, k is the information bits and t is the error correction capability. Figure 3.2.6 shows the structure of a block code. Bose-Chaudhuri-Hocquenghem (BCH) and Reed-Solomon (RS) are the example of

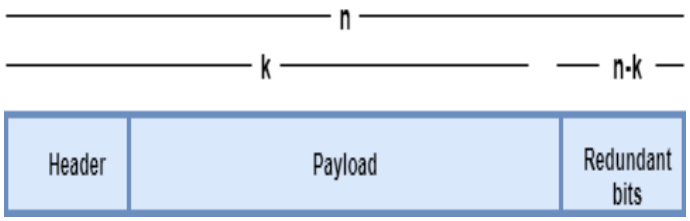

Figure 3.2.6. A structure of FEC block code

block codes. Convolution code is denoted by three numbers (n,k,L) in which n is output bits, k is the input (*i.e.,* information) bits and L is the total memory of encoder. Time delay is the smallest in convolution codes since it decodes data as soon as received. In this study, we consider the block codes,namely, BCH and RS.

For FEC, the transmission energy cost over link-(i,j) is given by

$$E_{tx,ij}^{FEC} = E_{enc} + E_{tx}(L_P). \tag{3.20}$$

The reception energy cost over link-(i,j) is given by

$$E_{rx,ij}^{FEC} = (E_{rx}(L_P) + E_{dec}(L_P)). \tag{3.21}$$

The energy needed for decoding data ($E_{dec}(L_P)$) is given by

$$E_{dec}(L_P) = P_{proc} T_{dec}(L_P), \tag{3.22}$$

where P_{proc} is the processing power . E_{enc} is the encoding energy which is negligible.

3.2.3 Hybrid Automatic Repeat Request (HARQ)

Hybrid Automatic Repeat Request (HARQ) takes advantages of both ARQ and FEC schemes. ARQ is better for good channel conditions whereas FEC is better for bad channel conditions [51]. In HARQ-I, uncoded packet is transmitted to receiver, if any error is detected, transmitter retransmits coded data so that receiver can correct the error. In HARQ-II, uncoded packet is transmitted to the receiver, if receiver detects any error, only the redundant bits are retransmitted so that receiver can correct the errors. HARQ-II needs storage elements to store earlier received packet. The representation of HARQ-I and

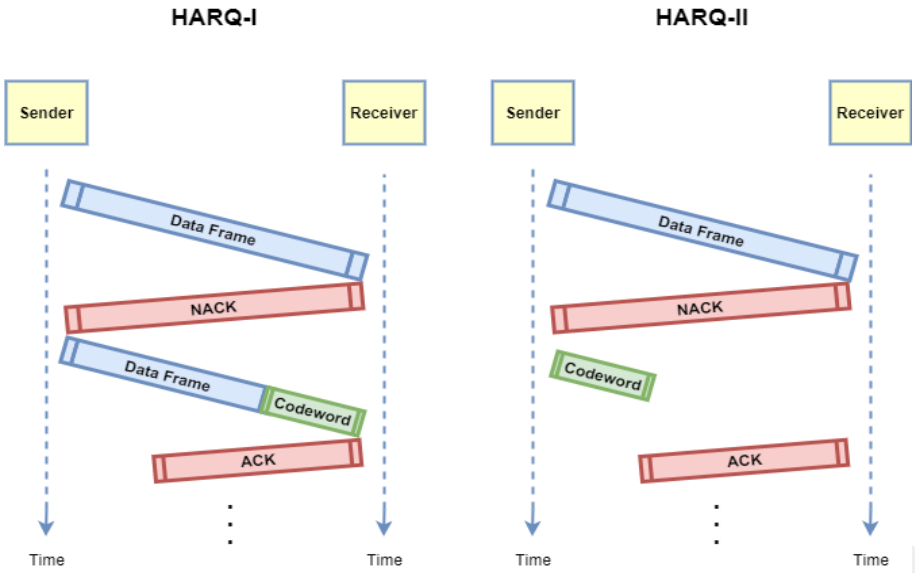

Figure 3.2.7. The representation of HARQ-I and HARQ-II schemes

HARQ-II is shown in Figure 3.2.7.

For HARQ, the transmission energy cost is given by

$$E_{tx,ij}^{HARQ} = E_{enc} + E_{tx}(L_{P_f}) + (1 - p_{ij}^{s}(L_{P_f}))\times \\ (E_{rx}(L_{P_n}) + E_{tx}(L_{P_s})), \tag{3.23}$$

where L_{P_f}, L_{P_s} and L_{P_n} refer to first packet size and second packet size and the NACK packet size, respectively. $p_{ij}^{s}(L_{P_f})$ denotes the probability of successful transmission. The reception energy cost is given by

$$E_{rx,ij}^{HARQ} = E_{rx}(L_{P_f}) + E_{dec}(L_{P_f}) + (1 - p_{ij}^{s}(L_{P_f}))\times \\ (E_{tx}(L_{P_n}) + E_{rx}(L_{P_s}) + E_{dec}(L_{P_s})). \tag{3.24}$$

The packet success rate is determined by

$$\phi_{ij}^{HARQ} = 1 - (PER_{ij}^{ARQ} \times PER_{ij}^{FEC}). \tag{3.25}$$

The data transmission time is given by

$$T_{tx,ij}^{HARQ} = T_{tx,ij}^{ARQ} + (1 - p_{ij}^{s}(L_{P_f})) \times T_{tx,ij}^{FEC}. \tag{3.26}$$

the data reception time is given by

$$T_{rx}^{HARQ} = T_{rx}^{ARQ} + (1 - p_{ij}^{s}(L_{P_f})) \times T_{rx}^{FEC}. \tag{3.27}$$

Chapter 4

Analyzing lifetime of energy harvesting wireless multimedia sensor nodes in industrial environments

4.1 Motivation

There has been great demand for Wireless Multimedia Sensor Networks (WMSNs) due to their low cost and expanded usage area (*e.g.,* many applications especially monitoring ones explained in Section 1.1.1). However, limited energy is the major challenge for wireless communication. Larger data size causes larger energy consumption in processing and communication. The excessive energy consumption leads sensor battery to run of of quickly. Permanent destruction may occur in industrial applications because of temporary interruption in monitoring systems. Therefore, saving energy of sensor nodes become vital for WMSNs applications in industrial environment.

To save the energy of sensor nodes, there have been several power management schemes are presented [16, 20, 114]. The method we considered in our thesis is schedule driven model where the power mode of sensor node alternates according to the duty cycle period [49]. In other words, the model changes power of sensor node when it is in active mode or sleep mode. The inter mode transition of sensor node is formulated by using semi-Markov chain. The other approach to save the sensor node energy during multimedia communication (*i.e.,* image transmission) is data size reduction methods. However, the processing energy cost emerges for image compression. Therefore, the computation cost should be evaluated. Discrete Cosine Transformation (DCT) based image compression methods are commonly used in literature. However, the computation cost of DCT is high. Thus, Fast-Zonal Binary DCT (BinDCT) method is utilized in this study. Finally,EH technologies are used for prolonging the sensor node lifetime. The available ambient

energy sources for industrial environment are solar, thermal and mechanical energy.

4.2 Related Work

Image compression methods have been studied for reducing the data size to be transmitted. For instance Nasri et. al [75] utilizes the JPEG image compression methods for data size reduction. In order to avoid overloading energy consumption of a sensor node, they have adopted to distributed image compression approaches. Huu et. al [45] also have applied the distributed image compression system to prevent overloading of one sensor node. To extend the lifetime of network, energy threshold algorithm which determines the relay node according to residual energy is utilized. Sun et. al [98] have proposed image compression method with low energy. The method performs compression with low ratio to interest part of image while high ratio to least important part of image. They achieved the dramatically extended the network lifetime. Wei et. al [117] have proposed image compression method that distributes the compression on several sensor nodes while transmitting to prolong the network lifetime. In this introduced method, different sensors have different roles. Camera sensors captures the image data. Then, common sensors compressed the image blocks to relay the cluster heads. Finally, cluster head nodes send the compressed image to the sink node.

On the other hand, EH methods supply the great solution for sensor node with limited battery. Solar, thermal and vibration are the available ambient energy sources for industrial environments. There are several studies that utilizes the solar EH methods for powering industrial sensor nodes [46, 60]. Besides solar EH methods, indoor solar EH methods are also used for industrial environments. Hande et. al [39] have improved an algorithm that harvests energy from 34 W fluorescent lights using monocrystaline solar cells. Elefsiniotis et. al [27] have described thermoelectric energy harvester which scavenges energy from temperature difference during aircraft operation. Ren et. al [86] have presented the use of vibration energy harvester in industrial applications. The comprehensive review of utilizing EH methods in WSN is given in Section 2. The literature overview of this chapter is presented in Table 4.2.6 where CM, IC, PM and LT denote channel model, image

Existing Studies	CM	IC	PM	LT	EH
[75], [45], [98]	✗	✓	✗	✓	✗
[117]	✗	✓	✗	✗	✗
[39]	✗	✗	✓	✗	✓
[27], [46]	✓	✓	✗	✓	✓
[60]	✗	✗	✓	✓	✓
Proposed System	✓	✓	✓	✓	✓

Table 4.2.6. Literature overview

compression, power management and lifetime, respectively.

4.3 Evaluated Methods

4.3.1 Image Compression Methods

Huge data size increases the the energy consumed in communication phase (*i.e.,* transmission and reception). Therefore, to reduce the data size by compressing before transmit is critical for energy efficiency of sensor node. However, the computation energy cost emerges to compress the image data. Thus, there is tradeoff between communication energy cost and computation energy cost.

Discrete Cosine Transformation (DCT) is utilized to transform image signal from spatial domain to frequency domain. DCT algorithm divides image into 8x8 block and then quantized and encode each block of image. To encode whole image leads to excessive energy consumption in computation. Therefore, reducing this computation cost is important. [66] introduced the fast zonal DCT approach in image compression to decrease the computational energy. Instead of computing 64 DCT coefficient, the fast zonal DCT approach selects subregion from coefficient to compute and encode. The value of k specifies the size of selected subregion which can be either square pattern or triangle pattern. Thus, as k gets smaller, the computation energy reduces. In addition, also Binary DCT (BinDCT) is proposed by authors. Only sum and shift operations are used in BinDCT approach , hence it eliminates the energy consumption caused by multiplication

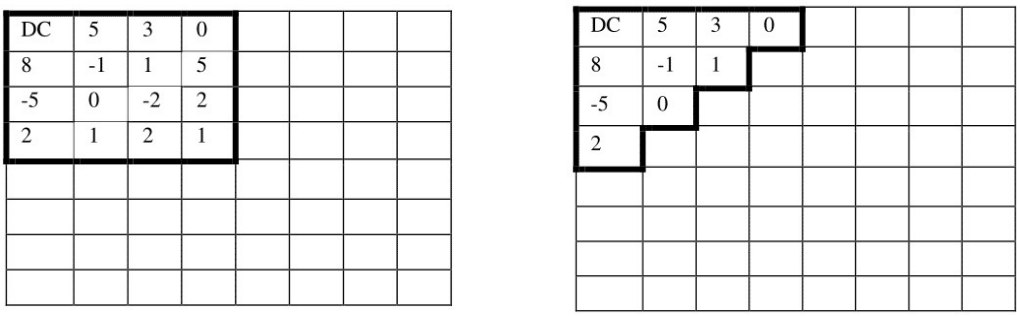

(a) square pattern (b) triangle pattern

Figure 4.3.8. The representation of 2-D 8-point DCT where $k = 4$

operations. The representation of selected subregion (*i.e.,* square pattern and triangle pattern) is shown in Figure 4.3.8.

4.3.2 Power Management Methods

The aim of the power management methods is to save the energy of sensor node by taking the currently not used components mode to off. In this way, the power usage control system increases the lifetime of sensor nodes. In this study, a schedule-driven power management method with MATSNL toolbox is utilized [49]. To save the energy, sensor nodes move to either sleep mode or awake mode in this method. The timer is used to switch between active mode and sleep mode. The time period of awake mode and sleep mode are denoted by T_w and T_s, respectively. Semi Markov chain is utilized to build state (*i.e.,* mode) transition diagram shown in Figure 4.3.9. There exists four stages in this diagram such as awake, sleep, process and communication stage. The awake stage involves the monitoring stage and idle stage. If the event is detected then sensor node switches to the monitoring stage from sleep stage, if it is not detected, sensor node stays in idle stage. The event is detected with β probability. After detecting event, sensor node certainly switches process stage to determine whether the event data is meaningful or not. In addition, the compressing is done in processing stage. After processing stage, the node switches to communication stage with α probability to transmit the data. Otherwise, the sensor nodes shifts to the sleep stage.

There exists three hardware units such as sensor, CPU and radio of sensor nodes to process. Not every unit needs to be process at every stage. This means that, only required

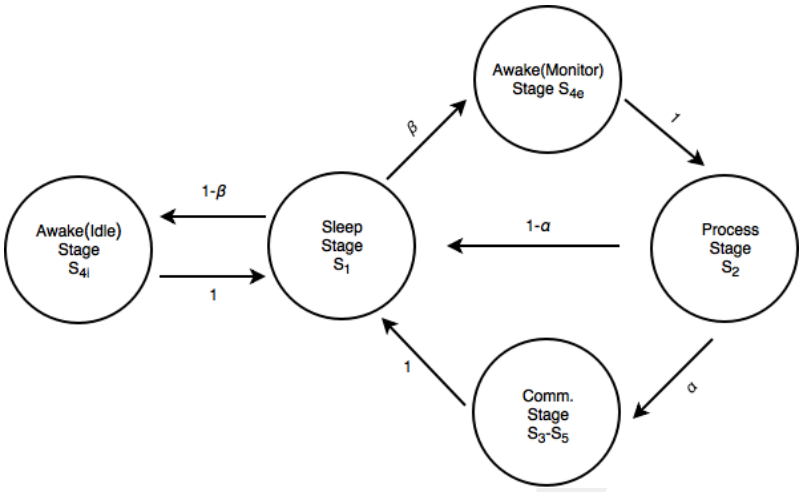

Figure 4.3.9. State transition diagram

Mode	Sensor	CPU	Radio
S1	Off	Off	Off
S2	Off	On	Off
S3	Off	On	Tx
S4	On	Idle	Off
S5	Off	On	Rx

Table 4.3.7. Schedule driven model

units are active in each stage. The five different modes (*i.e.,* S1, S2, S3, S4, S5) are defined to indicate the status of hardware units and presented in Table 4.3.7.

The average power consumption of sensor node for each task is determined by

$$P_{sch}(\beta) = \frac{P_e + \frac{\beta}{T_c} M_E}{1 + \frac{\beta}{T_c} M_T}. \tag{4.1}$$

The lifetime of sensor node is given by

$$T_L(\beta) = \frac{(1 + \frac{\beta}{T_c} M_T) E_{total}}{P_e + \frac{\beta}{T_c} M_E}, \tag{4.2}$$

where P_e denotes the average power consumed if there is no detected event. T_c refers to duty cycle time period. E_{total} refers to total energy of sensor node. M_E and M_T denote the average residual energy and time if there exist detected event, respectively. The average residual energy (M_E) is computed as:

$$M_E = T_{S2} * P_{S2} + \alpha * (T_{S3} * P_{S3} + C_R) - \frac{T_W * (T_W + 2 * T_E)}{2 * (T_W + T_E)} * P_{S4}. \tag{4.3}$$

The average residual time M_T is computed as

$$M_T = T_{S2} + \alpha * T_{S3} - \frac{T_W * (T_W + 2 * T_E)}{2 * (T_W + T_E} \tag{4.4}$$

The average power consumed if there is no detected event is computed as:

$$P_e = P_{S1} + d * (P_{S4} - P_{S1}) + \frac{C_P}{T_c} \tag{4.5}$$

In Equations 4.3, 4.4 and 4.5, T_{S2} denotes the average processing time and T_{S3} denotes the average transmission time per event. T_W refers to duration of CPU in awake mode. T_E refers to duration of event. P_{S1}, P_{S2}, P_{S3} and P_{S4} represents the required power in idle state, processing state, communication state, and monitoring state, respectively. C_P and C_R are wake-up energy cost of C_P and C_R, respectively. α is the shifting to communication stage probability of sensor node and d denotes the duty period. The improvement of lifetime is defined by

$$Lifetime_{Improvement} = \frac{Lifetime_{CompAndEH} - Lifetime_{unmodified}}{Lifetime_{unmodified}} * 100 \tag{4.6}$$

4.4 Performance Analysis

The lifetime of sensor nodes while transmitting image data is investigated in this thesis. As realistic channel model, we use the log-normal shadowing model to realize the channel characteristics defined in Section 3.1. The channel parameters of industrial environment is given in Table 4.4.8 [31]. Telos and Mica2 sensor motes are utilized in the simulations. In addition, Carrier Sense Multiple Access (CSMA) as a channel access scheme and Automatic Repeat Request (ARQ) as an error control scheme is used. Since, Telos and Mica2 use different modulation scheme, namely, Q-PSK and FSK, two different Packet Reception Rate (PRR) are evaluted to determine the number of retransmissions shown in Figure 4.4.10. The retransmission number is limited with 3.

The image compression scheme based on fast zonal DCT and BinDCT are considered

Channel Characteristics		
Sy/Ac/Vr	**Description**	**Value**
PL(d_0)	Path loss at distance, d_0	63.57 dB
d_0	Reference distance	0.5 m
n	Path loss exponent	2.40
σ	Shadowing standard deviation	4.79 dB
P_n	Noise Floor	-93.0 dBm
P_t	Output power	0 dB
B_N	Noise bandwidth	30 kHz kbps

Table 4.4.8. Channel parameters of industrial environment

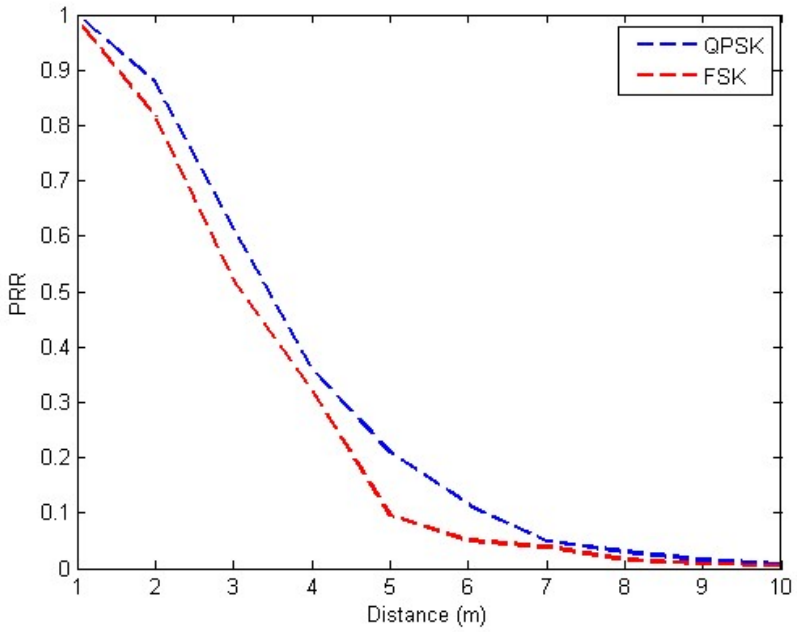

Figure 4.4.10. Packet reception rate wrt. distance for FSK and Q-PSK

to decrease the size of data. The execution time of compressing 256x256 image for these approaches with different k value are presented in Table 4.4.9. The image is encoded at 0.5 bit per pixel (bpp). The time spent for compression (*i.e.,* execution time) is added to time spent in processing stage (S2). Additionally, EH methods, namely indoor solar, thermal and vibration are used to prolong the sensor node lifetime. The average harvested power calculations in detail are given in Chapter 2. The simulation parameters of energy harvesting methods are given in Table 4.4.10. The generated power from harvesters is given in Table 4.4.11.

Figure 4.4.11 and Figure 4.4.12 present the lifetime improvement of various image

	Execution Times (ms)					
	DCT k=8 (S-8)	**DCT k=4 (S-4)**	**DCT k=2 (S-2)**	**BinDCT k=8 (P-8)**	**BinDCT k=4 (P-4)**	**BinDCT k=2 (P-2)**
Telos	44851	38502	27136	4018	2684	1428
Mica2	19760	11124	6288	1188	686	339

Table 4.4.9. Execution time for compressing 256x256 image

Indoor solar harvester			
Sy/Ac/Vr	**Description**	**Unit**	**Value**
T_C	Ambient temperature	K	295
n	Number of PV cells	-	15
I_0	Current of p-n nodes	A	$1 \times 10^{-}9$
I_{SC}	Current of light irradiance	μA	150
q	Charge of electron	C	$1.6022 \times 10^{-}19$
k	Boltzmans constant	$JK^{-}1$	$1.3807 \times 10^{-}23$
Thermal harvester			
Sy/Ac/Vr	**Description**	**Unit**	**Value**
ΔT	Temperature differences	K	10
n	Number of thermocouples	-	5200
α	Seebeck's coefficients	mV/K	0.21
R_s	Electrical resistance	$k\Omega$	82
Vibration harvester			
Sy/Ac/Vr	**Description**	**Unit**	**Value**
ω	Frequency	Hz	71
V	Voltage	V	48
I	Current	mA	0.05

Table 4.4.10. Simulation parameters for energy harvesters

Harvester	**Value**	**Unit**
Indoor solar	0.4947	mW
Thermal	0.3635	mW
Vibration	0.2400	mW

Table 4.4.11. Average harvested power

compression approaches as a function of duty cycle for Telos and Mica2, respectively. The distance between two sensor nodes is set to 10 m. For Telos, the lifetime improvement is greater when utilizing DCT based compression. Since, the processing power of Telos is low

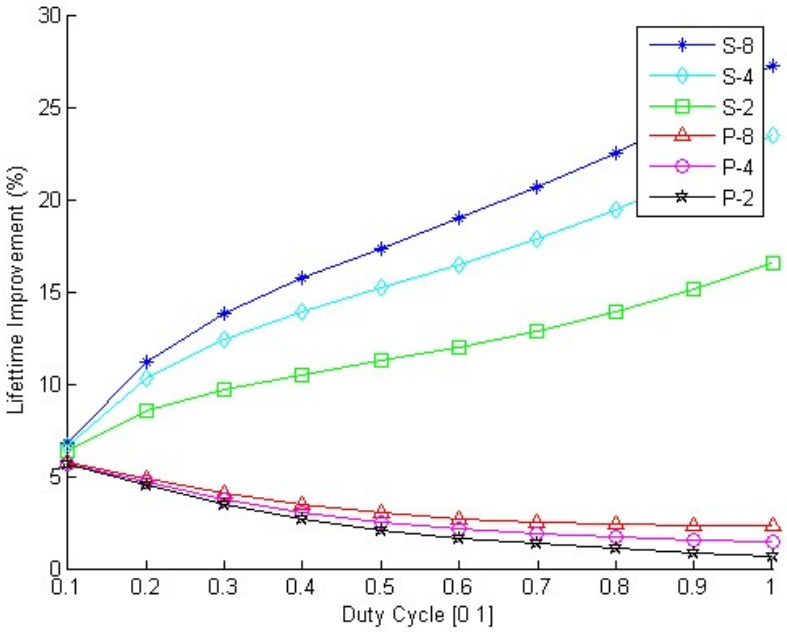

Figure 4.4.11. Lifetime improvement with various compression approaches wrt. duty cycle for Telos

and increase in processing stage duration, decrease the average power consumption. DCT based compression approaches (*i.e,* S-8, S-4, S-2) provides higher lifetime improvement as the duty cycle increases. However, BinDCT based image compression provides less lifetime improvement as the duty cycle increases. For Mica2, the lifetime improvement of DCT based image compression is smaller than the BinDCT based image compression before the duty cycle is 0.6. The reason for that, the average power consumption without compression is less than the power consumption of processing state. However, for duty cycle grater than 0.6, this situation is reversed. Therefore, DCT based image compression approaches give the better lifetime improvement.

Figure 4.4.13 and Figure 4.4.14 depict the lifetime improvement of with regard to distance for Telos and Mica2, respectively. Duty cycle is set to 0.1. As the distance increases, the effect of image compression methods increases for both Telos and Mica2. Since, the large data size and long distance cause higher energy consumption. Therefore, reducing the data size prolongs the lifetime. However, the negative effect is observed for Mica2 when it utilizes the method S-8 and distance is shorter than 5 m. The reason for that is the execution time of S8 and the processing power of Mica2 are high. It is more efficient when nodes are close enough due to less energy consumption in transmission. In other words, the transmission energy is less as the number of retransmission decreases at a

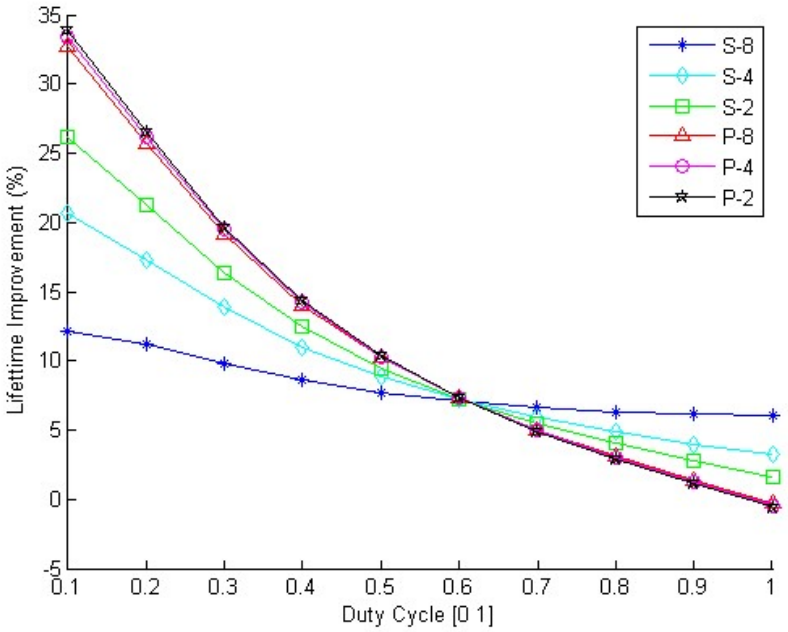

Figure 4.4.12. Lifetime improvement with various compression approaches wrt. duty cycle for Mica2

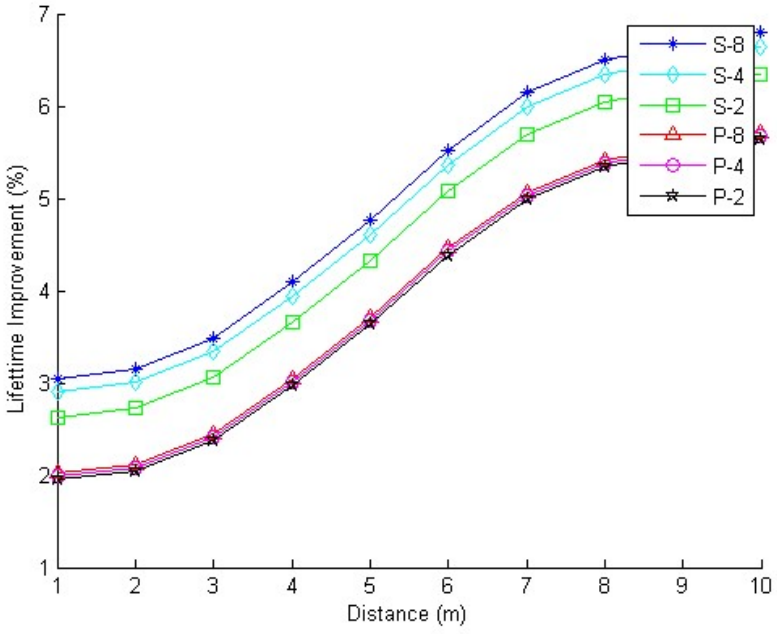

Figure 4.4.13. Lifetime improvement with various compression approaches wrt. distance for Telos

shorter distance. Thus, addition energy spent for processing decreases the sensor lifetime. DCT based image compression approach achieves the better lifetime improvement whereas BinDCT based image compression approach achieves better lifetime improvement for Mica2.

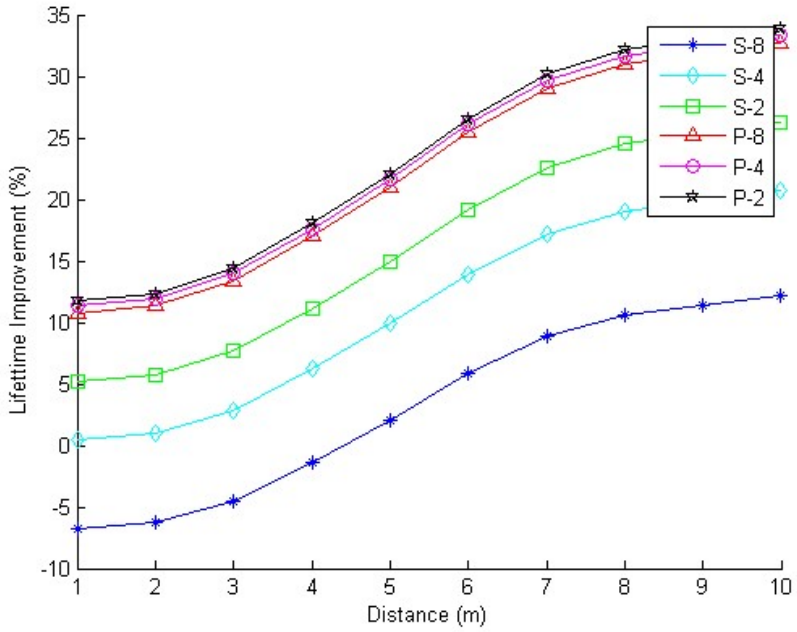

Figure 4.4.14. Lifetime improvement with various compression approaches wrt. distance for Mica2

Figure 4.4.15 and Figure 4.4.16 presents the lifetime improvement of joint utilization of compression methods and energy harvesting methods as a function of duty cycle for (a) Telos and (b) Mica2. Although greater lifetime improvement is observed at longer execution time when the average power consumption without compression is higher than the power consumption of S_2 state, it decreases the number of cycles (*i.e.,* measurements) throughout the sensor lifetime. Therefore, BinDCT (P-2) is selected as a compression method. The average harvested power from indoor solar harvester is higher than others which is 0.497 mW given in Table 4.4.11. For Telos, the lifetime improvement increases from 5.6%-0.7% to 14.5%-1.2% when jointly utilized compression and vibration harvester. The thermal and solar harvester provide even more improvement on lifetime. For Mica2, the lifetime improvement is increased to from between 33.9% and -0.6% to between 42.1% and -0.1% when both compression and vibration harvester are used.

Figure 4.4.17 and Figure 4.4.18 present the lifetime improvement of joint utilization of compression methods and energy harvesting methods as a function of distance for Telos and Mica2, respectively. For Telos, the lifetime improvement increases from 2%-5.6% to 10.6%-14.6% when jointly utilized compression and vibration harvester. The thermal and solar harvester provide even more improvement on lifetime. For Mica2, the lifetime improvement is increased to from between 11.8% and 33.9% to between 18.7% and 42.1%

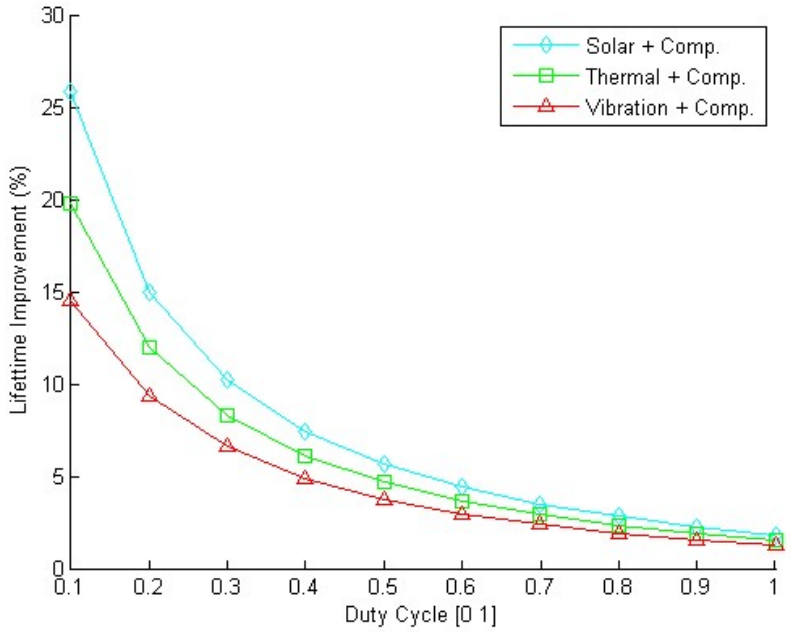

Figure 4.4.15. Lifetime improvement with joint utilization of compression and energy harvesting approaches wrt. duty cycle for Telos

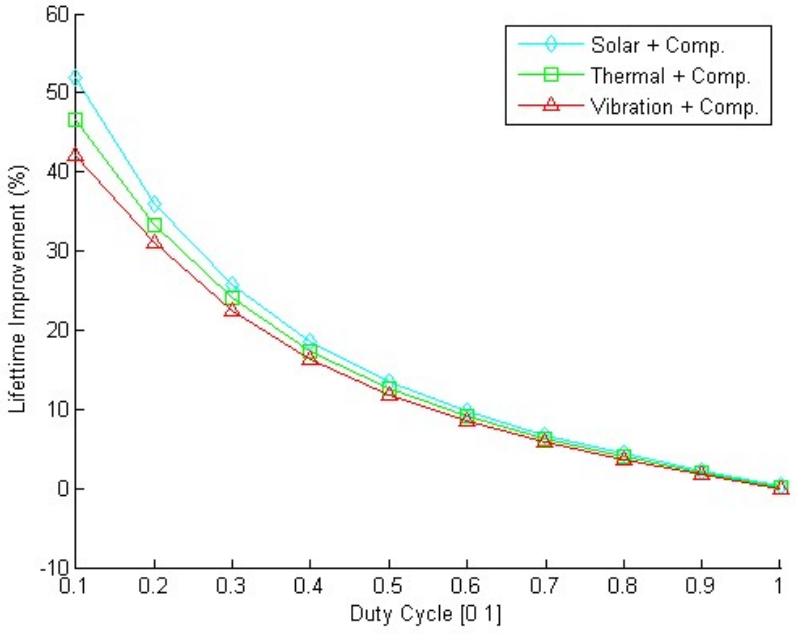

Figure 4.4.16. Lifetime improvement with joint utilization of compression and energy harvesting approaches wrt. duty cycle for Mica2

when both compression and vibration harvester are used. As a result, application needs determine the duty cycle and distance between sensor nodes.

In conclusion, the performance results show the joint utilization of image compression and energy harvesting methods prolongs the lifetime of sensor node

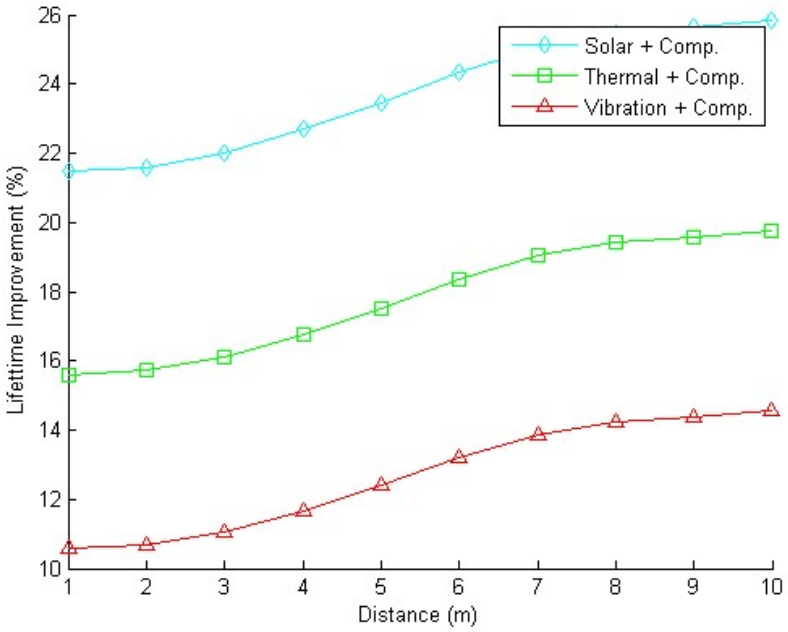

Figure 4.4.17. Lifetime improvement with joint utilization of compression and energy harvesting approaches wrt. distance for Telos

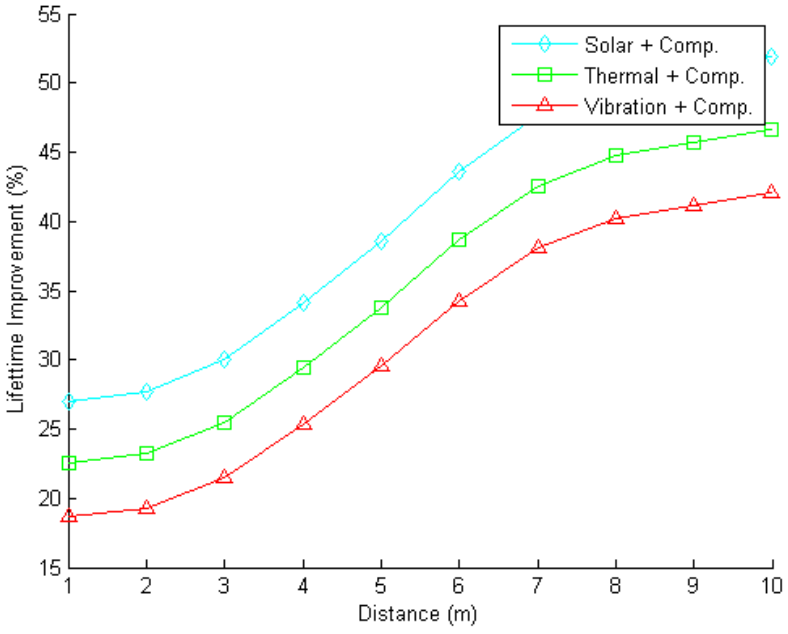

Figure 4.4.18. Lifetime improvement with joint utilization of compression and energy harvesting approaches wrt. distance for Mica2

significantly. The maximum lifetime improvement is 25.8 % for Telos while it is 51.8 % for Mica2.

Chapter 5

The Impact of Error Control Schemes on Lifetime of Energy Harvesting Wireless Sensor Networks in Industrial Environments

5.1 Motivation

Reliability is very critical especially for IWSNs due to the harsh channel conditions. The harsh channel conditions lead to packet drops and erroneous packet transmission. This poses a danger to industrial applications such as process control and maintenance where reliability is vital. For example, if controller can not be informed correctly about the broken machine which causes to stop whole system, it can create a huge waste of time and financially devastation. To reliably measure any fault in time prevents major environmental hazards. For instance, any detected liquid or gas leakage or fire information occurring in the industrial environment can cause destruction if not transmitted in a timely and reliable manner. Therefore, to provide reliable communication become essential. To address reliability requirement, there exist error control methods such as Automatic Repeat Request (ARQ), Forward Error Correction (FEC) and Hybrid ARQ (HARQ) in literature. In this study, we examine the EC methods performance in IWSNs whether they can reach the desired reliability rate of application or not.

On the other hand, providing reliable communication is energy costly. Energy consumption is of great importance for battery powered sensor nodes where the replace of them is highly difficult in industrial environment. Therefore, prolonging the network lifetime is also essential for industrial applications. We examine the impact of EC schemes on network lifetime. In addition, we provide energy harvesting methods that can be scavenged from industrial environment. The EH methods are based on indoor solar,

thermal and vibration. To optimize energy utilization of sensor nodes in the network is vital for extending network lifetime. To this end, we formulated the MIP model to maximize the network lifetime by jointly considering channel model, EC models and EH methods.

5.2 Related Work

In literature, [73, 111] investigate the energy efficiency of error control schemes for wireless sensor networks. Vuran et. al [111] analyzed EC schemes by jointly using channel model, Medium Access Control (MAC) and routing. They evaluated PER, energy consumption and latency performance of ARQ, FEC and HARQ. Nandi and Kundu [73] have examined the energy performance of ARQ and FEC by utilizing Rayleigh fading. They compared the ARQ with FEC in terms of energy efficiency and PER. Moreover, they analyzed the effect of packet length and Rayleigh fading FEC error correcting capability. They showed that the energy efficiency of FEC is greater than the ARQ. Islam [47] examined the BER and power consumption of FEC schemes a to identify the suitable error control schemes for wireless sensor networks. They showed that RS(31,21) performs the better performance when jointly considering power consumption and BER. Naderi et. al [70] examined the EC schemes for WMSNs. They have investigated the energy efficiency of ARQ, FEC, erasure coding , link-layer hybrid ARQ, and cross-layer hybrid error control methods. In addition to energy efficiency, they investigated the frame loss rate and Peak Signal to Noise Ratio (PSNR). Sarvi et. al [89] proposed adaptive cross layer EC protocol which arranges redundant bits considering loss rate of packet for WMSNs. Razali et. al [85] investigated the WSN while utilizing both CDMA and HARQ scheme in terms of energy consumption and lifetime.

There are some studies that introduced proper energy harvesting methods for WSNs while considering EC schemes. Jalali et. al [48] utilized the solar energy harvesting method to scavenge energy. To improve energy efficiency and reliability, they have proposed solution that utilize Cooperative ARQ method. In that method, retransmission is done by cooperator node so that energy consumption of source node is reduced. Sharma

Paper	CM	EC	NL	EH	AP	Hardware
[111],[73],[47]	✗	✓	✗	✗	✗	**Mica2, MicaZ**
[70]	✗	✓	✗	✗	✓	**MicaZ**
[89], [85]	✓	✓	✗	✗	✗	**MicaZ**
[48]	✗	✓	✗	✓	✗	**MicaZ**
[94]	✗	✓	✗	✗	✗	✗
[65]	✓	✓	✗	✓	✗	✗
[121], [50]	✗	✓	✗	✓	✗	✗
Proposed system	✓	✓	✓	✓	✓	**Mica2, Telos**

Table 5.2.12. Literature overview

et.al [94] investigated the Packet Drop Probability (PDR) of ARQ and HARQ schemes used on EH sensor nodes. They have also evaluated the impact of energy harvesting rate on EH sensor nodes. Mahdavi et. al [65] examined the Repetititon-HARQ and Incremental Redundancy HARQ (IR-HARQ) in terms of throughput. They perform energy harvesting only fro receiver node with limited harvesting rate. Yadav et. al [121] introduced the energy harvesting sensor node that uses adaptive ARQ scheme. The sensor nodes harvest energy with a fixed rate. The papers that we mentioned above have introduced EH methods with a rate, however in our study we consider realistic EH methods that can be utilized in industrial environment. Jung et. al [50] introduced the energy-aware Reed Solomon (EA-RS) scheme. In that scheme, the length of parity bits are adjusted according to remaining energy of sensor node. The overview of literature is presented in Table 5.2.12 where CM, NL and AR denote the channel model, network lifetime and application reliability, respectively.

5.3 Evaluated Methods

In this section, we present the methods that are used in the study. We utilize the log normal shadowing model as a channel model explained in Section 3.2. The detail explanation of utilized error control schemes is given in Section 3.2. The EH methods, namely, indoor solar, thermal and vibration for industrial environment are given in Section 2.1, 2.2 and 2.3, respectively. The proposed Mixed Integer Programming (MIP) model is

given below.

5.3.1 Mixed Integer Programming Model

The MIP model shown in Figure 5.2.19 is constructed to optimize the energy dissipation of sensor nodes. The lifetime of network is described as the time until the first node consumes all the battery energy.

The network topology is described as directed graph $G = (V, A)$ where V is the set

Maximize H
Subject to:

$$f_{ij} \geq 0, \forall (i,j) \in A \tag{5.1}$$

$$f_{1j} = 0, \forall (j) \in W \tag{5.2}$$

$$\sum_{(i,j)\in A} f_{ij} - \sum_{(j,i)\in A} f_{ji} \times \phi_{ji} = H \times s, \forall i \in W \tag{5.3}$$

$$\sum_{(j,1)\in A} f_{j1} \times \phi_{j,1} \geq \sum_{j\in W} s \times H \times r \tag{5.4}$$

$$\begin{aligned} T_{busy,i} = &\sum_{i\in W} T_{tx,ij} \times f_{ij} \times n_{ret,ij} \\ &+ \sum_{i\in W} T_{rx} \times f_{ji} \times n_{ret,ji} \\ &+ H \times T_{acq}, \forall i \in W \end{aligned} \tag{5.5}$$

$$\begin{aligned} &\sum_{j\in W} E_{tx,ij} \times f_{ij} + \sum_{j\in W} E_{rx,ji} \times f_{ji} \\ &+ (H \times E_{acq}) + P_{slp} \times (H \times T_{rnd} - T_{busy,i}) \\ &- P_{harv} \times (H \times T_{rnd} - T_{busy,i}) \leq \xi, \forall i \in W \end{aligned} \tag{5.6}$$

$$\begin{aligned} (L_P + L_A) \times &\sum_{j\in W} f_{ij} \times n_{ret,ij} + \sum_{j\in W} f_{ji} \times n_{ret,ji} \\ &\leq \varsigma \times H \times T_{rnd} \forall i \in V \end{aligned} \tag{5.7}$$

Figure 5.2.19. The MIP framework

of sensor nodes which involve sink node and A refers to the link pairs. The set of sensor nodes without sink node is denoted by W. Sink node is denoted by node-1. Sensor nodes in set V gather N bytes data to relay the sink node at each round during network lifetime. The number of data packet is estimated as $s = \lceil \frac{N}{L_P - L_H} \rceil$ where L_P and L_H are the size of payload and header, respectively. H is the number of rounds made throughout the network lifetime. T_{rnd} is the predefined time for the round. Accordingly, network lifetime is determined as $H \times T_{rnd}$. f_{ij} is the decision variable that denote the number of packet flows over link-(ij). ϕ_{ij} is the packet success rate (*i.e.,* successful transmission probability over link-(ij) explained in Section 3.2. $T_{busy,i}$ refers to total time duration of when node i is active mode. $T_{tx,ij}$ is the data transmission time over link-(ij). $n_{ret,ij}$ is the number of retransmission over link-(ij). The calculation of this value for ARQ is determined in Section 3.2. Since there is no retransmission in FEC and HARQ method, $n_{ret,ij}^{FEC} = 1$ and $n_{ret,ij}^{HARQ} = 1$. $E_{tx,ij}$ and $E_{rx,ij}$ are transmission energy cost and reception energy cost over link-(ij), respectively. Finally, P_{harv} is the average harvested power.

Equation (5.1) determines that flows can not be negative. Equation (5.2) ensures that node-1 does not produce packet hence flow. Equation (5.3) presents the flow balance constraint so that the sum of received and generated packets by node-i is equal to transmitted packets from node-i. The all packets generated from all sensor nodes may not reach to sink node because of packet losses. Therefore, Equation (5.4) ensures the reliability constraint so that at least r percent of generated data packets from all sensor nodes is received by node-1. Hence, r is the predefined reliability rate. Equation (5.5) estimates the total busy time of node-i. Equation (5.6) specifies that the energy consumed by node-i for acquisition, transmission and reception is limited by battery of power plus harvested power during network lifetime. Equation (5.7) guarantees that channel bandwidth is greater than the required bandwidth for communication.

5.4 Performance Analysis

the random disk shaped network topology where the radius of network is denoted as R_{net} is built. 50 sensor nodes are randomly placed in the network topology. The sink

node is placed to point of (0,0). R_{net} values change between 10 m to 20 m. The different values of L_P are defined as 128, 96, 48 and 24 byte. Furthermore, the various reliability rates which are 0.5, 0.6, 0.7, 0.8, 0.9 and 1 are analysed. Finally, four different industrial environment topographies where the channel parameters are given in Table 5.4.13 are examined [31]. The simulation parameters used in evaluations are given in Table 5.4.15. The contributions of EH methods on network lifetime is analyzed. The harvested average powers are given in Table 4.4.10. MATLAB is used to evaluate the channel model and energy calculations and General Algebraic Modelling System (GAMS) with CPLEX is used for solving the proposed MIP framework. The figures are obtained by taking average of results of 100 trials.

Topographical category	**Path loss exponent (n)**	**Shadowing deviation (σ)**
LOS	2.40	4.79
OBS (light clutter)	2.77	5.42
OBS (heavy clutter)	4.29	8.42
ALL LSF	3.44	8.63

Table 5.4.13. The channel parameters for different industrial topographies

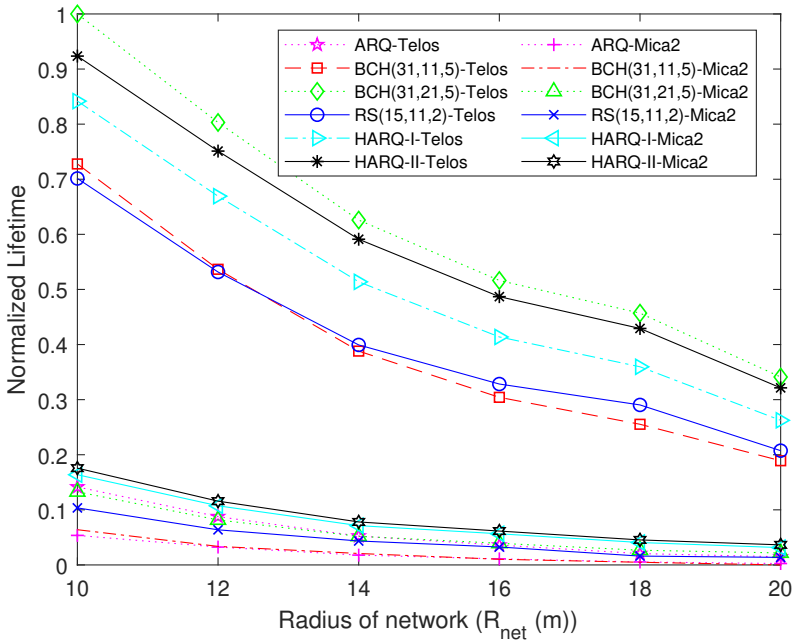

Figure 5.4.20. Normalized lifetime wrt. radius of network for Mica2 and Telos

The Figure 5.4.20, Figure 5.4.21 and Figure 5.4.22 are simulated in LOS environment. The Fig. 5.4.20 shows the normalized network lifetime for Mica2 and Telos with respect to

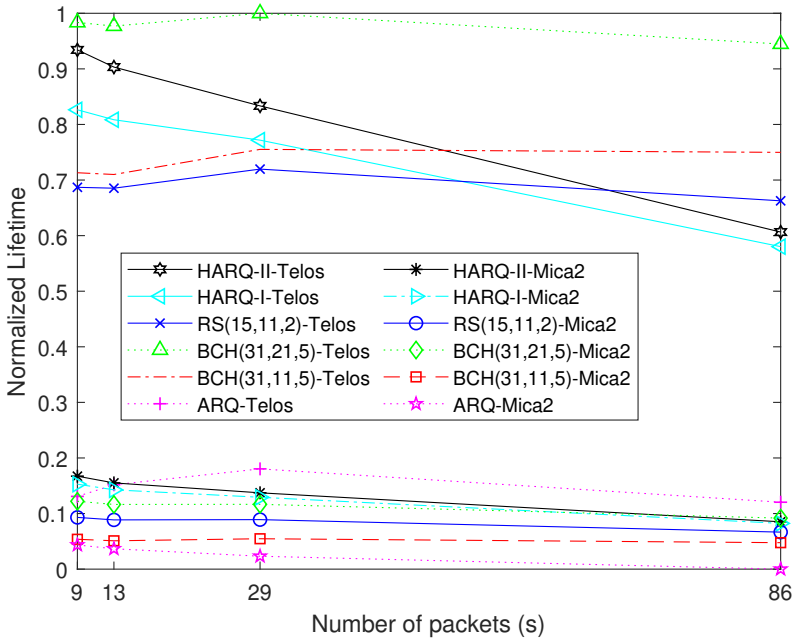

Figure 5.4.21. Normalized lifetime wrt. number of packets for Mica2 and Telos

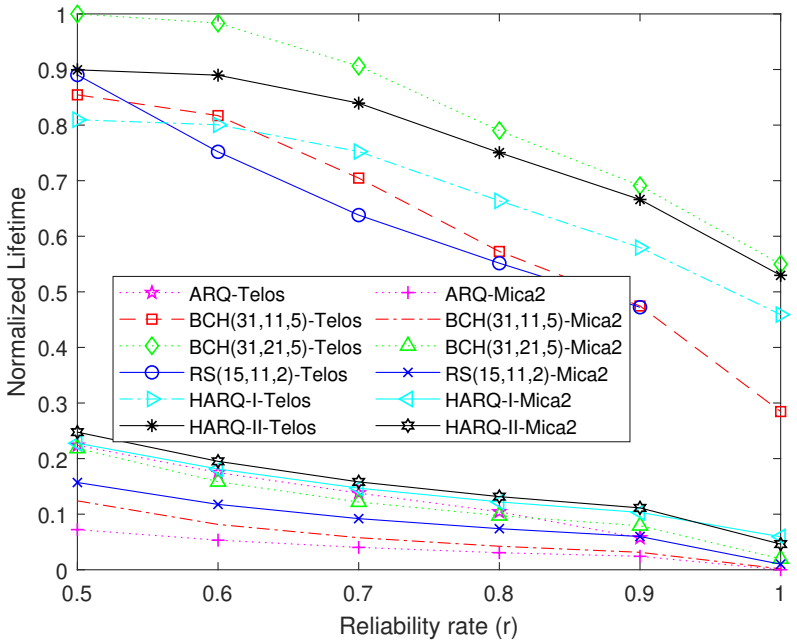

Figure 5.4.22. Normalized lifetime wrt. reliability rate for Mica2 and Telos

the R_{net} when r and L_P are set to 0.8 and 128 byte, respectively. For both Mica and Telos mote, the network lifetime for all EC schemes declines as the R_{net} increases. The network lifetime obtained with utilizing ARQ present least performance for both Mica2 and Telos mote. The reason for that increase in number of retransmission due to harsh channel condition of industrial environment. The increasing number of retransmission consumes

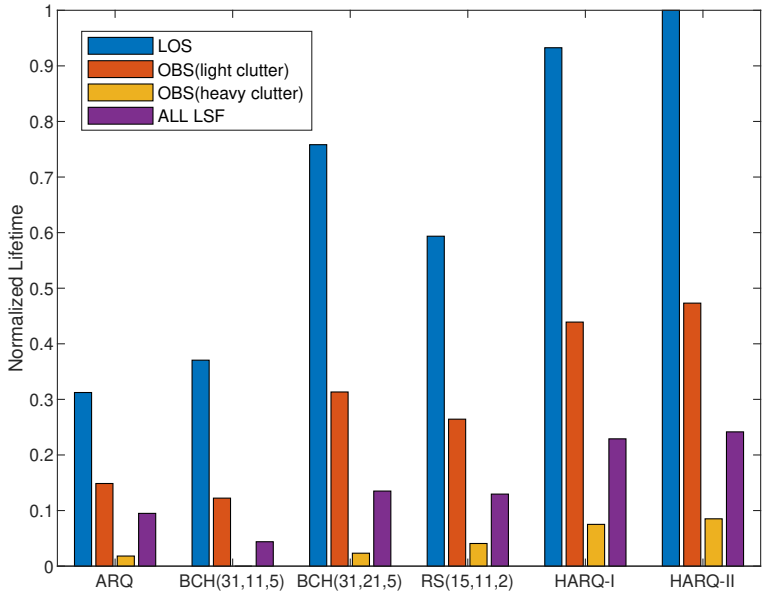

Figure 5.4.23. Normalized lifetime wrt. different topographies for Mica2

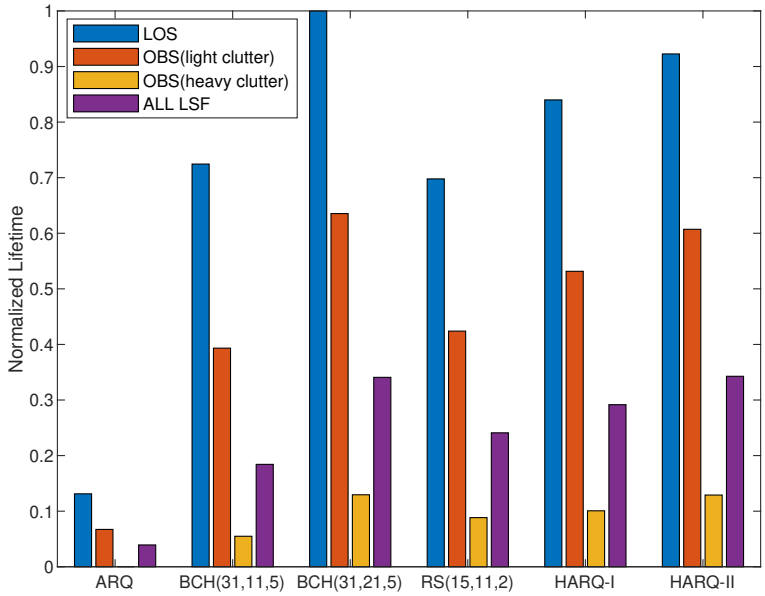

Figure 5.4.24. Normalized lifetime wrt. different topographies for Telos

more energy in transmission. If we compare the performance of Telos and Mica2, Telos gives better lifetime than Mica2. Since Telos has higher data rate and lower processing power than Mica2. That is why, BCH(31,21,5) outperforms the other EC schemes for Telos whereas it is HARQ-II for Mica2. Thus, lower processing power significantly effect the amount of energy consumption for decoding. The reason that the network lifetime with

HARQ-II exceed HARQ-I is that HARQ-II resend only the redundant bits. BCH(31,21,5) presents better network lifetime than BCH(31,11,5) because the less payload size of block increases the number of block therefore number of redundant bits to sent. The higher redundant bits cause higher energy consumption. The higher error correcting capability of BCH(31,11,5) compared to RS(15,11,2) induces higher energy consumption even if they both have same payload size of block. The Figure 5.4.21 shows the normalized network lifetime as a function of s where $R_{net} = 10m$ and $r = 0.8$. As the number of packets increases, packet flows also increases cause higher energy consumption. Therefore, for both Telos and Mica2 the network lifetime declines. Figure 5.4.22 presents the normalized network lifetime as a function of r for Telos and Mica2 mote. For both of them, the network lifetime decreases The number of routing path that provides the higher reliability rate decreases. Continuous use of the same routing paths to ensure the reliability rate causes energy to be consumed quickly. Therefore, for both Telos and Mica2, the network lifetime decreases as the reliability rate increases. In fact, Telos with RS(15,11,2) and ARQ could not provide the reliability criteria where $r = 1$.

Figure 5.4.23 and Figure 5.4.24 indicate the normalized network lifetime for all EC schemes as a function of changing topographies for Mica2 and Telos, respectively. The figures are obtained when R_{net} is 10 m and r is 0.8. For Mica2 and Telos, OBS (heavy clutter) gives the worst network lifetime since it has the path loss exponent. The higher path loss causes the higher BER. Therefore, to provide reliability become more energy costly. In addition, it is observed that BCH(31,11,5) gives the worst lifetime for all topographies except LOS for Mica2.

The Table 5.4.14 presents the lifetime improvement of EH methods as a function of R_{net}. The L_P and r are set to 128 byte and 0.8, respectively. Among all EH methods, indoor solar harvester performs the best network lifetime. The lifetime improvement is accomplished with at most $\%46$ for Mica2 with HARQ-II and $\%71$ for Telos with BCH(31,21,5) where R_{net} is 10 m.

		Lifetime Improvement (%)					
		Mica2					
R_{net} (m)	Harvester	ARQ	BCH(31,11,5)	BCH(31,21,5)	RS(15,11,5)	HARQ-I	HARQ-II
	Vibration	5.6	6	13	10	16	18
	Thermal	7	10	21	16	27	30
10	Indoor Solar	12	14	32	24	41	46
	Vibration	3.5	4	8	7	10	11
	Thermal	5	5	13	10	17	18
12	Indoor Solar	7	7	18	15	25	27
	Vibration	2	2	6	4	7	8
	Thermal	3	3.4	9	7	8	9
14	Indoor Solar	4	5	12	10	16	18
	Vibration	1.3	1.3	4	3	5	6
	Thermal	2	2	6	5	8	9
16	Indoor Solar	3	3	9	7	11	13
	Vibration	1	0.8	3	2	4	4
	Thermal	1.5	1.2	4	3	6	6
18	Indoor Solar	2	1.7	6	4	8	9
	Vibration	0.5	0.3	2	1.3	2.7	3
	Thermal	0.8	0.4	3	2	4	5
20	Indoor Solar	1	0.6	4	3	6	7
		Telos					
		ARQ	BCH,(31,11,5)	BCH(31,21,5)	RS(15,11,5)	HARQ-I	HARQ-II
	Vibration	4	18	25	17	20	23
	Thermal	6	29	44	28	35	39
10	Indoor Solar	8	45	71	43	54	62
	Vibration	3	13	20	13	16	18
	Thermal	4	21	33	21	26	30
12	Indoor Solar	7	31	52	30	40	46
	Vibration	2	9	15	10	12	14
	Thermal	3	15	24	15	19	23
14	Indoor Solar	4	21	37	22	29	34
	Vibration	1.5	7	12	8	10	11
	Thermal	2	11	20	12	15	18
16	Indoor Solar	3	16	29	17	22	26
	Vibration	1	6	11	7	8	10
	Thermal	1.5	9	17	11	13	16
18	Indoor Solar	2	13	24	16	19	23
	Vibration	0.8	4	8	5	6	7
	Thermal	1.3	7	12	7	9	11
20	Indoor Solar	1.7	9	17	10	13	16

Table 5.4.14. Lifetime improvement of different EH methods wrt. R_{net} and EC scheme

Simulation Parameters			
Sy/Ac/Vr	**Description**	**Unit**	**Value**
PL(d_0)	Path loss at distance, d_0 [31]	dB	63.57
d_0	Reference distance	m	0.5
P_n	Noise Floor	dBm	-93.0
P_t	Output antenna power	dB	0
q	Size of frame	bytes	128
γ_{ij}	Signal to Noise Ratio (SNR) over the link-(i,j)	dB	-
P_b	Bit Error Rate (BER)		-
B_N	Noise bandwidth	kHz	30
R	Data rate [1, 81]	kbps	19.2 (Mica2) and 250 (Telos)
H	Number of rounds	-	-
f_{ij}	Packet flows over link-(ij)	-	-
s_i	Generated data packet number	-	-
d_{ij}	Distance over link-(ij)	m	-
$p^s_{ij}(q)$	Packet success rate over link-(ij)	-	-
p^f_{ij}	Packet failure rate over link-(ij)	-	-
P_{tx}	Transmission power [96]	mW	5
P_{rx}	Reception power [96]	mW	21 (Mica2) and 69 (Telos)
P_{proc}	Processing power [2, 110]	mW	24 (Mica2) 0.9 (Telos)
P_{slp}	Sleep power [28]	mW	0.3 (Mica2) 0.16 (Telos)
E^k_{tx}	Transmission energy cost where $\forall k \in \{ARQ, FEC, HARQ\}$	J	-
E^k_{rx}	Reception energy cost where $\forall k \in \{ARQ, FEC, HARQ\}$	J	-
E_{dec}	Decoding energy cost	-	-
E_{acq}	Acquisition energy cost [7]	μJ	600
E_{elec}	Electronics energy cost [15]	nJ	50
$n_{ret,ij}$	Number of retransmission over the link-(i,j)	-	-
ϕ_{ij}	Packet success rate after retransmissions [123]	-	-
r	Reliability criteria		0.8
$T_{tx,ij}$	Transmission time	s	-
T_{rx}	Reception time	s	-
T_{rnd}	Turnaround time	s	20
T_{acq}	Acquisition time [7]	ms	20
$T_{busy,i}$	Busy time of node-i		-
t_{cycle}	Time period of cycle [81, 110]	ns	250 (Mica2) and 62.5 (Telos)
P_{harv}	Average harvested power [102]	mW	-
ξ	Battery energy	kJ	25
L_P	Size of packet	byte	128
L_A	Size of acknowledgement packet	byte	20
N	Size of data	byte	1024

Table 5.4.15. Simulation parameters

Chapter 6

Analysis of Compressive Sensing and Energy Harvesting for Wireless Multimedia Sensor Networks

6.1 Motivation

Wireless multimedia sensor networks (WMSNs) are qualified with transmitting and receiving multimedia data such as image and video. The main drawback of WMSNs applications is the huge data size that leads to extreme energy consumption in communication. Therefore, data size reduction methods to overcome this problem become necessary for WMSNs applications. Several image compression algorithms are introduced in literature [34, 64, 76]. However, while transmission energy cost decreases due to reduced data size, processing energy cost increases. Therefore, there is a trade-off between communication energy cost and computation energy cost in compression algorithms.

In recent years, Compressive Sensing (CS) algorithms are developed to reduce data to be transmitted. CS algorithms achieve the data with relatively fewer measurements than Nyquist theory. CS reduces the data at low complexity while sensing in order to decrease energy consumption in transmission. In addition, Energy Harvesting (EH) methods are utilized to extend the network lifetime. Therefore, the aim of this study is to examine the effect of the TC, CS and BCS methods on the WMSNs lifetime while considering the Error Control (EC) schemes to ensure the reliability. A novel Mixed Integer Programming (MIP) model which jointly considers EC schemes, data size reduction methods and EH methods to maximize the network lifetime.

6.2 Related Work

To provide energy efficient multimedia communication, there are studies that utilize data size reduction methods namely, compressive sensing and image compression and. Lecuire et. al [57] have introduced fast zonal Discrete Cosine Transofmation (DCT) design to reduce the energy consumption in processing stage. The number of operations are decreased without changing quality of image to save the energy hence, extend the lifetime of sensor node. Sun et. al [98] have suggested image compression with low energy algorithm. In that algorithm, they reduced the energy consumption by compressing interest point of image with low ratio whereas the remaining parts with high ratio. Therefore, the algorithm maintains the image quality. The performance results show that the algorithm can extend the network lifetime significantly. Wang et. al [116] have proposed the image compressive method which is energy efficient and low complexity. The block-based compressive sensing method divides image according to its interest region to decrease the energy consumption. Zang et. al [125] have introduced the adaptive block compressive sensing approach that varies the sampling rate based on whether the block of image is compressible or not. Blocks with interest region are less compressible while block with background are more compressible. Nandihini et. al [72] have introduced the novel sensing method based on Toeplitx matrix for compressive sensing approach. They have compared the proposed scheme with conventional Gausian matrix approach in terms of peak signal-to-noise ratio (PSNR), computational time, transmission energy and latency. Cao et. al [18] have introduced data collection algorithm by using CS to improve the network lifetime. They have proved that the proposed algorithm extend the network lifetime importantly. Hemalatha et. al [40] have suggested the image transmission approach by utilizing CS to reduce the data size hence, the transmission energy cost. They have developed the specific encoding algorithm based on Bernoulli matrix for CS measurement. The literature overview is presented in Table 6.2.16 where CM and AR denote channel model and application reliability, respectively.

Existing Studies	CM	EC	CS	AR	EH
[57]	✗	✗	✗	✗	✗
[98]	✗	✗	✗	✗	✗
[116]	✗	✗	✓	✓	✗
[125]	✗	✗	✓	✗	✗
[71]	✗	✗	✓	✗	✗
[18]	✗	✗	✓	✗	✗
[40]	✗	✗	✓	✗	✗
Proposed System	✓	✓	✓	✓	✓

Table 6.2.16. Literature overview

6.3 Evaluated Methods

In this section, we present the methods that are used in the study. We utilize the log normal shadowing model explained in Section 3.2. The detail explanation of utilized error control schemes is given in Section 3.2. The EH methods are given in Section 2.1, 2.2 and 2.3, respectively. The image transmission methods and compressive sensing are shown below. Finally, the proposed MIP model with node-level EC strategy is given below.

6.3.1 Compressive Sensing Method

A signal is obtained with Nyquist rate to properly reconstruct it in traditional signal processing. The representation of obtained signal is given by $x \in R^N$ [17]. Any vector in R^N is defined as a linear combination of basis vectors, $\{\psi_i\}_i^N$ which is given by

$$x = \sum_{i=1}^{N} s_i \psi_i \qquad x = \Psi s, \tag{6.1}$$

where ψ is the basis matrix with i^{th} column ψ_i. N is required number of measurements to obtain the full signal.

A signal is called K-sparse if there are K number of non-zero coefficients. In image compression, the all signal (*i.e.,* N measurements) is obtained and only the K coefficients of the signal where $K < N$ are encoded for transmission. However, in CS only the number

of random measurements determined by $M \geq \alpha K \log(N/K)$ are obtained and transmitted. For truly reconstruct the signal, M number of measurements where $M << N$ are required.

The signal recovery is done by solving the minimum l_1-norm optimization problem shown below

$$\min \|s\|_{l_1} \quad s.t. \quad y = \Phi \Psi s. \tag{6.2}$$

6.3.2 Image Transmission Methods

The N byte raw image data is acquired and relayed to the sink node with one or more hop in No Processing (NP) method. Since there is no processing, the energy is consumed only by transmission and reception. Thus, only transmission and reception energy are calculated for NP method in lifetime analysis. However, in image compression (*i.e.,* Transform Coding (TC)) method, the obtained N byte raw image is processed to be compressed. The raw image is separated into 8x8 image blocks. Each block is transformed into frequency domain by using DCT. K greatest values are computed to acquire K-sparse signal. The compressed K-sparse signal is transmitted. The received K values are decoded and located to their positions. Finally, Inverse DCT (IDCT) is implemented to reconstruct the image.

In CS method, the image is separated into 8x8 blocks to make them sparse by using DCT. The number of measurements (*i.e.,* M) determined in accordance with sparsity level are obtained and transmitted to the receiver. The receiver reconstructs the image from K-sparse signals. The BCS method introduced by Hemelatha et. al [40] makes separated image blocks to sparse by utilizing Binary DCT (BinDCT). BinDCT eliminates the multiplication operations in order to reduce computation complexity. For TC, CS and BCS besides communication energy (*i.e.,* transmission and reception energy), the computation energy is also examined in the network lifetime analysis. The computation energy is determined by

$$E_{cmp} = P_{proc} \times T_{cmp}, \tag{6.3}$$

where P_{proc} and T_{cmp} denote the processing power and the computation time.

6.3.3 Mixed Integer Programming Model

The aim of the MIP with node-level EC strategy framework presented in Figure 6.3.25 is to optimize lifetime. The MIP model with network-level MIP model approach presented at previous chapter is extended to node-level EC scheme approach. In this approach, each sensor node selects the EC schemes in each transmission from the set E (*i.e.,* E ={ARQ, BCH(31,11,5), BCH(31,21,5), RS(15,11,2), HARQ-I, HARQ-II}). For instance, node-5 may utilize the ARQ while transmitting data to node-10 whereas

Maximize H
Subject to:

$$f_{ij}^{k} \geq 0, \forall (i,j) \in A, \forall (k) \in E \tag{6.4}$$

$$f_{1j}^{k} = 0, \forall (j) \in W, \forall (k) \in E \tag{6.5}$$

$$\sum_{k \in E} \sum_{(i,j) \in A} f_{ij}^{k} - \sum_{k \in E} \sum_{(j,i) \in A} f_{ji}^{k} \times \phi_{ji}^{k} = H \times s_i, \forall i \in W \tag{6.6}$$

$$\sum_{k \in E} \sum_{(j,1) \in A} f_{j1}^{k} \times \phi_{j,1}^{k} \geq \sum_{i \in W} s_i \times H \times r, \forall i \in W \tag{6.7}$$

$$\begin{aligned} T_{busy,i} = & \sum_{k \in E} \sum_{i \in W} T_{tx,ij}^{k} \times f_{ij}^{k} \times n_{ret,ij}^{k} \\ & + \sum_{i \in W} T_{rx,ji}^{k} \times f_{ji}^{k} \times n_{ret,ji}^{k} \\ & + H \times (T_{acq} + T_{cmp}), \forall i \in W \end{aligned} \tag{6.8}$$

$$\begin{aligned} & \sum_{k \in E} \sum_{j \in W} E_{tx,ij}^{k} \times f_{ij}^{k} + \sum_{k \in E} \sum_{j \in W} E_{rx,ji}^{k} \times f_{ji}^{k} \\ & + H \times (E_{acq} + E_{cmp}) + P_{slp} \times (H \times T_{rnd} - T_{busy,i}) \\ & - P_{harv} \times T_{harv} \times H \leq \xi, \forall i \in W \end{aligned} \tag{6.9}$$

$$\begin{aligned} (L_P + L_A) \times & \sum_{k \in E} \sum_{j \in W} f_{ij}^{k} \times n_{ret,ij}^{k} + \sum_{k \in E} \sum_{j \in W} f_{ji}^{k} \times n_{ret,ji}^{k} \\ & \leq \varsigma \times H \times T_{rnd} \forall i \in V \end{aligned} \tag{6.10}$$

Figure 6.3.25. The MIP framework

may utilize BCH(31,21,5) to node-25. In this chapter, the N byte image transmission is analyzed, hence s_i is estimated as $s_i = \lceil \frac{N}{L_P - L_H} \rceil$.

f_{ij}^k denotes the packet flows by using EC method type-k over link-(ij). Equation (7.1) and (7.2) defines the flow constraints of sensor nodes and sink node, respectively. Equation (7.1) ensures that the flows can not take negative value. Equation (7.2) ensures sink node does not produce packet. Equation (7.3) provides the flow balance constraint so that the outgoing packets from node-i is equal to the sum of incoming packet to node-i and generated packet of node-i. Equation (7.4) ensures the reliability criteria where at least r percent of all generated packets should be received by sink node. In equation (7.5), $T_{busy,i}$ calculates the busy time of node-i. $n_{ret,ij}^k$ is the number of retransmission by using EC scheme type k. Equation (7.6) indicates the energy balance constraint which guarantees that total amount of energy that node-i consumes for communication, acquisition and computation can not exceed the summation of battery energy and harvested energy. P_{harv} and T_{harv} are average harvested power and harvesting duration, respectively. Equation (7.7) states that channel bandwidth should be larger than the required bandwidth for communication.

6.4 Performance Analysis

In performance evaluations, the random disk shaped network topology where the radius of network is denoted as R_{net} is created. The sink node (*i.e.,* node-1) is paced at point-(0,0). In every hour, sensor nodes relay the N byte image to the sink node. The four types image transmission methods (*i.e.,* NP, TC, CS and BCS) are defined in this study. The MIP with node-level EC strategy is formulated by considering energy dissipation of EC schemes and communication and computation energy consumption of image transmission methods for lifetime maximization. Moreover, in order to prolong the network lifetime, the EH methods scavenge energy for 10 minutes in each round. The communication and computation energy calculations are done by using MATLAB while the MIP model is solved by utilizing General Algebraic Modelling System (GAMS). The presented simulation results in figures are acquired by taking average values of 100

Channel Characteristics		
	Description	**Value**
PL(d_0)	Path loss at distance, d_0 [31]	63.57 dB
d_0	Reference distance	0.5 m
n	Path loss exponent	2.40
σ	Shadowing standard deviation	4.79 dB
P_n	Noise Floor	-93.0 dBm
P_t	Output power	0 dB
R	Data rate	19.2 kbps
B_N	Noise bandwidth	30 kHz kbps
Hardware Characteristics		
	Description	**Value**
P_{tx}	Transmission power	5 mW
P_{rx}	receiving power [96]	21 mW
P_{proc}	Processing power [110]	24 mW
P_{slp}	Sleep power [28]	0.3 mW
ξ	Initial battery energy	25 kJ
t_{cycle}	Cycle duration [110]	250 ns
E_{acq}	Acquisition energy [10]	600 μJ
T_{acq}	Acquisition time	20 ms
E_{elec}	Electronics energy	50 nJ
L_P	Payload size	128 byte
L_A	Acknowledgement size	20 byte

Table 6.3.17. Channel and hardware parameters

different trials. Channel and hardware parameters are presented in Table 6.3.17.

Figure 6.4.26 presents the lifetime improvement of TC, CS, BCS methods as a function of R_{net}. The lifetime improvement is estimated by determining the percent increment between when network utilizes TC, CS or BCS and when network utilizes NP. BCS improve the lifetime at most compared to other methods. Since the required computational energy for compressing the image is very low in BCS method. In smaller network, when R_{net} is less than 12 m, to compress image with TC and CS is not energy efficient. Therefore, in that case the lifetime improvement takes negative values. The lifetime improvement of TC is higher than CS. Despite the fact that the computation energy needed for TC and CS are close, the transmission energy of CS is higher due to lower compression ratio. Figure 6.4.27 illustrates the lifetime improvement with respect

Method	Compression rate (bpp)		
	K = 2	**K = 3**	**K = 4**
TC	0.55	0.8	1.03
CS	1.49	2.25	3.17
BCS	0.59	1.44	2.26
Method	**Execution Times (ms)**		
	K=2	**K=3**	**K=4**
TC	80.39	80.58	80.77
CS	79.09	80.85	83.74
BCS	12.50	14.74	17.59

Table 6.4.18. Rate and execution times of compressing an 8x8 image block wrt. different sparsity level

	Average Solution Times (s)			
$\mathbf{R_{net}(m)}$	**NP**	**TC**	**CS**	**BCS**
10	2.24	1.30	1.50	1.33
12	2.05	1.25	1.40	1.38
14	1.95	1.44	1.36	1.35
16	2.04	1.43	1.26	1.30
18	1.79	1.09	1.40	1.31
20	1.73	1.06	1.33	0.88

Table 6.4.19. Average solution times for different image transmission methods

to the reliability rate. As the reliability rate of network increases, the network lifetime decreases. Since, mostly communicate over certain nodes to ensure the reliability reduces the network lifetime. However, the reason for the increase in lifetime improvement as the reliability rate gets higher is that the effect of TC, CS and BCS becomes more evident. In other words, the contribution of TC, CS and BCS are greater when the desired application reliability is high. Figure 6.4.28 illustrates the lifetime improvement of TC, CS and BCS as a function of sparsity level. The execution time and compression ratio for various sparsity level is given in Table 6.4.18 [40]. As the sparsity level increases, both the compressed data size and the execution times for TC, CS and BCS increase. The increase of compressed data size means the increase of data to be transmitted which leads more energy consumption in communication. In addition, the increase in execution times cause more energy consumption in computation of image. Therefore, the lifetime improvement decreases.

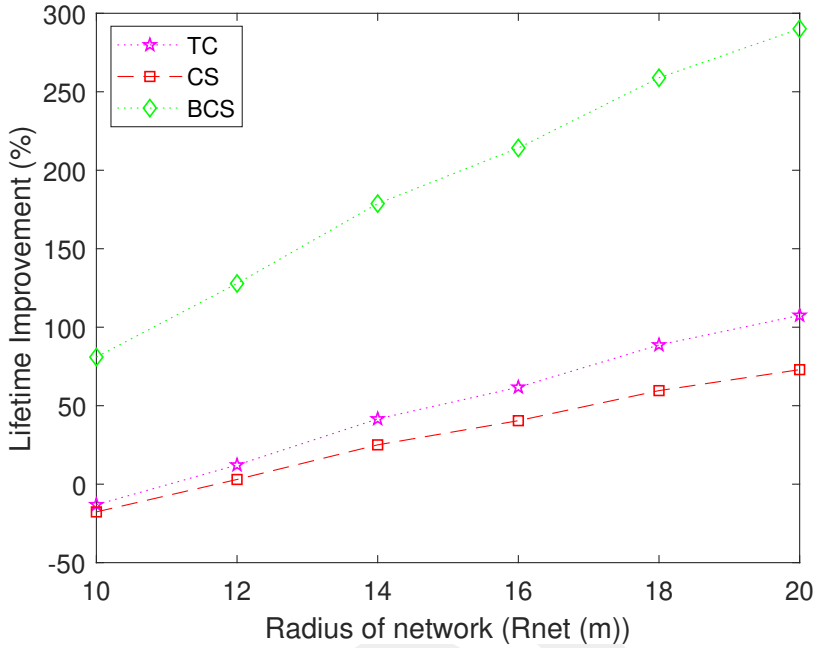

Figure 6.4.26. Lifetime improvement of various data size reduction methods wrt. radius of network

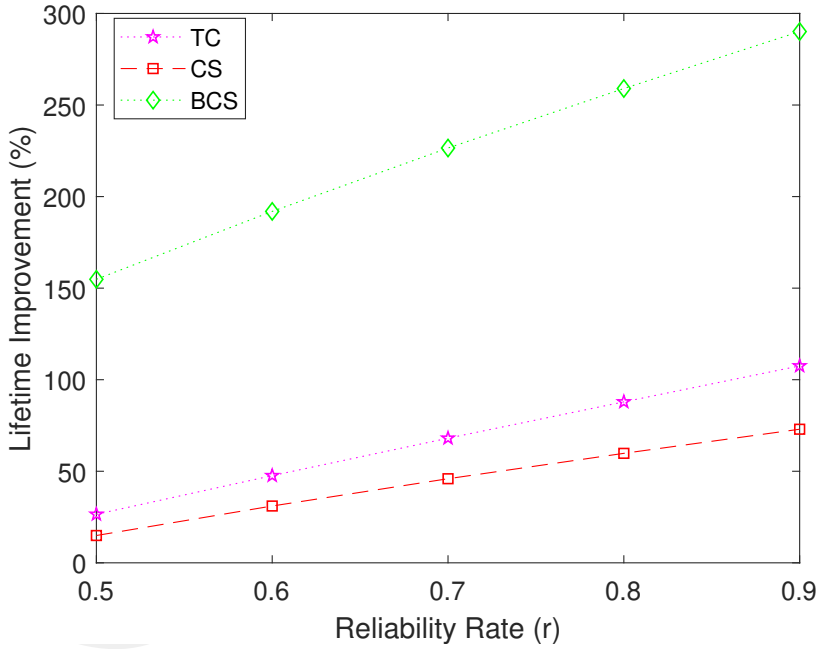

Figure 6.4.27. Lifetime improvement of various data size reduction methods wrt. sparsity level

Figure 6.4.29 illustrates the contribution of EH methods on lifetime as a function of R_{net} when network utilizes NP as a image transmission method. The lifetime improvement of EH methods decreases while R_{net} is increasing. ISH acquires the gratest improvement compared to other EH methods which is at most 13 $\%$ where R_{net}, r and K are set to 10

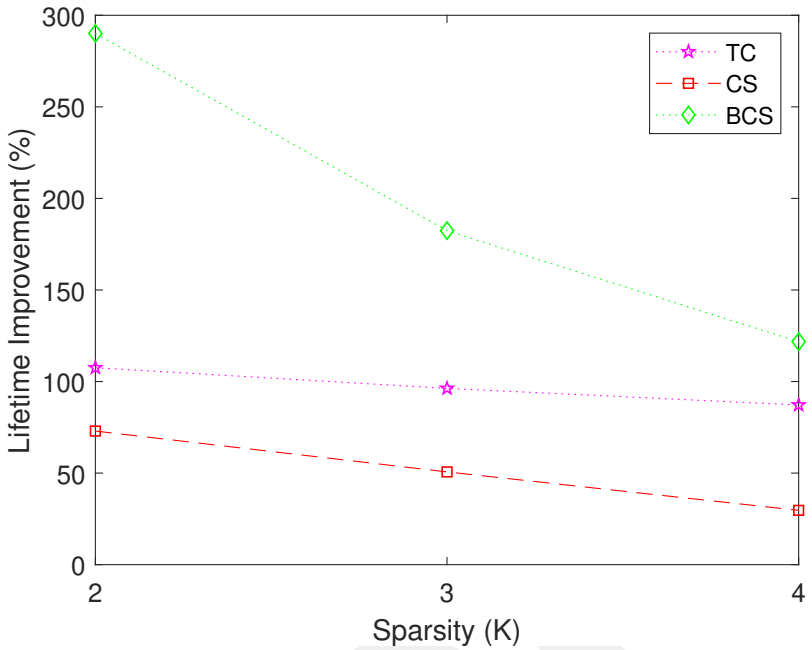

Figure 6.4.28. Normalized lifetime of various data size reduction methods wrt. reliability rate

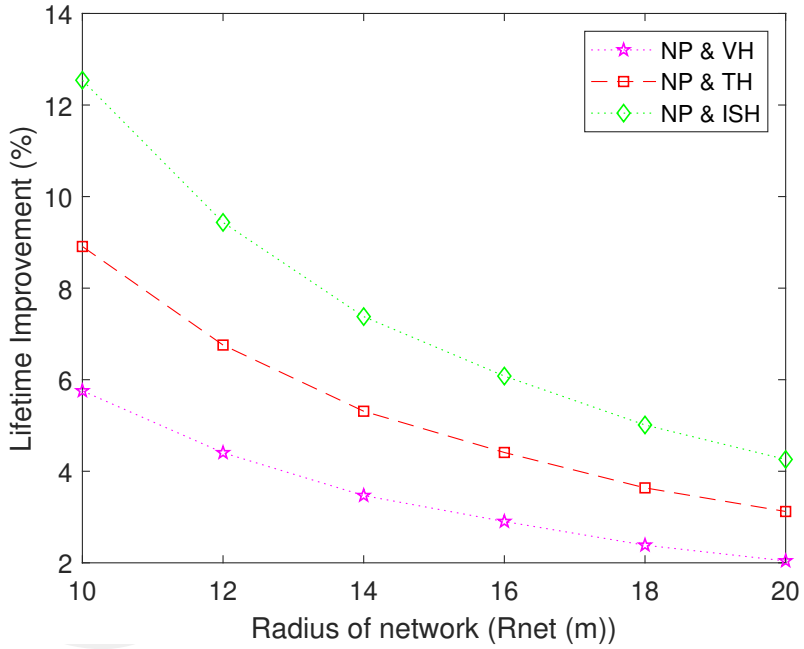

Figure 6.4.29. Lifetime improvement of various EH methods wrt. radius of network

m, 0.9 and 2, respectively. Figure 6.4.30 shows the lifetime improvement of EH methods with regard to r. As the r increases, the contribution of EH methods decreases. The 13 $\%$ improvement when r is set to 0.9 increases to 22 $\%$ when r is set to 0.5. Since the performance of ISH is the best for lifetime improvement, ISH is used as EH methods for

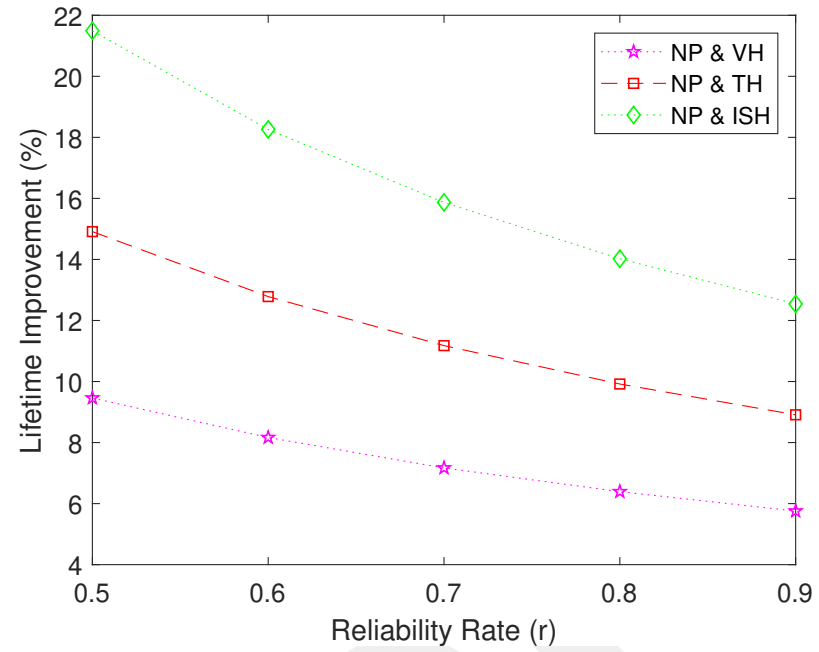

Figure 6.4.30. Lifetime improvement of various EH methods wrt. reliability rate

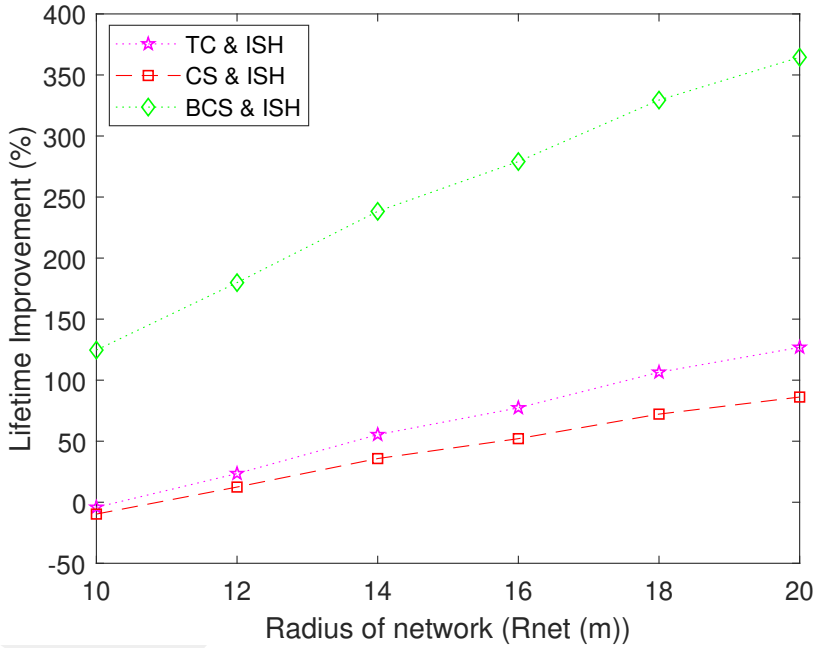

Figure 6.4.31. Lifetime improvement of joint utilization of EH methods and data size reduction methods wrt. radius of network

the next simulations. Figure 6.4.31 presents the lifetime improvement when the network utilizes TC, CS and BCS with ISH as a function of R_{net}. The network using TC with ISH improves the lifetime with 126 %. The network using CS with ISH improves the lifetime with 86 %. The best lifetime with 364 % is observed when network uses BCS with ISH.

The proposed MIP model is a NP-hard problem thus the time complexity of solving this problem is very high. To reduce the time complexity, the efficient heuristics are used. In this study, Linear Programming (LP) relaxation method is performed to provide solution in a polynomial time. The average solution times are given in Table 6.4.19. The simulations are performed on Intel i5 machine with 12 GB RAM. The average solution time for BCS is at most 1.38 s and at least 0.88 s. The average solution time for CS is at most 1.50 s and at least 1.26 s. Finally, the average solution time for NP is at most 2.24 s and at least 1.73 s.

Chapter 7

Node-Level Error Control Strategies for Prolonging the Lifetime of Industrial Wireless Sensor Networks

7.1 Motivation

The limited energy of sensor nodes and providing reliability are two main drawbacks of IWSNs applications. To improve the reliability of applications, Error Control (EC) schemes such as ARQ, FEC, HARQ are utilized. However, utilizing EC schemes to ensure the reliability of network burdens significant energy consumption to sensor nodes. Therefore, there is a decrease in network lifetime. In Chapter 5, we developed Mixed Integer Programming (MIP) model with network-level EC scheme approach (*i.e.,* all sensor nodes utilize the same type of EC scheme) for lifetime maximization. However, utilizing ARQ and HARQ are efficient in terms of energy cost for shorter links whereas utilizing FEC is energy efficient for longer longer links. To this end, we provide MIP model with node-level EC scheme approach (*i.e.,* each node selects optimum type of EC methods for different links in terms of and reliability and energy cost). MIP with node-level EC scheme approach further extends the network lifetime compared to network-level EC scheme approach. On the other hand, to obtain exact solution of MIP model with node-level EC scheme approach in a polynomial time is not feasible especially for larger networks. For this purpose, we develop various meta-heuristics in order to reduce time complexity of MIP model. In this study, we perform Golden Section Search (GSS), Extended GSS (EGSS), Simulated Annealing (SA), Extended SA (ESA) and Genetic Algorithms (GA) algorithms as a meta-heuristic solution for our MIP model with node-level EC scheme approach.

7.2 Related Work

There are number of studies that utilize the mathematical programming in optimization problems for WSNs [29, 52, 126]. Fateh et. al [29] proposed Mixed Integer Linear Programming (MILP) to optimize the energy consumption of network which is interference aware. In addition, they provide three phase heuristics for their minimization problem. Kahjogh et. al [52] proposed MIP framework to evaluate the effect of disabling critical nodes in terms of latency. Tan et. al [100] have proposed MIP model to optimize both network lifetime and video encoding rate by performing network coding and ARQ as an EC scheme. Zhang et. al [124] have proposed the energy efficient HARQ. They have formulated to maximize the network lifetime while considering the reliability.

Meta-heuristic methods are significant for practically solving the optimization problems in WSNs. The meta-heuristic methods are designed for providing a near optimal solution in feasible time. Since WSNs optimization problems are mostly NP-hard where there is no solution in polynomial time, there are studies employ the meta-heuristics to their problem [69, 91, 115, 119, 122]. Xenakis et. al [119] performed Simulated Annealing (SA) heuristics to combined optimization of topology and transmit power for lifetime maximization. In another study [118], they also have studied the cross layer aware topology optimization by using SA. In cross layer approach, they consider both channel model and EC methods in consumed energy minimization. Pinto et. al [80] proposed self optimization approach by utilizing SA heuristic to provide autonomous communication efficiency. Shekofteh et. al [95] employed tabu search and SA heuristics in localization of WSNs. Yildiz et. al [122] presented MIP framework to maximize network lifetime while providing non-repudiation security. They consider communication energy and computation energy model of Digital Signature (DS) algorithm. To solve their NP-hard MIP problem in a polynomial time, they provide heuristic such as SA and GSS. Hosseini et. al [41] presented GA heuristic for their multi-objective optimization problem where reliability and power consumption are evaluated. In addition, they proposed GA with hierarchical sub-chromosome to solve the problem in less time. Abo-Zahhad et. al [4] developed the clustering algorithm based on GA. The algorithm identifies the optimum number of cluster nodes for network maximization. Bhatia [14] et. al introduced routing

Existing Studies	CM	EC	MP	LM	HM
[29]	✗	✗	✓	✗	✓
[52]	✗	✗	✓	✗	✗
[124]	✗	✓	✗	✓	✗
[100]	✗	✓	✓	✓	✗
[91], [115], [69], [122]	✗	✗	✓	✗	✓
[118]	✓	✓	✗	✓	✓
Proposed System	✓	✓	✓	✓	✓

Table 7.2.20. Literature overview

protocol based on GA for WSNs. They utilized GA to optimally determine the cluster head nodes in the WSNs. They defined fitness function by jointly evaluating the remaining energy of node and distance between cluster heads to other sensor nodes. The literature overview is presented in Table 7.2.20 where CM, MP, LM and HM denote the channel model, mathematical programming, lifetime maximization and heuristic methods, respectively.

In Chapter 5, we developed MIP model for network-level EC scheme approach [104] and nodel-level EC control scheme approach on multimedia communication [103] to maximize the network lifetime. Although MIP model gives the exact solution, its time complexity limits the number of sensor nodes to be computed. Hence, in this thesis, we propose meta-heuristics algorithm such as GSS, EGSS, SA, ESA and GA to overcome time complexity of our MIP problem.

7.3 Evaluated Methods

In this section, we provide methods that are used in this chapter. The MIP model with node-level EC scheme approach is formulated. The utilized meta-heuristic methods are explained. The channel model and energy dissipation of link layer model are given in Chapter 3.

Maximize H
Subject to:

$$f_{ij}^{k} \geq 0, \forall (i,j) \in A, \forall (k) \in E \tag{7.1}$$

$$f_{1j}^{k} = 0, \forall (j) \in W, \forall (k) \in E \tag{7.2}$$

$$\sum_{k \in E} \sum_{(i,j) \in A} f_{ij}^{k} - \sum_{k \in E} \sum_{(j,i) \in A} f_{ji}^{k} \times \phi_{ji}^{k} = H \times s_i, \forall i \in W \tag{7.3}$$

$$\sum_{k \in E} \sum_{(j,1) \in A} f_{j1}^{k} \times \phi_{j,1}^{k} \geq \sum_{i \in W} s_i \times H \times r, \forall i \in W \tag{7.4}$$

$$\begin{aligned} T_{busy,i} = & \sum_{k \in E} \sum_{i \in W} T_{tx,ij}^{k} \times f_{ij}^{k} \times n_{ret,ij}^{k} \\ & + \sum_{i \in W} T_{rx}^{k} \times f_{ji}^{k} \times n_{ret,ji}^{k} \\ & + H \times T_{acq}, \forall i \in W \end{aligned} \tag{7.5}$$

$$\begin{aligned} & \sum_{k \in E} \sum_{j \in W} E_{tx,ij}^{k} \times f_{ij}^{k} + \sum_{k \in E} \sum_{j \in W} E_{rx,ji}^{k} \times f_{ji}^{k} \\ & + H \times E_{acq} + P_{slp} \times (H \times T_{rnd} - T_{busy,i}) \leq \xi, \forall i \in W \end{aligned} \tag{7.6}$$

$$\begin{aligned} (L_P + L_A) \times \sum_{k \in E} \sum_{j \in W} f_{ij}^{k} \times n_{ret,ij}^{k} + \sum_{k \in E} \sum_{j \in W} f_{ji}^{k} \times n_{ret,ji}^{k} \\ \leq \varsigma \times H \times T_{rnd} \forall i \in V \end{aligned} \tag{7.7}$$

Figure 7.3.32. The MIP framework with node-level EC strategy

7.3.1 Mixed Integer Programming Model

The main difference between model formulated in Chapter 6 Figure 6.3.25 and the MIP model defined in this chapter is that the type of data. In Chapter 6, we consider the image data to be transmitted and we provide data size reduction methods to decrease the size of data. Therefore, the computation energy should be considered in energy balance constraint of that model. In addition, we use EH methods that also effect the energy constraint of the MIP model. However, we provide MIP model with node-level EC scheme approach for scalar data transmission to compare it with MIP model with network-level EC

scheme approach defined in Chapter 5 Figure 5.2.19. In network-level approach, a single EC scheme type is applied to all data transmission. In other words, all sensor nodes in the network use the same type EC scheme while transmitting data. In node-level approach as shown in Figure 7.3.32, each node selects the different EC scheme according to link quality. k takes value of one of the EC scheme types from set E (*i.e.,* E =ARQ, BCH(31,11,5), BCH(31,21,5), RS(15,11,2), HARQ-I, HARQ-II) for each node. V indicates the set of all sensor nodes whereas W indicates set of all sensor nodes except sink node (*i.e.,* $W = V \backslash \{1\}$). A denotes the link between node pairs. s_i is number of data that sensor nodes produce in every round where it is calculated as $s_i = \lceil \frac{N}{L_P - L_H} \rceil$ where N is the data size in byte. L_P and L_H denote the packet payload and header size, respectively. The network lifetime is described as duration until the first node in the network deplete its all energy. The network lifetime is detemined by $H \times T_{rnd}$ where T_{rnd} is the time period of a round and H is the number of round.

f_{ij}^k is the packet flows by using EC schemes type-k over link-(i,j). Equation (7.1) and (7.2) defines the flow constraints of sensor nodes and sink node, respectively. Equation (7.1) ensures that flows can not take negative value. Equation (7.2) guarantees that sink node does not generate packet. Equation (7.3) provide flow balance so that he sum of incoming packets (*i.e.,* $\sum_{k \in E} \sum_{(j,i) \in A} f_{ji}^k \times \phi_{ji}^k$) and generated packets during the lifetime (*i.e.,* $H \times s_i$) should be equal to the number of outgoing packets (*i.e.,* $\sum_{k \in E} \sum_{(i,j) \in A} f_{ij}^k$). Equation (7.4) is the reliability constraint that states at least r percent of all generated data packets during network lifetime (*i.e.,* $\sum_{i \in W} s_i \times H \times r$) is received by sink node. In equation (7.5), $T_{busy,i}$ calculates the busy time of node-i. $n_{ret,ij}^k$ is the number of retransmission by using EC scheme type-k. Equation (7.6) indicates the energy balance constraint which guarantees that total amount of consumed energy should be less than battery energy. Equation (7.7) states that the required bandwidth for communication is less than the channel bandwidth.

7.3.2 Heuristic Methods

From the simulations of node-level approach on small size of network, we noticed that sensor nodes mostly utilize HARQ-II and BCH(31,21,5) as an error control scheme in order to reach maximum solution. Thus, our problem is turned into binary selection

problem. In other words, which sensor node use HARQ-II and which use BCH(31,21,5) to optimize the lifetime.

The sensor nodes in the network are represented in a set (*i.e.,* $\mathbb{S} = \{S_1, S_2, S_3, ...S_{|V|}\}$) where N is the number of sensor nodes. A solution is defined as vector whose size is number of nodes (*e.g.,* S=[0 0 1 .... 1]) in which each element corresponds a sensor node in a network. The sensors took value of 0 use BCH(31,21,5) and 1 use HARQ-II (*e.g.,*. $S_2 = 1$, node-2 uses HARQ-II). This solution vector structure is utilized by all heuristic methods below.

7.3.2.1 Golden Section Search

The golden-section search method is utilized for searching an maximum of objective function inside a specified interval in our problem. The main idea is to determine how many sensor nodes use HARQ-II and how many of them use BCH(31,21,5) to find an maximum lifetime. GSS linearizes the MIP model by pre-determining the which nodes use which error control scheme.

The numbers $|V|$, lb, ub and Φ denote the number of sensor nodes in the network, lower bound and upper bound of interval and the golden ratio, respectively. Initially, we set the boundaries lb to 0 and ub to number of sensor nodes minus 1. We define interior points λ_1 and λ_2 (*i.e.,* $lb < \lambda_1 < ub$) to determine which nodes use HARQ-II and which use BCH(31,21,5). In other words, started from the second nodes to $\lambda_1 + 1$ nodes use HARQ-II (*i.e.,* $S_i = 1, \forall i \in \{2, 3, .., \lambda_1 + 1\}$), the rest of them use BCH(31,21,5) (*i.e.,* $S_i = 0, \forall i \in \{\lambda_1 + 2, ..., |V|\}$). The same step is done for λ_2. Then, the lifetime values are computed according to λ_1 and λ_2 values and assigned to β_1 and β_2, respectively. While searching the maximum lifetime, GSS updates the interval according to current lifetimes. If $\beta_1 < \beta_2$, the upper bound of interval is updated to $ub = \lambda_2$. If $\beta_1 >= \beta_2$, the lower bound of is updated to $lb = \lambda_2$. Repeat this narrowing process until interval is less than 1 (*i.e.,* $[ub - lb] < 1$). The algorithm returns lb that indicates the threshold number of sensor nodes that use HARQ-II. To be more clear, from sensor node 2 to lb use HARQ-II and from $lb + 1$ to $|V|$ use BCH(31,21,5). Therefore, the maximum lifetime is obtained by this optimum interval value.

In addition, we observed that the sensor nodes closer to the sink node mostly utilize HARQ-II and further nodes mostly utilize the BCH(31,21,5) in node-level EC scheme

approach. The reason for that closer sensor nodes are often used as relay nodes result in more energy consumption. Therefore, for these nodes energy efficient EC schemes become more critical. On the other hand, further nodes utilize multi-hop transmission. Each hop they may loose the data or have error on received data. Therefore, it is more important for them to reliable transmission than the energy efficiency. Based on this, we extended our GSS heuristic (EGSS) so that HARQ-II is set to sensor nodes closer to the sink and BCH(31,21,5) is set to further ones. This means that, $\lambda_1 + 1$ (or $\lambda_2 + 1$) nodes closest to the sink node use HARQ-II and the others use BCH(31,21,5). At each iteration the lifetime values (*i.e.,* β_1 and β_2) is calculated according to the this rule.

Algorithm 1: Golden Section Search

1: Input parameter: Number of nodes ($|V|$).
2: Initialize parameters: Lower bound ($lb \leftarrow 0$), Upper bound ($ub \leftarrow |V| - 1$), Golden ratio ($\Phi \leftarrow (-1 + \sqrt{(5)})/2$). Compute $\lambda_1 \leftarrow \lceil (ub - \Phi \times (ub - lb) \rceil$ and $\lambda_2 \leftarrow \lfloor (lb + \Phi \times (ub - lb) \rfloor$.
3: Apply the first $\lambda_1 + 1$ nodes to HARQ-II and the other nodes to BCH(31,21,5). Compute the lifetime and assign it to the β_1. Apply the first $\lambda_2 + 1$ nodes to HARQ-II and the other nodes to BCH(31,21,5). Compute the lifetime and assign it to the β_2. Compare lifetime values, β_1 and β_2. Narrow the interval, accordingly.

if *($\beta_1 < \beta_2$)* **then**

$ub \leftarrow \lambda_2$;
$\lambda_2 \leftarrow \lambda_1$;
$\lambda_1 \leftarrow \lceil ub - \Phi \times (ub - lb) \rceil$;

else

$lb \leftarrow \lambda_1$;
$\lambda_1 \leftarrow \lambda_2$;
$\lambda_2 \leftarrow \lfloor lb + \Phi \times (ub - lb) \rfloor$;

4: Repeat step 3 until termination criteria ($\mid ub - lb \mid < 1$) is met.
5: Output result: $2 < i < lb \leftarrow$ HARQ-II and $lb + 1 < i < |V| \leftarrow$ BCH(31,21,5)

7.3.2.2 Simulated Annealing

We also apply Simulated Annealing (SA) heuristic algorithm to search near optimal solution for our optimization model. The basic idea of SA is that it selects the random move while searching local optimal instead of best move. If it is better, it is always accepted. Otherwise, the random move is accepted with a probability which decreases exponentially depending on the badness of move. The reason for the worse move acceptance is to prevent being stuck in local optimal and to search optimal globally.

The SA algorithm applied to our problem is presented in Algorithm 2. In this algorithm, input parameters which are number of nodes ($|V|$), temperature (q), cooling parameter (α), and maximum cycle number (maxCycle) are defined.

Initially, the half of the current solution is set to 1 (*i.e.,* $S_i = 1, \forall i \in \{2, 3, .., \lceil \frac{|V|}{2} \rceil\}$) and remaining of them to 0 (*i.e.,* $S_i = 1, \forall i \in \{\lceil \frac{|V|}{2} \rceil + 1, ..., |V|\}$). The means of that half of the sensor nodes use HARQ-II and the remaining ones use BCH(31,21,5). The current lifetime is obtained from current solution. Then, candidate solution which is found by complementing error control schemes (*i.e.,* HARQ-II or BCH(31,21,5)) of a randomly selected neighbour node is created. For instance, if a randomly selected neighbour node uses HARQ-II, it switches to use BCH(31,21,5) or vice versa. The candidate lifetime is calculated by using candidate solution. If candidate lifetime is greater than the current lifetime, update current solution and lifetime with candidate solution and lifetime. Otherwise, update the current solution and lifetime with a probability (*i.e.,* $rand() < e^{(\Delta Obj/q)}$). The algorithm search for candidate solution until maximum number of cycle is reached.

As we did in GSS, we extend SA algorithm (ESA) to reach optimal solution. To this end, the initial solution vector is constructed as the half of the sensor nodes closest to the sink use HARQ-II and the others use BCH(31,21,5). While creating candidate solution, the distance of random neighbour node to the sink is checked. If distance is smaller than some threshold distance value, it is forced to use HARQ-II. Otherwise, it is forced to use BCH(31,21,5). Therefore, sensor nodes close to the sink up to a certain threshold mostly use HARQ-II and others use BCH(31,21,5).

7.3.2.3 Genetic Algorithm

Genetic Algorithm (GA) starts with defining population with set of solution vectors called chromosomes. Each chromosome in population is evaluated considering fitness function. The fitness function is maximization in our problem. While searching more fit chromosome from population, crossover and mutation stages are applied to chromosomes. Mutation is used in GA to avoid the local optimum values.

The GA algorithm applied to our problem is presented in Algorithm 3. In this algorithm, input parameters which are population size ($popSize$), maximum generation ($maxGen$) and mutation probability ($mutProb$) are initialized. Initially, population (P)

Algorithm 2: Simulated Annealing

1: Input parameters: Number of nodes ($|V|$), Initial temperature (q), Cooling parameter (α), and Maximum cycle number ($maxCycle$)
2: Initialize the parameters: Count ($count \leftarrow 0$), and Best Lifetime ($bestLifetime \leftarrow 0$). Find initial solution, keep them as a current solution and best solution ($currentSolution$ and $bestSolution$). Compute the lifetime by using current solution and keep it as a current lifetime and also best lifetime ($currentLifetime$ and $bestLifetime$).
3: Assign the temperature ($q \leftarrow q \times \alpha$). Find the candidate solution ($candidateSolution$) by taking complement of one element in current solution. Compute its lifetime and set it as a candidate lifetime ($candidateLifetime$).

if *candidateLifetime>currentLifetime* **then**
$currentLifetime \leftarrow candidateLifetime$;
$currentSolution \leftarrow candidateLifetime$;
if $candidateLifetime > bestLifetime$ **then**
$bestLifetime \leftarrow candidateSolution$;
$bestSolution \leftarrow candidateSolution$;

$count = count + 1$;
$\Delta Obj \leftarrow currentLifetime - bestLifetime$. Assign $candidateSolution$ to $currentSolution$ with $e^{(-\Delta Obj/q)}$ probability.
4: Repeat step 3 until termination criteria (count > maxCycle) is met.
5: Output result : bestLifetime

Algorithm 3: Genetic Algorithm

1: Input parameters: Population size ($popSize \leftarrow 10$), Maximum generation ($maxGen \leftarrow 100$), Mutation probability ($mutProb \leftarrow 0.15$)
2: Initialize parameters: Generation ($gen \leftarrow 0$), Generate population with random chromosomes ($P \leftarrow \{C_1, C_2, ...C_{popSize}\}$) , Determine the chromosome with best lifetime from population ($bestLifetime \leftarrow BestLifetime(P)$).
3: Select two chromosomes according to Roulette Wheel selection algorithm $\{C^{P1}, C^{P2}\} \leftarrow RoulettteWheel(P)$. Crossover the selected chromosomes $C^{new} \leftarrow CrossOver(C^{P1}, C^{P2})$ Mutate random gene of chromosome with a probability $C^{new} \leftarrow Mutation(C^{new})$
4: Calculate the lifetime of new chromosome (C^{new}).
$newLifetime \leftarrow CalculateLifetime(C^{new})$;

if $newLifetime > bestLifetime$ **then**
Select chromosome with worst lifetime from population
$C^{worst} \leftarrow SelectWorseChromosome(P)$;
Remove it from population
P.remove(C^{worst});
Add new chromosome to population
P.add(C^{new});

gen=gen+1;
5: Repeat steps 3-4 until termination criteria ($gen > maxGen$) is met.
6: Output: bestLifetime

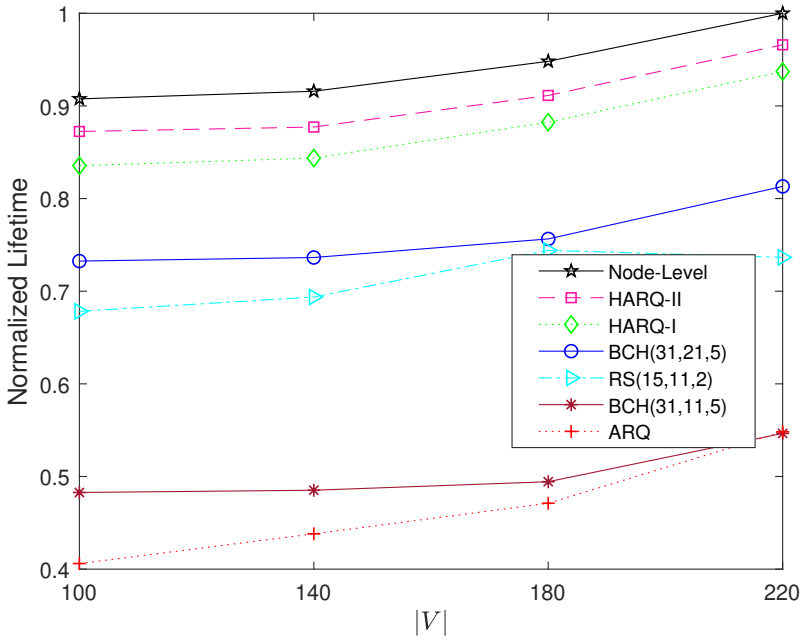

Figure 7.3.33. Normalized lifetime comparison of Network-level EC scheme approaches against Node-Level EC scheme approach

contains random solution vectors which are called chromosome as much as population size (*i.e.,* $P \leftarrow \{C_1, C_2, ..., C_{popSize}\}$). Then, lifetime of each chromosome is evaluated and the best lifetime is declared. By using Roulette Wheel selection [35], two parent chromosomes from population (P) are selected (*i.e.,* $C^{P1} = C_i$, $C^{P2} = C_j$ $\forall i, j \in \{1, 2, ..., popSize\}$ s.t. $i \neq j$). In this method, selection process is done randomly according to the lifetime values where the chromosomes with higher lifetime have a higher chance to be selected for crossover. The parent chromosomes (*i.e.,* C^{P1} and C^{P2}) go through the crossover and mutation stages, respectively. In crossover stage, new child chromosome is produced by swapping genes of two parent after random cut point (*e.g.,* $C^{P1} = [\mathbf{0\ 0\ 1}\ 0\ 1\ 1\ 0]$ and $C^{P2} = [1\ 0\ 1\ \mathbf{0\ 1\ 1\ 1}] \rightarrow C^{new} = [\mathbf{0\ 0\ 1\ 0\ 1\ 1\ 1}]$). The mutation stage occurs at the randomly selected gene with a pre-defined probability. If the value of selected gene is 1, it changes to 0 or vice versa (*e.g.,* $\mathcal{C}^{new} = [0\ 0\ 1\ 0\ 1\ 1\ 1] \rightarrow \mathcal{C}^3 mut = [0\ 0\ 1\ \mathbf{1}\ 1\ 1\ 1]$). The lifetime of new chromosome is calculated. If the lifetime is greater than the best lifetime, the new child chromosome is added to the population (*i.e.,* $P \cup \{C^{new}\}$) and the chromosome with worst lifetime is removed from the population (*i.e.,* $P \backslash \{C^{worst}\}$). These stages are done until the termination criteria is met.

Symbol	Description	Value
B_N	Noise bandwidth	30 kHz
c	Speed of light in air	3×10^8 m/s
d_e	Edge length of the network	20 m
d_0	Reference distance	0.5 m
E_{acq}	Acquisition energy	600 μJ
E_{elec}	Transmitter electronics energy	50 nJ/bit
ξ	Initial battery energy	25 kJ
L_A	ACK packet size	160 bits
L_H	Header size	96 bits
L_P	Payload size	1024 bits
N	Raw data size	1024 bytes
PL_0	Path loss at d_0	63.57 dB
P_n	Noise floor	–93.0 dBm
P_{proc}	Processing power	24 mW
P_{rx}	Reception power	21 mW
P_{slp}	Sleep power	0.3 mW
P_{std}	Standby power	75 μW
P_t	Output antenna power	0 dBm
P_{tx}	Transmission power	5 mW
R	Data rate	19.2 kbps
T_{acq}	Acquisition time	20 ms
t_{cycle}	Cycle duration	250 ns
T_{rnd}	Round duration	600 s
$\|W\|$	Number of sensor nodes	100–220
n	Path loss exponent	2.40
r	Reliability criteria	0.8
σ	Std. deviation	4.79 dB

Table 7.3.21. Simulation parameters

7.4 Performance Analysis

In this section, the random square shaped topology is considered. The one edge of two dimensional square shaped network is taken as 20 m (*i.e.,* $d_{net} = 20$). The round duration is considered to be 600 sec (*i.e.,* $T_{rnd} = 600$). This means that in every 600 second each sensor gathers N byte data to relay. (*i.e.,* $N = 1024$). The simulation parameters of

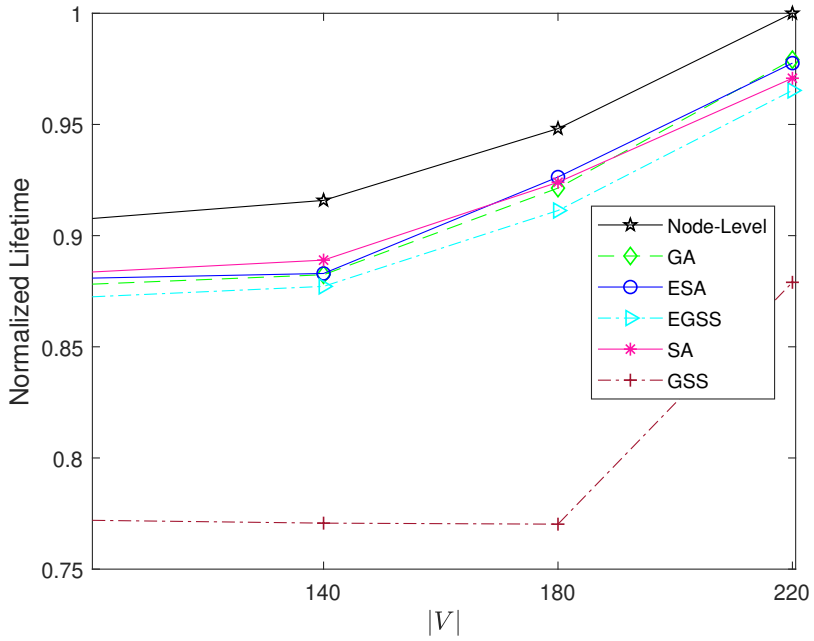

Figure 7.3.34. Normalized lifetime comparison of Node-Level EC scheme approach against meta-heuristic approaches

industrial channel and Mica2 are given in Table 5.4.15. To evaluate the MIP model and heuristic methods, General Algebraic Modelling System (GAMS) and MATLAB are used. The performance results are obtained with the average of 20 trials. The reliability rate is set to 0.8 for all simulations in this thesis. The normalized lifetime is determined by the absolute lifetime divided by maximum lifetime. The executions are performed on HP Z640 Workstation with 16GB RAM. As the number of sensors in the network increase, the average solution time significantly increases. To solve MIP model in polynomial time, we apply Linear Programming (LP) relaxation method for the simulations. The simulation parameters are given in Table 7.3.21.

Figure 7.3.33 demonstrates the comparison of network-Level EC scheme and node-Level EC scheme approach in terms of network lifetime as a function of $|V|$. The network-level with HARQ-II outperforms the other EC schemes among the network-level approaches. HARQ-II yields normalized lifetime between 0.87 and 0.96. ARQ gives the worst normalized lifetime values which are between 0.40 and 0.54. However, the lifetime obtained by utilizing node-level EC scheme approach which are between 0.9 and 1.0 is even better than network-level with HARQ-II. Node-level EC scheme approach extends the network lifetime up to 4.2 $\%$.

Figure 7.3.34 presents the comparison between the normalized lifetime of node-

level EC approach and meta-heuristics approaches (*i.e.,* Node-Level vs GA, SA, ESA, GSS, EGSS). GSS gives the worst normalized lifetimes which are between 0.77 and 0.87. The extended version of GSS (*i.e.,* E-GSS) enhances the normalized lifetimes which are between 0.87 and 0.96. SA and E-SA yield roughly close normalized lifetimes which are between 0.88 and 0.97. Finally, GA gives the normalized lifetime which are between 0.87 and 0.97. As a result, all meta-heuristic approaches except GSS provide shorter lifetime than node-level EC scheme approach at most 4.2 $\%$.

	Average Solution Times (s)					
$\|V\|$	**Node-Level**	**GSS**	**EGSS**	**SA**	**ESA**	**GA**
100	15	12	15	71	66	74
140	125	30	37	180	164	190
180	538	56	87	350	297	359
220	1114	121	116	588	496	619

Table 7.4.22. Average solution times for node-level EC scheme approach and meta-heuristics approaches

Table 7.4.22 presents the average solution time of node-level EC scheme approach and meta-heuristics. As the number of sensor nodes is the network increase, the average solution time of all methods are importantly increase. GSS gives the best results in terms of average solution time which are at least 12 and at most 121 second. Although EGSS gives better lifetime than GSS, the average solution time me of EGSS that are between 15 and 87 seconds is little longer than GS until V=180. After that point EGSS improves the average solution time (*i.e.,* 116 sec) which is greater than GSS. The average solution time of SA is between 71 and 588 second whereas for ESA is between 66 and 496 seconds.

Chapter 8

Conclusions and Future Propects

8.1 Conclusions

In this thesis, the lifetime of EH WMSNs in industrial environments is analytically quantified. Recently, EH methods are promising solution to prolong the network lifetime which includes many sensor nodes with rechargeable battery. EH methods available in industrial environments, namely, indoor solar, thermal and vibration that are comprehensively reviewed. At first, the lifetime of sensor node communicating with image data is analyzed by using a log-normal shadowing model as the channel model and a schedule-driven algorithm as power management scheme [102]. The impact of image compression methods and energy harvesting methods on sensor node lifetime is analyzed.

Reliability is a huge challenge due to harsh channel conditions of IWSNs. In addition, to provide reliability by utilizing EC schemes in industrial applications leads to substantial energy consumption that reduces the network lifetime. The impact of EC schemes on EH IWSNs lifetime is investigated. MIP model is designed to maximize the network lifetime by jointly utilizing energy dissipation of EC schemes and EH methods [104]. Moreover, image transmission which has huge data size poses critical problem for network lifetime. Therefore, the effect of CS and image compression algorithms on EH IWSNs lifetime are examined [103]. MIP with node-level EC scheme approach where each node selects the optimum EC type in each transmission is formulated to maximize the network lifetime. Finally, time complexity of MIP model with node-level EC scheme approach is analyzed. The developed meta-heuristic methods are compared in terms of network lifetime and time complexity.

The main conclusions are given as follows.

- Utilizing compression methods prolongs the sensor node lifetime especially when the

transmission distance is long. Since, the energy spent for extra processing operations during compression is smaller than the difference between the communication energy requirements of the original and compressed images. Furthermore, the analyses show that EH methods greatly extend the sensor node lifetime. According to simulation results, sensor node lifetime can be extended by jointly utilizing BinDCT and indoor solar harvesting method for Mica2 at most 51.8 % while for Telos at most 25. 8 %. As a result, image compression and EH methods are viable solutions to the limited energy problem of sensor nodes when used with proper power management methods tailored to application requirements.

- For Mica2, the maximum lifetime is achieved when sensor nodes uses HARQ-II as an EC scheme to ensure the reliability of application. However, for Telos, BCH(31,21,5) outperforms the other EC scheme in terms of lifetime. The reason for that, the lower processing power of Telos reduces the decoding energy cost for FEC schemes. At the same time, the lifetime of Telos is greater than that of Mica2 because of low the processing power and high data rate capability of Telos. Furthermore, the indoor solar harvester improves the lifetime of Mica2 by 46 % at most whereas the lifetime of Telos by 71 % at most.

- In WMSNs lifetime analysis, ISH outperforms the other harvesters, namely, VH and TH when data size reduction methods are not utilized. ISH can provide the lifetime improvement at least 5 % and at most 13 % when the reliability rate is 0.9.

- For WMSNs in industrial environment, BCS achieves better lifetime than the other data size reduction methods. Since, the computation energy to reduce the data size is very low in BCS method. As a result, BCS enhances the network lifetime up to 300 %. Furthermore, the joint utilization of BCS and indoor solar harvester prolongs the WMSNs lifetime up to 364 %.

- The MIP with node-level EC approach outperforms the MIP with network-level EC approach (*i.e.,* for all type of EC scheme) in terms of the network lifetimes regardless of the network density. The lifetimes obtained by using the network-level EC approach can be improved by at 4.2% using the node-level EC approach with the cost of extra computation time. For the network-level EC strategies, HARQ-II yields the best lifetimes while the classical ARQ has the worst lifetime performance.

- For the MIP with node-level EC approach, HARQ-II is the preferred EC method for the nodes which are close to the sink node since HARQ-II is an energy-efficient EC method. On the other hand, BCH$(31, 21, 5)$ is the favorite EC method for the nodes which are away from the sink node to combat against packet losses.

- The lifetime performance and time complexity of meta-heuristics which are GSS, E-GSS, SA, E-SA and GA are analyzed.The analysis highlights the importance of using the GSS algorithm to reduce the computational complexity of the node-level EC approach. More specifically, the E-GSS algorithm can reduce the time complexity of the MIP model by 89.5$\%$ with 3.4 shorter lifetime whereas the E-SA algorithm can reduce by 55.4$\%$ with 2.2$\%$ shorter lifetimes.

8.2 Contribution to Global Sustainability

WSNs technologies are used to improve the public welfare for the future of society. However, to construct and maintain WSNs applications require an enormous budget. Especially, to power WSNs applications which consist of battery-powered sensor nodes is a major challenge. Since, the sensor nodes with limited energy restrict the sustainability of these applications which makes them unfavorable. In addition, battery replacement of sensor nodes is not feasible when they are deployed in unreachable and hazardous places. Therefore, EH methods which converts natural and artificial ambient energy into electrical energy to provide the sustainability of WSNs applications.

On the other hand, sustainable WSNs applications contributes greatly to global sustainability such as environmental protection and economic development. Use of renewable energies in WSNs application which increases the energy efficiency reduces the environmental pollution. Batteries that do not need replacing reduce waste which is very difficult to destroy in nature. In terms of economical manner, the equipment and maintenance cost are decreased by utilizing sustainable energy sources in WSNs.

8.3 Future Prospects

As a future prospect, the cross layer communication approaches which determine all network layers to enhance the network lifetime and reliability. In this thesis, we consider physical layer (*i.e.,* channel model), link layer (*i.e.,* EC scheme) and their effect on network lifetime and reliability. MIP model deals with network layer (*i.e.,* routing protocols) such that optimum routing path is find to maximize the network lifetime by balancing energy dissipation of the all layers. In addition, energy efficient congestion control algorithms can be implemented to the proposed system to improve end to end delay. For real time industrial applications and video communication, latency is of vital challenge. Therefore, the future work may focus on to enhance the proposed MIP framework to maximize network lifetime by jointly meeting reliability and latency criteria. Although Mica2 and Telos commonly used sensor motes in industrial environment, Tmote Sky and IRIS etc. which provide high data rate become popular, recently . Therefore, the performance of Tmote Sky and IRIS etc can be investigated by using appropriate parameters of them. Another future work can be to simulate the proposed system with other heuristics such as particle swarm optimization or artificial bee colony. Furthermore, machine learning based algorithms such as neural networks can be applied to the proposed system to predict optimum EC scheme or WSN parameters to provide reliable and extended network lifetime. The computation cost to train machine learning algorithms may be very high, however once it is trained, the testing process can be done with low computation cost. In this way, the machine learning algorithms may provide solution for dynamically changing industrial environment. Finally, the experimental evaluations of proposed approaches via IWSN testbeds can be investigated in the future.

BIBLIOGRAPHY

[1] Mica2 Datasheet.

[2] Msp430 Datasheet.

[3] Abdal-Kadhim, A. M. and Leong, K. S. (2017). Application of thermal energy harvesting from low-level heat sources in powering up wsn node. In *2017 2nd International Conference on Frontiers of Sensors Technologies (ICFST)*, pages 131–135. IEEE.

[4] Abo-Zahhad, M., Ahmed, S. M., Sabor, N., and Sasaki, S. (2014). A new energy-efficient adaptive clustering protocol based on genetic algorithm for improving the lifetime and the stable period of wireless sensor networks. *International Journal of Energy, Information and Communications*, 5(3):47–72.

[5] Adu-Manu, K. S., Adam, N., Tapparello, C., Ayatollahi, H., and Heinzelman, W. (2018). Energy-harvesting wireless sensor networks (eh-wsns) a review. *ACM Transactions on Sensor Networks (TOSN)*, 14(2):1–50.

[6] Akbar, M. and Curiel-Sosa, J. (2016). Piezoelectric energy harvester composite under dynamic bending with implementation to aircraft wingbox structure. *Composite Structures*, 153:193–203.

[7] Akbas, A., Yildiz, H. U., Tavli, B., and Uludag, S. (2016). Joint optimization of transmission power level and packet size for wsn lifetime maximization. *IEEE Sensors Journal*, 16(12):5084–5094.

[8] Ali, A., Khelil, A., Shaikh, F. K., and Suri, N. (2012). Efficient predictive monitoring of wireless sensor networks. *International Journal of Autonomous and Adaptive Communications Systems*, 5(3):233–254.

[9] Allmen, L., Bailleul, G., Becker, T., Decotignie, J.-D., Kiziroglou, M. E., Leroux, C., Mitcheson, P. D., Müller, J., Piguet, D., Toh, T. T., et al. (2017). Aircraft strain wsn powered by heat storage harvesting. *IEEE Transactions on Industrial Electronics*, 64(9):7284–7292.

[10] Anastasi, G., Falchi, A., Passarella, A., Conti, M., and Gregori, E. (2004). Performance measurements of motes sensor networks. In *Proceedings of the 7th ACM international symposium on Modeling, analysis and simulation of wireless and mobile systems*, pages 174–181. ACM.

[11] Aoki, Y. (2017). Photovoltaic performance of organic photovoltaics for indoor energy harvester. *Organic Electronics*, 48:194–197.

[12] Baghaee, S., Ulusan, H., Chamanian, S., Zorlu, O., Kulah, H., and Uysal-Biyikoglu, E. (2013). Towards a vibration energy harvesting wsn demonstration testbed. In

2013 24th Tyrrhenian international workshop on digital communications-green ICT (TIWDC), pages 1–6. IEEE.

[13] Berger, A., Hörmann, L. B., Leitner, C., Oswald, S. B., Priller, P., and Springer, A. (2015). Sustainable energy harvesting for robust wireless sensor networks in industrial applications. In *2015 IEEE Sensors Applications Symposium (SAS)*, pages 1–6. IEEE.

[14] Bhatia, T., Kansal, S., Goel, S., and Verma, A. (2016). A genetic algorithm based distance-aware routing protocol for wireless sensor networks. *Computers & Electrical Engineering*, 56:441–455.

[15] Bicakci, K., Bagci, I. E., and Tavli, B. (2012). Communication/computation tradeoffs for prolonging network lifetime in wireless sensor networks: The case of digital signatures. *Information Sciences*, 188:44–63.

[16] Byun, H. and Yu, J. (2012). Adaptive duty cycle control with queue management in wireless sensor networks. *IEEE Transactions on Mobile Computing*, 12(6):1214–1224.

[17] Caione, C., Brunelli, D., and Benini, L. (2013). Compressive sensing optimization for signal ensembles in wsns. *IEEE Transactions on Industrial Informatics*, 10(1):382–392.

[18] Cao, G., Yu, F., and Zhang, B. (2011). Improving network lifetime for wireless sensor network using compressive sensing. In *2011 IEEE International Conference on High Performance Computing and Communications*, pages 448–454. IEEE.

[19] Carvalho, C. and Paulino, N. (2014). On the feasibility of indoor light energy harvesting for wireless sensor networks. *Procedia Technology*, 17:343–350.

[20] Castagnetti, A., Pegatoquet, A., Le, T. N., and Auguin, M. (2014). A joint duty-cycle and transmission power management for energy harvesting wsn. *IEEE Transactions on Industrial Informatics*, 10(2):928–936.

[21] Chen, Y., Shen, W., Huo, H., and Xu, Y. (2010). A smart gateway for health care system using wireless sensor network. In *2010 Fourth International Conference on Sensor Technologies and Applications*, pages 545–550. IEEE.

[22] Chottirapong, K., Manatrinon, S., Dangsakul, P., and Kwankeow, N. (2015). Design of energy harvesting thermoelectric generator with wireless sensors in organic fertilizer plant. In *2015 6th International Conference of Information and Communication Technology for Embedded Systems (IC-ICTES)*, pages 1–6. IEEE.

[23] Decker, A. (2013). Solar energy harvesting for autonomous field devices. *IET Wireless Sensor Systems*, 4(1):1–8.

[24] Dondi, D., Napoletano, G., Bertacchini, A., Larcher, L., and Pavan, P. (2012). A wsn system powered by vibrations to improve safety of machinery with trailer. In *SENSORS, 2012 IEEE*, pages 1–4. IEEE.

[25] Dong, C., Li, S., Han, R., He, Q., Li, X., and Xu, D. (2019). Self-powered wireless sensor network using event-triggered energy harvesters for monitoring and identifying intrusion activities. *IET Power Electronics*, 12(8):2079–2085.

[26] Eidaks, J., Tjukovs, S., and Pikulins, D. (2017). Exploration of possible energy sources for hybrid power system of indoor wsn. In *2017 5th IEEE Workshop on Advances in Information, Electronic and Electrical Engineering (AIEEE)*, pages 1–5. IEEE.

[27] Elefsiniotis, A., Kokorakis, N., Becker, T., and Schmid, U. (2013). Performance of a low temperature energy harvesting device for powering wireless sensor nodes in aircrafts applications. In *2013 Transducers & Eurosensors XXVII: The 17th International Conference on Solid-State Sensors, Actuators and Microsystems (TRANSDUCERS & EUROSENSORS XXVII)*, pages 2276–2279. IEEE.

[28] Eris, C., Saimler, M., Gungor, V. C., Fadel, E., and Akyildiz, I. F. (2014). Lifetime analysis of wireless sensor nodes in different smart grid environments. *Wireless networks*, 20(7):2053–2062.

[29] Fateh, B. and Govindarasu, M. (2013). Joint scheduling of tasks and messages for energy minimization in interference-aware real-time sensor networks. *IEEE transactions on mobile computing*, 14(1):86–98.

[30] Furtak, J., Zieliński, Z., and Chudzikiewicz, J. (2016). Security techniques for the wsn link layer within military iot. In *2016 IEEE 3rd World Forum on Internet of Things (WF-IoT)*, pages 233–238. IEEE.

[31] Gao, G., Zhang, H., and Li, L. (2014). Performance evaluation of wsns-based link quality estimation metrics for industrial environments. In *Advanced Technologies in Ad Hoc and Sensor Networks*, pages 69–79. Springer.

[32] Garg, S., Sharma, A. K., and Tyagi, A. (2016). An introduction to various error detection and correction schemes used in communication. *International Journal of Applied Research 2016*, 2(8):216–218.

[33] Ghayvat, H., Mukhopadhyay, S., Gui, X., and Suryadevara, N. (2015). Wsn-and iot-based smart homes and their extension to smart buildings. *Sensors*, 15(5):10350–10379.

[34] Ghorbel, O., Ayedi, W., Jmal, M. W., and Abid, M. (2012). Images compression in wsn: Performance analysis. In *2012 IEEE 14th International Conference on Communication Technology*, pages 1363–1368. IEEE.

[35] Goldberg, D. E. and Holland, J. H. (1988). Genetic algorithms and machine learning.

[36] Grumazescu, C., Vlăduţă, V.-A., and Subaşu, G. (2016). Wsn solutions for communication challenges in military live simulation environments. In *2016 International Conference on Communications (COMM)*, pages 319–322. IEEE.

[37] Guan, M., Wang, K., Xu, D., and Liao, W.-H. (2017). Design and experimental investigation of a low-voltage thermoelectric energy harvesting system for wireless sensor nodes. *Energy Conversion and Management*, 138:30–37.

[38] Gungor, V. C., Hancke, G. P., et al. (2009). Industrial wireless sensor networks: Challenges, design principles, and technical approaches. *IEEE Trans. Industrial Electronics*, 56(10):4258–4265.

[39] Hande, A., Polk, T., Walker, W., and Bhatia, D. (2007). Indoor solar energy harvesting for sensor network router nodes. *Microprocessors and Microsystems*, 31(6):420–432.

[40] Hemalatha, R., Radha, S., and Sudharsan, S. (2015). Energy-efficient image transmission in wireless multimedia sensor networks using block-based compressive sensing. *Computers & Electrical Engineering*, 44:67–79.

[41] Hosseini, E. S., Esmaeelzadeh, V., and Eslami, M. (2015). A hierarchical sub-chromosome genetic algorithm (hsc-ga) to optimize power consumption and data communications reliability in wireless sensor networks. *Wireless Personal Communications*, 80(4):1579–1605.

[42] Hou, L., Tan, S., Yang, L., Zhang, Z., and Bergmann, N. (2017). Autonomous wireless sensor node with thermal energy harvesting for temperature monitoring of industrial devices. *International Journal of Online and Biomedical Engineering (iJOE)*, 13(04):75–82.

[43] Hou, L., Tan, S., Zhang, Z., and Bergmann, N. W. (2018). Thermal energy harvesting wsns node for temperature monitoring in iiot. *IEEE Access*, 6:35243–35249.

[44] Huang, Q., Lu, C., and Shaurette, M. (2010). Feasibility study of indoor light energy harvesting for intelligent building environment management.

[45] Huu, P. N., Tran-Quang, V., and Miyoshi, T. (2010). Energy threshold adaptation algorithms on image compression to prolong wsn lifetime. In *2010 7th International Symposium on Wireless Communication Systems*, pages 834–838. IEEE.

[46] Ibrahim, R., Chung, T. D., Hassan, S. M., Bingi, K., and Salahuddin, S. (2017). Solar energy harvester for industrial wireless sensor nodes. *Procedia Computer Science*, 105(C):111–118.

[47] Islam, M. R. (2010). Error correction codes in wireless sensor network: An energy aware approach. *International Journal of Computer and Information Engineering*, 4(1):59–64.

[48] Jalali, F., Khodadoustan, S., and Ejlali, A. (2012). Error control schemes in solar energy harvesting wireless sensor networks. In *Communications and Information Technologies (ISCIT), 2012 International Symposium on*, pages 979–984. IEEE.

[49] Jung, D., Teixeira, T., and Savvides, A. (2009). Sensor node lifetime analysis: Models and tools. *ACM Transactions on Sensor Networks (TOSN)*, 5(1):1–33.

[50] Jung, J., Kang, M., Yoon, I., and Noh, D. K. (2016). Adaptive forward error correction scheme to improve data reliability in solar-powered wireless sensor networks. In *Information Science and Security (ICISS), 2016 International Conference on*, pages 1–4. IEEE.

[51] Kadel, R., Islam, N., Ahmed, K., and Halder, S. J. (2019). Opportunities and challenges for error correction scheme for wireless body area network—a survey. *Journal of Sensor and Actuator Networks*, 8(1):1.

[52] Kahjogh, B. O., Demirkol, I., Careglio, D., and Pascual, J. D. (2017). The impact of critical node elimination on the latency of wireless sensor networks. In *2017 Ninth International Conference on Ubiquitous and Future Networks (ICUFN)*, pages 182–187. IEEE.

[53] Kassan, S., Gaber, J., and Lorenz, P. (2019). Autonomous energy management system achieving piezoelectric energy harvesting in wireless sensors. *Mobile Networks and Applications*, pages 1–12.

[54] Kim, M.-K., Kim, M.-S., Lee, S., Kim, C., and Kim, Y.-J. (2014). Wearable thermoelectric generator for harvesting human body heat energy. *Smart Materials and Structures*, 23(10):105002.

[55] Kim, Y. J., Gu, H. M., Kim, C. S., Choi, H., Lee, G., Kim, S., Kevin, K. Y., Lee, S. G., and Cho, B. J. (2018). High-performance self-powered wireless sensor node driven by a flexible thermoelectric generator. *Energy*, 162:526–533.

[56] Kumar, V., Jain, A., Barwal, P., et al. (2014). Wireless sensor networks: security issues, challenges and solutions. *International Journal of Information and Computation Technology (IJICT)*, 4(8):859–868.

[57] Lecuire, V., Makkaoui, L., and Moureaux, J.-M. (2012). Fast zonal dct for energy conservation in wireless image sensor networks. *Electronics Letters*, 48(2):125–127.

[58] Lee, S., Lee, I., Kim, S., Lee, S., and Bovik, A. C. (2013). A pervasive network control algorithm for multicamera networks. *IEEE Sensors Journal*, 14(4):1280–1294.

[59] Leonov, V. (2013). Thermoelectric energy harvesting of human body heat for wearable sensors. *IEEE Sensors Journal*, 13(6):2284–2291.

[60] Li, K., Shu, L., Mukherjee, M., Wang, D., and Hu, L. (2016). Prolonging network lifetime with sleep scheduling for solar harvesting industrial wsns. In *2016 IEEE 18th International Conference on High Performance Computing and Communications; IEEE 14th International Conference on Smart City; IEEE 2nd International Conference on Data Science and Systems (HPCC/SmartCity/DSS)*, pages 1532–1533. IEEE.

[61] Li, X., Li, D., Wan, J., Vasilakos, A. V., Lai, C.-F., and Wang, S. (2017). A review of industrial wireless networks in the context of industry 4.0. *Wireless networks*, 23(1):23–41.

[62] Liu, X., Cao, J., Lai, S., Yang, C., Wu, H., and Xu, Y. L. (2011). Energy efficient clustering for wsn-based structural health monitoring. In *2011 Proceedings IEEE INFOCOM*, pages 2768–2776. IEEE.

[63] Low, K. S., Win, W. N. N., and Er, M. J. (2005). Wireless sensor networks for industrial environments. In *null*, pages 271–276. IEEE.

[64] Ma, T., Hempel, M., Peng, D., and Sharif, H. (2012). A survey of energy-efficient compression and communication techniques for multimedia in resource constrained systems. *IEEE Communications Surveys & Tutorials*, 15(3):963–972.

[65] Mahdavi-Doost, H. and Yates, R. D. (2015). Hybrid arq in block-fading channels with an energy harvesting receiver. In *Information Theory (ISIT), 2015 IEEE International Symposium on*, pages 1144–1148. IEEE.

[66] Makkaoui, L., Lecuire, V., and Moureaux, J.-M. (2010). Fast zonal dct-based image compression for wireless camera sensor networks. In *2010 2nd International Conference on Image Processing Theory, Tools and Applications*, pages 126–129. IEEE.

[67] Meng, J.-H., Wang, X.-D., and Chen, W.-H. (2016). Performance investigation and design optimization of a thermoelectric generator applied in automobile exhaust waste heat recovery. *Energy Conversion and Management*, 120:71–80.

[68] Mihajlovic, Z., Joza, A., Milosavljevic, V., Rajs, V., and Zivanov, M. (2015). Energy harvesting wireless sensor node for monitoring of surface water. In *2015 21st International Conference on Automation and Computing (ICAC)*, pages 1–6. IEEE.

[69] Molina, G. and Alba, E. (2008). Wireless sensor network deployment using a memetic simulated annealing. In *2008 International Symposium on Applications and the Internet*, pages 237–240. IEEE.

[70] Naderi, M. Y., Rabiee, H. R., Khansari, M., and Salehi, M. (2012). Error control for multimedia communications in wireless sensor networks: A comparative performance analysis. *Ad Hoc Networks*, 10(6):1028–1042.

[71] Nandhini, S. A., Radha, S., Nirmala, P., and Kishore, R. Compressive sensing for images using a variant of toeplitz matrix for wireless sensor networks. *Journal of Real-Time Image Processing*, pages 1–16.

[72] Nandhini, S. A., Radha, S., Nirmala, P., and Kishore, R. (2019). Compressive sensing for images using a variant of toeplitz matrix for wireless sensor networks. *Journal of Real-Time Image Processing*, 16(5):1525–1540.

[73] Nandi, A. and Kundu, S. (2011). Energy level performance of error control schemes in wsn over rayleigh fading channel. In *Industrial Electronics and Applications (ISIEA), 2011 IEEE Symposium on*, pages 194–199. IEEE.

[74] Nasiri, A., Zabalawi, S. A., and Mandic, G. (2009). Indoor power harvesting using photovoltaic cells for low-power applications. *IEEE Transactions on Industrial Electronics*, 56(11):4502–4509.

[75] Nasri, M., Helali, A., Sghaier, H., and Maaref, H. (2010). Adaptive image transfer for wireless sensor networks (wsns). In *5th International Conference on Design & Technology of Integrated Systems in Nanoscale Era*, pages 1–7. IEEE.

[76] Nasri, M., Helali, A., Sghaier, H., and Maaref, H. (2011). Adaptive image compression technique for wireless sensor networks. *Computers & Electrical Engineering*, 37(5):798–810.

[77] Othman, A. and Maga, D. (2018). Indoor photovoltaic energy harvester with rechargeable battery for wireless sensor node. In *2018 18th International Conference on Mechatronics-Mechatronika (ME)*, pages 1–6. IEEE.

[78] Panthongsy, P., Isarakorn, D., Sudhawiyangkul, T., and Nundrakwang, S. (2015). Piezoelectric energy harvesting from machine vibrations for wireless sensor system. In *2015 12th International Conference on Electrical Engineering/Electronics, Computer, Telecommunications and Information Technology (ECTI-CON)*, pages 1–6. IEEE.

[79] Petrini, F. and Gkoumas, K. (2018). Piezoelectric energy harvesting from vortex shedding and galloping induced vibrations inside hvac ducts. *Energy and Buildings*, 158:371–383.

[80] Pinto, A. R., Cansian, A., Machado, J. M., and Montez, C. (2012). Self-optimization of dense wireless sensor networks based on simulated annealing. In *2012 13th Latin American Test Workshop (LATW)*, pages 1–6. IEEE.

[81] Polastre, J., Szewczyk, R., and Culler, D. (2005). Telos: enabling ultra-low power wireless research. In *Information Processing in Sensor Networks, 2005. IPSN 2005. Fourth International Symposium on*, pages 364–369. IEEE.

[82] Pubill, D., Serra, J., and Verikoukis, C. (2018). Harvesting artificial light indoors to power perpetually a wireless sensor network node. In *2018 IEEE 23rd International Workshop on Computer Aided Modeling and Design of Communication Links and Networks (CAMAD)*, pages 1–6. IEEE.

[83] Radmand, P., Talevski, A., Petersen, S., and Carlsen, S. (2010). Comparison of industrial wsn standards. In *4th ieee international conference on digital ecosystems and technologies*, pages 632–637. IEEE.

[84] Rasheduzzaman, M., Pillai, P. B., Mendoza, A. N. C., and De Souza, M. M. (2016). A study of the performance of solar cells for indoor autonomous wireless sensors. In *2016 10th International Symposium on Communication Systems, Networks and Digital Signal Processing (CSNDSP)*, pages 1–6. IEEE.

[85] Razali, S. M., Mamat, K., and Bashah, N. S. K. (2016). Implementation of hybrid arq (harq) error control algorithm for lifetime maximization and low overhead cdma wireless sensor network (wsn). In *Wireless Sensors (ICWiSE), 2016 IEEE Conference on*, pages 71–76. IEEE.

[86] Ren, L., Chen, R., Xia, H., and Zhang, X. (2016). Energy harvesting performance of a broadband electromagnetic vibration energy harvester for powering industrial wireless sensor networks. In *Active and Passive Smart Structures and Integrated Systems 2016*, volume 9799, page 97993P. International Society for Optics and Photonics.

[87] Roshani, H., Dessouky, S., Montoya, A., and Papagiannakis, A. (2016). Energy harvesting from asphalt pavement roadways vehicle-induced stresses: A feasibility study. *Applied Energy*, 182:210–218.

[88] Sankman, J. and Ma, D. (2014). A 12-μw to 1.1-mw aim piezoelectric energy harvester for time-varying vibrations with 450-na $i\_\{\backslash bmQ\}$˙ *IEEE Transactions on Power Electronics*, 30(2):632–643.

[89] Sarvi, B., Rabiee, H. R., and Mizanian, K. (2017). An adaptive cross-layer error control protocol for wireless multimedia sensor networks. *Ad Hoc Networks*, 56:173–185.

[90] Schwieger, K., Kumar, A., and Fettweis, G. P. (2005). On the impact of the physical layer on energy consumption in sensor networks. In *EWSN*, pages 13–24.

[91] Sembroiz, D., Ojaghi, B., Careglio, D., and Ricciardi, S. (2019). A grasp meta-heuristic for evaluating the latency and lifetime impact of critical nodes in large wireless sensor networks. *Applied Sciences*, 9(21):4564.

[92] Ševčík, P. and Kovář, O. (2013). Power unit based on supercapacitors and solar cell module. In *SCIECONF*. University of Zilina.

[93] Sharma, H., Haque, A., and Jaffery, Z. A. (2019). Maximization of wireless sensor network lifetime using solar energy harvesting for smart agriculture monitoring. *Ad Hoc Networks*, 94:101966.

[94] Sharma, M. K. and Murthy, C. R. (2014). Packet drop probability analysis of arq and harq-cc with energy harvesting transmitters and receivers. In *Signal and Information Processing (GlobalSIP), 2014 IEEE Global Conference on*, pages 148–152. IEEE.

[95] Shekofteh, S. K., Yaghmaee, M. H., Khalkhali, M. B., and Deldari, H. (2010). Localization in wireless sensor networks using tabu search and simulated annealing. In *2010 The 2nd International Conference on Computer and Automation Engineering (ICCAE)*, volume 2, pages 752–757. IEEE.

[96] Shnayder, V., Hempstead, M., Chen, B.-r., Allen, G. W., and Welsh, M. (2004). Simulating the power consumption of large-scale sensor network applications. In *Proceedings of the 2nd international conference on Embedded networked sensor systems*, pages 188–200. ACM.

[97] Simjee, F. I. and Chou, P. H. (2008). Efficient charging of supercapacitors for extended lifetime of wireless sensor nodes. *IEEE Transactions on power electronics*, 23(3):1526–1536.

[98] Sun, E., Shen, X., and Chen, H. (2011). A low energy image compression and transmission in wireless multimedia sensor networks. *Procedia Engineering*, 15:3604–3610.

[99] Suryadevara, N. K., Mukhopadhyay, S. C., Kelly, S. D. T., and Gill, S. P. S. (2014). Wsn-based smart sensors and actuator for power management in intelligent buildings. *IEEE/ASME transactions on mechatronics*, 20(2):564–571.

[100] Tan, C., Zou, J., Wang, M., and Zhang, R. (2011). Network lifetime optimization for wireless video sensor networks with network coding/arq hybrid adaptive error-control scheme. *Computer Networks*, 55(9):2126–2137.

[101] Tang, X., Mones, Z., Wang, X., Gu, F., and Ball, A. D. (2018). A review on energy harvesting supplying wireless sensor nodes for machine condition monitoring. In *2018 24th International Conference on Automation and Computing (ICAC)*, pages 1–6. IEEE.

[102] Tekin, N., Erdem, H. E., and Gungor, V. C. (2018). Analyzing lifetime of energy harvesting wireless multimedia sensor nodes in industrial environments. *Computer Standards & Interfaces*, 58:109–117.

[103] Tekin, N. and Gungor, V. C. (2020a). Analysis of compressive sensing and energy harvesting for wireless multimedia sensor networks. *Ad Hoc Networks*, page 102164.

[104] Tekin, N. and Gungor, V. C. (2020b). The impact of error control schemes on lifetime of energy harvesting wireless sensor networks in industrial environments. *Computer Standards & Interfaces*, page 103417.

[105] Thielen, M., Sigrist, L., Magno, M., Hierold, C., and Benini, L. (2017). Human body heat for powering wearable devices: From thermal energy to application. *Energy conversion and management*, 131:44–54.

[106] Toh, W. Y., Tan, Y. K., Koh, W. S., and Siek, L. (2014). Autonomous wearable sensor nodes with flexible energy harvesting. *IEEE sensors journal*, 14(7):2299–2306.

[107] Uchida, K., Takahashi, S., Harii, K., Ieda, J., Koshibae, W., Ando, K., Maekawa, S., and Saitoh, E. (2008). Observation of the spin seebeck effect. *Nature*, 455(7214):778.

[108] Ullah, S., Higgins, H., Braem, B., Latre, B., Blondia, C., Moerman, I., Saleem, S., Rahman, Z., and Kwak, K. S. (2012). A comprehensive survey of wireless body area networks. *Journal of medical systems*, 36(3):1065–1094.

[109] Verma, G. and Sharma, V. (2018). A novel thermoelectric energy harvester for wireless sensor network application. *IEEE Transactions on Industrial Electronics*, 66(5):3530–3538.

[110] Vuran, M. C. and Akyildiz, I. F. (2006). Cross-layer analysis of error control in wireless sensor networks. In *Sensor and Ad Hoc Communications and Networks, 2006. SECON'06. 2006 3rd Annual IEEE Communications Society on*, volume 2, pages 585–594. IEEE.

[111] Vuran, M. C. and Akyildiz, I. F. (2009). Error control in wireless sensor networks: a cross layer analysis. *IEEE/ACM Transactions on Networking (TON)*, 17(4):1186–1199.

[112] Wahbah, M., Alhawari, M., Mohammad, B., Saleh, H., and Ismail, M. (2014). Characterization of human body-based thermal and vibration energy harvesting for wearable devices. *IEEE Journal on emerging and selected topics in circuits and systems*, 4(3):354–363.

[113] Wang, C., Zhao, J., Li, Q., and Li, Y. (2018). Optimization design and experimental investigation of piezoelectric energy harvesting devices for pavement. *Applied Energy*, 229:18–30.

[114] Wang, Q. and Yang, W. (2007). Energy consumption model for power management in wireless sensor networks. In *2007 4th Annual IEEE Communications Society Conference on Sensor, Mesh and Ad Hoc Communications and Networks*, pages 142–151. IEEE.

[115] Wang, X., Ma, J.-J., Wang, S., and Bi, D.-W. (2007). Distributed particle swarm optimization and simulated annealing for energy-efficient coverage in wireless sensor networks. *Sensors*, 7(5):628–648.

[116] Wang, Y., Wang, D., Zhang, X., Chen, J., and Li, Y. (2016). Energy-efficient image compressive transmission for wireless camera networks. *IEEE Sensors Journal*, 16(10):3875–3886.

[117] Wei, Z., Lijuan, S., Jian, G., and Linfeng, L. (2016). Image compression scheme based on pca for wireless multimedia sensor networks. *The Journal of China Universities of Posts and Telecommunications*, 23(1):22–30.

[118] Xenakis, A., Foukalas, F., and Stamoulis, G. (2016). Cross-layer energy-aware topology control through simulated annealing for wsns. *Computers & Electrical Engineering*, 56:576–590.

[119] Xenakis, A., Foukalas, F., Stamoulis, G., and Khattab, T. (2013). Energy-aware joint power, packet and topology optimization by simulated annealing for wsns. In *2013 7th IEEE GCC Conference and Exhibition (GCC)*, pages 17–21. IEEE.

[120] Xiong, H. and Wang, L. (2016). Piezoelectric energy harvester for public roadway: On-site installation and evaluation. *Applied Energy*, 174:101–107.

[121] Yadav, A., Goonewardena, M., Ajib, W., Dobre, O. A., and Elbiaze, H. (2017). Energy management for energy harvesting wireless sensors with adaptive retransmission. *IEEE Transactions on Communications*, 65(12):5487–5498.

[122] Yildiz, H. U., Bicakci, K., Tavli, B., Gultekin, H., and Incebacak, D. (2016a). Maximizing wireless sensor network lifetime by communication/computation energy optimization of non-repudiation security service: Node level versus network level strategies. *Ad Hoc Networks*, 37:301–323.

[123] Yildiz, H. U., Tavli, B., and Yanikomeroglu, H. (2016b). Transmission power control for link-level handshaking in wireless sensor networks. *IEEE Sensors Journal*, 16(2):561–576.

[124] Zhang, J. and Long, J. (2017). An energy-aware hybrid arq scheme with multi-acks for data sensing wireless sensor networks. *Sensors*, 17(6):1366.

[125] Zhang, J., Xiang, Q., Yin, Y., Chen, C., and Luo, X. (2017). Adaptive compressed sensing for wireless image sensor networks. *Multimedia Tools and Applications*, 76(3):4227–4242.

[126] Zhou, F., Chen, Z., Guo, S., and Li, J. (2016). Maximizing lifetime of data-gathering trees with different aggregation modes in wsns. *IEEE Sensors Journal*, 16(22):8167–8177.

[127] Zuniga, M. and Krishnamachari, B. (2004). Analyzing the transitional region in low power wireless links. In *2004 First Annual IEEE Communications Society Conference on Sensor and Ad Hoc Communications and Networks, 2004. IEEE SECON 2004.*, pages 517–526. IEEE.